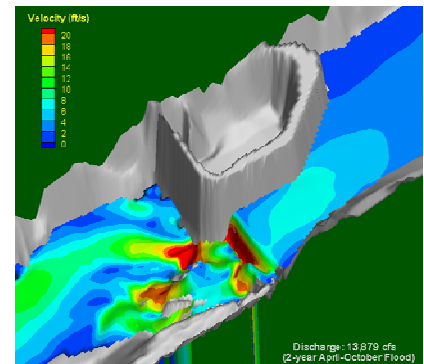
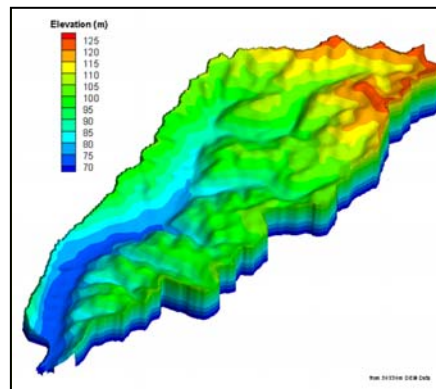
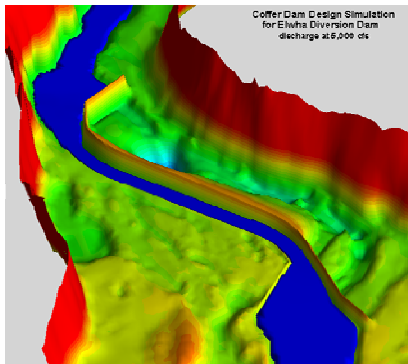


# RECLAMATION

*Managing Water in the West*

## Theory and User Manual for SRH-W Version 1.1

Sedimentation and River Hydraulic – Watershed model



U.S. Department of the Interior  
Bureau of Reclamation  
Technical Service Center  
Denver, Colorado

November 2006



# **Theory and User Manual for SRH-W Version 1.1**

**Sedimentation and River Hydraulics – Watershed model**

**Prepared by**

**Yong G. Lai, Ph.D., Hydraulic Engineer**

**Bureau of Reclamation  
Technical Service Center  
Sedimentation and River Hydraulics Group**



**U.S. Department of the Interior  
Bureau of Reclamation  
Technical Service Center  
Denver, Colorado**

**November 2006**

## **Mission Statements**

The mission of the Department of the Interior is to protect and provide access to our Nation's natural and cultural heritage and honor our trust responsibilities to Indian Tribes and our commitments to island communities.

---

The mission of the Bureau of Reclamation is to manage, develop, and protect water and related resources in an environmentally and economically sound manner.

## **Acknowledgments**

A number of engineers and researchers have made contributions to the review and testing of SRH-W Version 1.1 and the manual. Their effort has greatly enhanced the quality of the work reported. In particular, the following individuals are acknowledged for their contributions: Timothy Randle, Blair Greimann, Robert Hildale, Jennifer Bountry, Victor Huang, and David Mooney at the Sedimentation and River Hydraulics Group at the Bureau of Reclamation, and Chih Ted Yang at the Colorado State University. Peer review of the manual by Robert Hildale is greatly appreciated.

The work reported was funded by a number of sources, including the Environmental Protection Agency (EPA) under the Interagency Agreement No.DW14948044, Reclamation's Science and Technology Program, and other Reclamation projects.

## **Disclaimer**

No warranty is expressed or implied regarding the usefulness or completeness of the information contained in this report. References to commercial products do not imply endorsement by the Bureau of Reclamation and may not be used for advertising or promotional purposes.



# CONTENTS

ABSTRACT.....	1
CHAPTER 1 .....	3
INTRODUCTION .....	3
1.1 Background.....	3
1.2 Modeling Concepts and Capabilities .....	4
1.3 Limitations .....	7
1.4 Acquiring SRH-W .....	8
1.5 Disclaimer .....	8
CHAPTER 2 .....	9
GETTING STARTED.....	9
2.1 Model Structure .....	9
2.1.1 Mesh Generation Program .....	9
2.1.2 SRH-W Solver Module.....	10
2.1.3 Post-Processing Program .....	11
2.2 Solution Procedure.....	11
2.2.1 Mesh Generation.....	11
2.2.2 Preprocessor Execution.....	11
2.2.3 Main Solver Execution .....	12
2.3 SRH-W Output Files.....	13
2.3.1 _RES File .....	13
2.3.2 _OUT File .....	13
2.3.3 _RST File .....	13
2.3.4 Result Output File .....	13
CHAPTER 3 .....	15
TUTORIAL.....	15
3.1 A Subcritical Flow in a Channel.....	15
3.2 Water Runoff from a 2D Surface.....	19
CHAPTER 4 .....	23
INPUT COMMANDS .....	23
CHAPTER 5 .....	39
GOVERNING EQUATIONS.....	39
5.1 Flow Equations .....	39
5.2 Equations with Diffusive Wave Approximation .....	41
5.3 Sub-Models for Watershed Runoff Simulation .....	42
5.3.1 Introduction.....	42

5.3.2 Rainfall Component .....	44
5.3.3 Interception Component.....	45
5.3.4 Infiltration Component.....	46
5.3.5 Diffusive Wave Channel Network Solver .....	49
CHAPTER 6 .....	53
INITIAL AND BOUNDARY CONDITIONS .....	53
6.1 Initial Conditions .....	53
6.2 Inlet Boundary .....	53
6.3 Exit Boundary .....	54
6.4 Solid Wall Boundary .....	55
6.5 Symmetry Boundary .....	56
CHAPTER 7 .....	57
NUMERICAL METHODS .....	57
7.1 Diffusive Wave Solver for Flow.....	57
7.2 Dynamic Wave Solver for Flow .....	60
7.2.1 Discretization .....	60
7.2.2 Side Normal Velocity Calculation and Elevation Correction Equation .....	63
7.2.3 Summary of Solution Procedure .....	65
CHAPTER 8 .....	67
VERIFICATION CASES .....	67
8.1 1D Surface Runoff .....	67
8.2 2D Surface Runoff .....	70
8.3 1D Subcritical Flow in a Channel.....	73
8.4 1D Transcritical Flow in a Channel.....	74
8.5 2D Diversion Flow in a Channel .....	76
CHAPTER 9 .....	81
APPLICATION CASES .....	81
9.1 Goodwin Creek Experimental Watershed Runoff .....	81
9.1.1 Watershed Description .....	81
9.1.2 Digital Elevation Model.....	82
9.1.3 Soil Types .....	83
9.1.4 Land Use .....	84
9.1.5 Precipitation .....	86
9.1.6 Channel Network and Cross Section Data.....	86
9.1.7 Event Selection and Input Data.....	87
9.1.8 Description of Mesh Topologies.....	89
9.1.9 Results and Discussion .....	93
9.2 Savage Rapids Dam Removal Study .....	101
9.2.1 Topography and Mesh .....	101

9.2.2 Case Modeled, Boundary Conditions, and Other Parameters.....	102
9.2.3 Comparison of Water Surface Elevation .....	103
9.2.4 Comparison of Velocities and Flow Patterns.....	103
9.3 Study of Sandy River and Columbia River Interaction .....	106
9.3.1 Solution Domain, Mesh, and Flow Roughness.....	107
9.3.2 Input Data.....	111
9.3.3 Comparison of Water Surface Elevation .....	112
9.3.4 Comparison of Flow Velocity.....	114
9.4 Other Application Cases .....	121
REFERENCES .....	123
APPENDIX A.....	129
ON MESH GENERATION USING SMS.....	129
APPENDIX B .....	133
INPUT AND OUTPUT FORMATS .....	133
B.1 SMS Format .....	133
B.2 TECPLOT Format.....	133
B.3 PLOT3D Format .....	133
B.4 GENERIC Format.....	134
APPENDIX C .....	135
DYNAMIC INPUT FILE (DIP) .....	135
APPENDIX D.....	137
SPECIAL TREATMENT IN MESH ZONES .....	137

## TABLES

Table 1. Computed and documented catchment areas (Blackmarr 1995) .....	82
Table 2. Average channel width and depth of each reach in Figure 36.....	87
Table 3. Soil infiltration parameters for each soil type at the Goodwin Creek ...	89
Table 4. Land use parameters for each land use class at the Goodwin Creek .....	89
Table 5. Calibrated Manning's Coefficients in Different Zones Shown in Figure 62.....	111

## FIGURES

Figure 1. Conceptual illustration of zonal modeling used by SRH-W .....	5
Figure 2. Illustration of zone partition and mesh layout for a typical river simulation.....	5
Figure 3. A sample mesh used by SRH-W; quadrilateral cells are used along the main channel and levees and mixed coarser cells are in the floodplains.....	6
Figure 4. A sample mesh for SRH-W that uses a combination of structured and unstructured meshes.....	7
Figure 5. An 81-by-4 mesh used for simulation for test 1 of MacDonald (1996)	16
Figure 6. A sample window session running <i>srhpre11</i> for the tutorial case 1 .....	16
Figure 7. A sample window session running <i>srhw11</i> for the tutorial case 1 .....	17
Figure 8. A sample window session running <i>srhpre11</i> for the tutorial case 2 .....	20
Figure 9. A sample window session running <i>srhw11</i> for the tutorial case 2 .....	21
Figure 10. Illustration of the Green-Ampt infiltration model .....	47
Figure 11. Schematic illustrating two neighboring cells with a common side .....	58
Figure 12. Schematic illustrating a polygon P along with one of its neighboring polygons N .....	61
Figure 13. Schematic of the 1D Surface Runoff Case (Therrien et al., 2003).....	68
Figure 14. Comparison of Hydrographs for Case I with $F_0 = 0.5$ $K = 10$ .....	69
Figure 15. Comparison of Hydrographs for Case II with $F_0 = 1.5$ $K = 3$ .....	69
Figure 16. Geometry of the V-Shaped Catchment (diGiammarco et al., 1996) ...	70
Figure 17. Structured mesh (on the left) and unstructured mesh (on the right) used for simulation of the 2D V-Catchment Case.....	71
Figure 18. Comparison of Discharges at the Overland Exit into the Channel (GTAR-W is the former name of SRH-W).....	72
Figure 19. Comparison of Discharges at the Channel Exit (GTAR-W is the former name of SRH-W) .....	72

Figure 20. An 81-by-4 mesh used for simulation for test 1 of MacDonald (1996)	73
Figure 21. Comparison of simulated water surface elevation with analytical solution for test case 1 of MacDonald (1996)	74
Figure 22. Comparison of simulated water depth with analytical solution for test case 1 of MacDonald (1996)	74
Figure 23. 3D view of bed elevation and simulated water surface elevation for test case 6 of MacDonald (1996)	75
Figure 24. Comparison of simulated water surface elevation with analytical solution for test case 6 of MacDonald (1996)	76
Figure 25. Comparison of simulated water depth with analytical solution for test case 6 of MacDonald (1996)	76
Figure 26. Part of the quadrilateral mesh used for simulation of the diversion flow	77
Figure 27. Comparison of water surface elevation along both walls of the main channel for the Shettar and Murthy (1996) case	78
Figure 28. Comparison of water surface elevation along both walls of the side channel for the Shettar and Murthy (1996) case	78
Figure 29. Comparison of x-velocity (U) profiles at selected x locations in the main channel for the Shettar and Murthy (1996) case	79
Figure 30. Comparison of y-velocity profiles at selected y locations in the side channel for the Shettar and Murthy (1996) case	79
Figure 31. Goodwin Creek Watershed Location and Topography	82
Figure 32. Digital elevation model and subcatchments used in the Goodwin Creek watershed.	83
Figure 33. Soil type distribution at the Goodwin Creek	84
Figure 34. Land Use Class Map at Goodwin Creek	85
Figure 35. Locations of all rain gages at the Goodwin Creek	86
Figure 36. Delineated Channel Network and Reach IDs at Goodwin Creek	87
Figure 37. Storm intensity time series and locations of 16 rain gages for the event of Oct. 17, 1981 at Goodwin Creek	88

Figure 38. 30-meter Raster Mesh Used for CASC2D .....	91
Figure 39. Active 30-Meter Raster Mesh Used for SRH-W.....	91
Figure 40. Mixed Element Unstructured Mesh Used for SRH-W .....	92
Figure 41. Zoomed-In View of the Unstructured Mesh Near Exit .....	92
Figure 42. Comparison of Hydrographs: Raster Mesh (GTAR-W is the former name of SRH-W) .....	95
Figure 43. Comparison of Hydrographs: Unstructured Mesh with 0.035 Channel Manning Coefficient (GTAR-W is the former name of SRH-W) .....	96
Figure 44. Comparison of Hydrographs: Unstructured Mesh with Increased Channel Length (GTAR-W is the former name of SRH-W) .....	97
Figure 45. Comparison of Hydrographs: Unstructured Mesh with 0.06 Channel Manning Coefficient (GTAR-W is the former name of SRH-W) .....	98
Figure 46. Rainfall Intensity Spatial Distribution at Different Times .....	99
Figure 47. Simulated Water Depth Distribution over Watershed at Different Times.....	100
Figure 48. Plainview and bed elevation contours of the simulated area for the Savage Rapids Dam removal project.....	101
Figure 49. A Perspective View of the Topography of the Modeled River Reach. .....	102
Figure 50. Comparison of Predicted and Measured Water Surface Elevations..	103
Figure 51. Velocity Measurement Points for the Simulated River Reach (Points are Shown in Red).....	104
Figure 52. Comparison of Predicted and Measured Velocity Vectors at Cross Sections 1 to 4.....	105
Figure 53. Comparison of Predicted and Measured Velocity Vectors at Cross Sections 5 to 8.....	105
Figure 54. Comparison of Velocity Vectors and Flow Patterns downstream of the Dam.....	106
Figure 55. Aerial photo of the study area at the Sandy River Delta .....	107
Figure 56. Solution domain for the Sandy River Delta simulation. West (left) side of the Columbia River is the exit boundary, east (right) side is the inlet	

boundary, and south (bottom) side is the inlet boundary of the Sandy River .....	108
Figure 57. Mesh for the Sandy River Delta project: entire solution domain. ....	108
Figure 58. Mesh for the Sandy River Delta project: the Sandy River Delta area	109
Figure 59. Mesh for the Sandy River Delta project: Dam area. ....	109
Figure 60. Contour plot of the bed elevation for the Sandy River Delta project	110
Figure 61. 3D perspective view of the topography for the solution domain. ....	110
Figure 62. Roughness zones used for the Sandy River Delta Project.....	111
Figure 63. Comparison of simulated and field-measured water surface elevations along the Sandy River reach for October 12, 2005 flow conditions (GTAR- W is the former name of SRH-W) .....	113
Figure 64. Comparison of simulated and field-measured water surface elevations along the Columbia River reach for October 12, 2005 flow conditions (GTAR-W is the former name of SRH-W).....	114
Figure 65. Comparison of simulated and field-measured velocity magnitudes along the Sandy River reach for October 12, 2005 flow conditions (GTAR- W is the former name of SRH-W) .....	115
Figure 66. Comparison of simulated and field-measured velocity magnitudes along the Columbia River reach for October 12, 2005 flow conditions (GTAR-W is the former name of SRH-W).....	116
Figure 67. Seven regions (blue boxes) used for velocity vector comparison; Red points are the locations where velocity measurements were made.....	116
Figure 68. Comparison of velocity vectors in Region 1 (GTAR-W is the former name of SRH-W) .....	117
Figure 69. Comparison of velocity vectors in Region 2 (GTAR-W is the former name of SRH-W) .....	117
Figure 70. Comparison of velocity vectors in Region 3 (GTAR-W is the former name of SRH-W) .....	118
Figure 71. Comparison of velocity vectors in Region 4: Left is upstream and right is downstream portion of the region (GTAR-W is the former name of SRH- W) .....	118



Figure 72. Comparison of velocity vectors in Region 5: Left is upstream and right is downstream portion of the region (GTAR-W is the former name of SRH-W) .....	119
Figure 73. Comparison of velocity vectors in Region 6: Left is upstream and right is downstream portion of the region. (GTAR-W is the former name of SRH-W) .....	120
Figure 74. Comparison of velocity vectors in Region 7 (GTAR-W is the former name of SRH-W) .....	120



# **ABSTRACT**

SRH-W, Sedimentation and River Hydraulics - Watershed, is a two-dimensional (2D) hydraulic model for river systems and watersheds under development at the Bureau of Reclamation. SRH-W was originally developed for Reclamation internal use for various projects. Now SRH-W version 1.1 is released for public use as it is deemed to benefit the public. This report serves as both the theory and user's manuals for SRH-W v1.1, a version released for hydraulic flow simulation in rivers and runoff from watersheds, but without the sediment capability. The manual provides an overall introduction to SRH-W v1.1, its capability, and its potential applications. Mathematical formulation, numerical methods and algorithms, and physical process models are presented. Sample calibration and verification cases are discussed; and a number of practical project applications are included. The manual also provides guides to train a user to solve river hydraulic flows and watershed runoff using SRH-W v1.1. This manual is sufficient for a user to learn how to apply the model to projects.

SRH-W v1.1 solves the 2D dynamic wave equations (the standard depth-averaged St. Venant equations) that are mainly used for river simulation. In addition, the diffusive wave solver is also offered for watershed runoff simulation though it may also be used for river simulation. SRH-W v1.1 is comparable to many existing models such as RMA-2 (US Army Corps of Engineers 1996) and MIKE21 (DHI software 1996) in its river simulation capability. For watershed applications, SRH-W v1.1 is a distributed model for event based runoff simulation and has capabilities similar to CASC2D (Julien et al. 1995).

Chapters 1, 2 and 3 are the recommended materials to read if one is a new user of SRH-W v1.1. The rest of the chapters are for references only.



# CHAPTER 1

## INTRODUCTION

This documentation serves as the theory and user's manuals for SRH-W version 1.1, a version released for simulation of hydraulic flows in rivers and water runoff from watershed, without the erosion and sediment transport modules. The manual provides an overall introduction to SRH-W v1.1, its capabilities, and its potential applications. Details on the mathematical formulation, numerical methods and algorithms, and physical process models are presented. Sample calibration and verification cases are discussed, and a number of practical project results are included. The manual also provides guides to train a user to solve river hydraulic flows and watershed runoff problems using SRH-W v1.1. This manual is sufficient for a user to learn how to use and apply the model.

### 1.1 Background

SRH-W, Sedimentation and River Hydraulics - Watershed, is a two-dimensional (2D) hydraulic model for rivers and watersheds under development at the Bureau of Reclamation. It is primarily for internal use to solve various hydraulic problems. Once the model is deemed mature, it is released for public use. The current version, SRH-W v1.1, is the first release of the model with capabilities limited to water flow and runoff simulation. The intended application areas are: river flow simulation and/or watershed runoff simulation. Erosion and sediment modeling capabilities are under development and will be released in the future. It is noted that SRH-W has been tested more extensively and applied to more projects in river flows and less for the watershed runoff applications.

In river applications, SRH-W may be applied but not limited to:

- Flow in one or multiple river reaches including the main channel and floodplain; single or multiply connected streams and side channels may be simulated together;
- Flow in reservoirs with specified flow release;
- Flow around in-stream structures such as weirs, diversion dams, release gates, coffer dams, etc., and flow spill over banks and levees; and
- Flow over vegetated areas and interaction with main channel flows.

Some modeling and application issues were discussed by Lai (2005) and Bountry et al. (2006).

In watershed runoff applications, SRH-W is a physically based distributed model that, given a storm event, simulates water runoff from a watershed to a channel

network and then flows through the channel network. It consists of two major modules: an overland runoff model and a channel network model, with a seamless integration between the two. A thorough review of existing watershed models may be found in Yang et al. (2003) and Lai and Yang (2004). SRH-W was developed in an attempt to improve several aspects of the existing models with modeling capabilities similar to CASC2D, the CASCade of planes in Two Dimensions (Julien et al. 1995 and Johnson et al. 2000). The paper by Lai (2006) is recommended for further reference.

SRH-W was developed with a vision to provide reliable solutions with reasonable computer turnaround in its category. Solution algorithms have been developed to be robust so that SRH-W may provide solutions with little parameter turning. SRH-W was also developed with the objective that a 2D model does not have to be too complex to use. With SRH-W, a user does not have to memorize many commands as a user will be guided by an interactive user interface. Most user input errors may be automatically detected during the setup phase so errors may be removed before carrying out a final analysis.

## 1.2 Modeling Concepts and Capabilities

SRH-W adopts an approach for coupled modeling of channel, floodplain, and overland flows. Major features include the following:

**Zonal Modeling:** SRH-W divides a watershed or river reaches into modeling zones. A zone may represent a 1D river reach or a 2D feature that may be solved with suitable models. This layered hybrid approach facilitates the use of most appropriate models and solvers for each zone; it also extends the model to larger spatial and time scales. Flow routing includes diffusive wave and dynamic wave equations and the numerical solver uses the implicit scheme, in addition to various process models.

Zonal modeling, and the associated mesh cell layout, is illustrated for a watershed application in Figure 1 and river simulation in Figure 2. A watershed or a river system is partitioned into zones or polygons. A zone may represent a catchment, a river reach, or an arbitrary flow area. Typically, zones are delineated based on natural features such as the topography, land use, and soil types. Each zone may be assigned different properties such as the roughness coefficient.

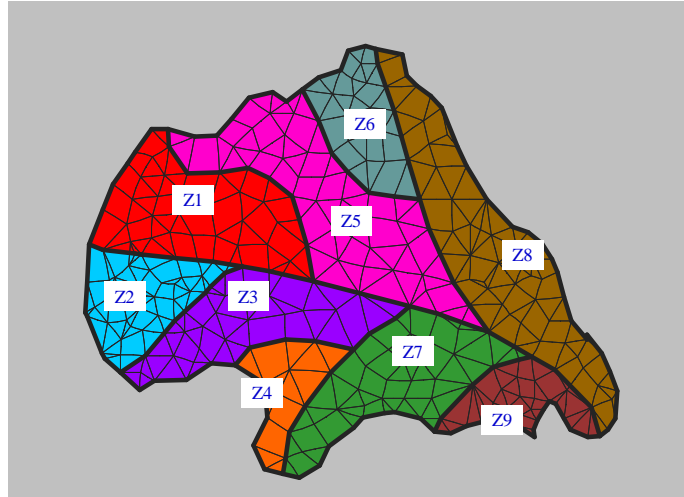


Figure 1. Conceptual illustration of zonal modeling used by SRH-W

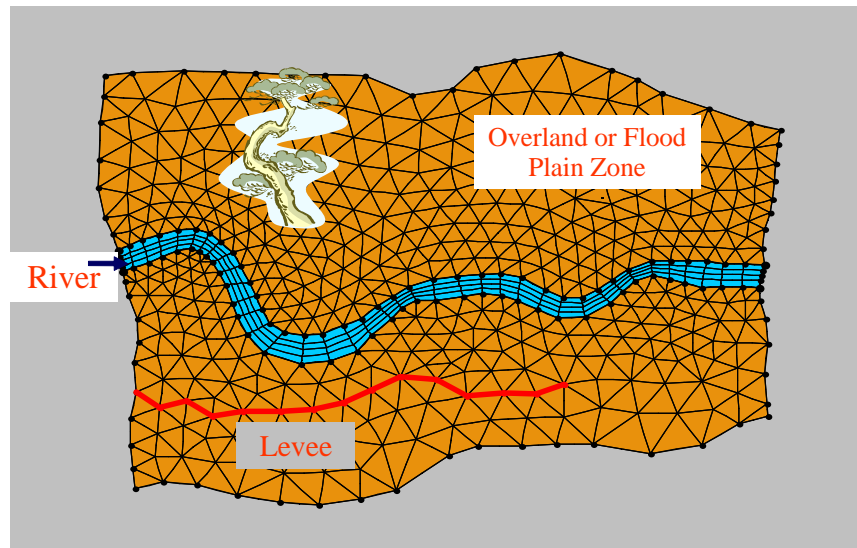


Figure 2. Illustration of zone partition and mesh layout for a typical river simulation

**Geometry Representation:** The arbitrarily shaped element method (ASEM) of Lai (1997, 2000) is adopted for geometry representation. This unstructured meshing strategy is flexible which facilitates the implementation of the zonal modeling concept and allows easy mesh representation. SRH-W essentially allows the use of most existing meshing methods available. For example, it allows a natural representation of a channel network in 1D or 2D, as well as the surrounding flood plains or overland zones. With ASEM, a tight integration between the watershed and channel system is achieved and a truly mesh-convergent solution may be obtained. Sample meshes are shown in Figure 3 and Figure 4 for illustrative purpose. More examples may be found in Chapter 9.

Major capabilities of SRH-W are listed below:

- SRH-W solves the 2D depth-averaged form of the diffusive wave or the dynamic wave equations. The dynamic wave equations are the standard St. Venant depth-averaged equations;
- Both the diffusive wave and dynamic wave solvers use the implicit scheme to achieve solution robustness and efficiency;
- Both steady or unsteady flows may be simulated;
- Unstructured or structured 2D meshes, with arbitrary element shapes, may be used with SRH-W. In most applications, a combination of quadrilateral and triangular meshes works the best. Cartesian or raster mesh is just a special mesh that may also be used by SRH-W;
- All flow regimes, i.e., subcritical, transcritical, and supercritical flows, may be simulated simultaneously without the need of a special treatment;
- Solution domain may include a combination of main channels, floodplains, and overland;
- Solved variables include water surface elevation, water depth, and depth averaged velocity. Output information includes above variables, plus flow inundation, Froude number, and bed shear stress.

SRH-W is a 2D model and it is particularly useful for problems where 2D effects are important. Examples include flows with in-stream structures, through bends, with perched rivers, and with multiple channel systems. A 2D model may also be needed if one is interested in local flow velocities, eddy patterns and flow recirculation, lateral variations, and flow spills over banks and levees.

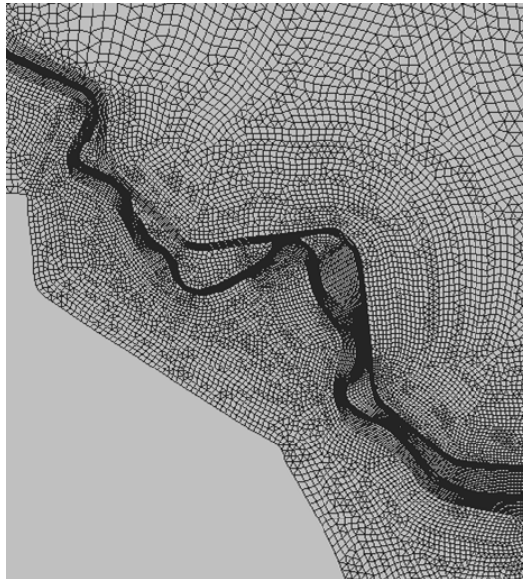


Figure 3. A sample mesh used by SRH-W; quadrilateral cells are used along the main channel and levees and mixed coarser cells are in the floodplains



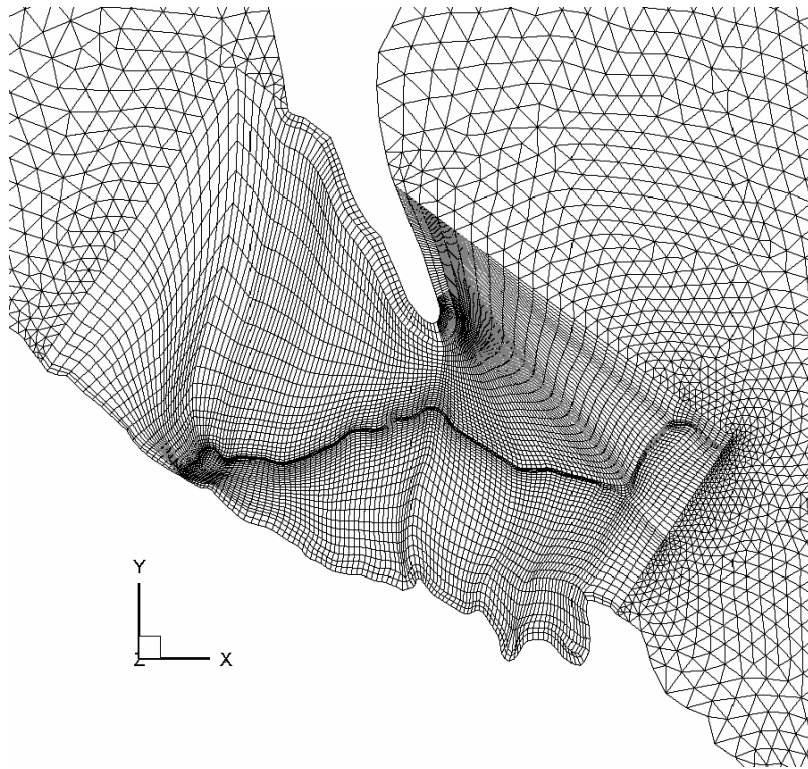


Figure 4. A sample mesh for SRH-W that uses a combination of structured and unstructured meshes

### 1.3 Limitations

SRH-W has the following limitations:

- Only flow hydraulics and water runoff are modeled. Erosion and sediment transport are not available at present;
- Only the flow routing module has been developed and released. A user will need other software packages for mesh generation and result post-processing. One of the recommended packages is SMS, the Surface Water Modeling System ([www.scientificsoftwaregroup.com](http://www.scientificsoftwaregroup.com)). ArcGIS and TECPLOT may also be used for result post-processing. Details are discussed later in this manual; and
- Only Personal Computers with Windows 2000/NT/XP operating systems are supported.

## **1.4 Acquiring SRH-W**

The latest information about SRH-W may be found on the Web by accessing <http://www.usbr.gov/pmts/sediment> and following the link on the web page.

SRH-W is currently under continuous development and improvement. Users are encouraged to check the SRH-W web page for updates.

## **1.5 Disclaimer**

SRH-W and related information in the manual are developed for use at the Bureau of Reclamation. Despite many successful applications of SRH-W to projects, Reclamation does not guarantee the performance of the program. Reclamation assumes no responsibility for the correct use of SRH-W and makes no warranties concerning the accuracy, completeness, reliability, usability, or suitability for any particular purpose of the software or the information contained in this manual. SRHW is a program that requires engineering expertise to be used and interpreted correctly. Like other computer programs, SRHW is potentially fallible. All results obtained from the use of the program should be carefully examined by an experienced engineer to determine if they are reasonable and accurate. Reclamation will not be liable for any special, collateral, incidental, or consequential damages in connection with the use of the software.

# CHAPTER 2

## GETTING STARTED

This chapter provides an overview of the SRH-W model and what a user needs to know before using SRH-W. This chapter is recommended for a new user.

### 2.1 Model Structure

Three programs are needed for a complete analysis with SRH-W: (1) a mesh generation program; (2) SRH-W package; and (3) a post-processing graphical program.

Each of the three programs is described next.

#### 2.1.1 Mesh Generation Program

Currently, SRH-W does not contain the mesh generation program. Instead, SRH-W relies on a third-party mesh generation program to provide a 2D mesh. SRH-W adopts a flexible unstructured mesh with arbitrary shapes, and therefore, most 2D mesh generation programs may be used. In general, a combination of quadrilaterals and triangles are the most common mesh type used by SRH-W, but purely quadrilateral mesh or triangular mesh, or special meshes such as the Cartesian mesh, may also be used (sample meshes are shown in Figure 3 and Figure 4).

One of the recommended mesh generation programs is SMS, the Surface Water Modeling System. SMS is a pre- and post-processor for surface water modeling and design. SMS may be purchased with a reasonably-priced license fee. The following website link provides more information for the software: [www.scientificsoftwaregroup.com](http://www.scientificsoftwaregroup.com). Note that only the Map, Mesh, and Scatter modules are needed to run SRH-W.

[APPENDIX A](#) provides an in-depth discussion on how to use SMS to prepare a 2D mesh for use by SRH-W.

In addition to the unstructured mesh, a multi-block structured mesh with quadrilateral elements in the PLOT3D format may also be used for problems with less complex geometry. Many mesh generation packages provide the option for generating such a mesh with the PLOT3D format. [APPENDIX B](#) of this manual provides a description of the PLOT3D format. Note that, with PLOT3D format, the mesh does not provide the boundary patch and type information; they are set up using commands in the SRH-W preprocessor, *srhpre11*, to be discussed later.

## 2.1.2 SRH-W Solver Module

SRH-W package consists of two programs: *srhpre11* and *srhw11*

*srhpre11* is a text-based interactive user interface that guides a user to set up the SRH-W simulation in an easy-to-understand manner. It may be interpreted as a preprocessor to prepare an input file to run SRH-W. The interface is designed such that a user does not need to memorize many input commands. Only occasional references to this manual may be needed. The interface has a comprehensive error checking mechanism so that errors may be detected before running SRH-W program. Note that a pre-generated 2D mesh, using, e.g. SMS, should be available before starting *srhpre11*.

*srhw11* is the main solver that reads the input data generated by *srhpre11*, carries out the simulation, and outputs the final results to data files in a format accessible to graphical post-processing packages. The output data files contain the final results and may be viewed and processed using selected graphic packages such as SMS, TECPLOT, or ArcGIS (see [APPENDIX B](#) for formats).

Among a number of output files, a restart or hot-start file - named *\_RSTn* file where *n* is an integer or may be empty - will be created whenever *srhw11* is executed. The *\_RSTn* file contains all results and may be generated periodically during the program execution. It serves several purposes:

- (1) In the event of a computer crash, the program may be continued from the previously saved restart file so that the simulation is not completely lost.
- (2) A time-consuming and computation intensive job may be run in several steps; a user has the opportunity to examine results at the end of each step to monitor the solution progress or check whether a steady-state solution has been achieved. The job may be continued to the next or final stage by restarting from the previous run using the *\_RSTn* file. For some instances, more result output variables may be added after the completion of a solution.
- (3) For more difficult simulations sensitive to initial conditions, the converged solutions (saved in the *\_RSTn* file) of another run (but with the same mesh) may be used to supply the initial conditions.
- (4) The *\_RSTn* file of a steady-state solution may also be used as the initial conditions for an unsteady simulation.

The use of the restart file is controlled by a parameter named *IREST*. This parameter may be setup with *srhpre11* or more conveniently using the SRH-W dynamic input file as explained in [APPENDIX C](#).

### 2.1.3 Post-Processing Program

SRH-W outputs intermediate and final results to output files that may be viewed and examined by post-processing graphical programs. Three formats are currently available from SRH-W: SMS, TECPLOT, and GENERIC. SMS output files may be imported into SMS or ArcGIS programs; TECPLOT format is suited for result post-processing using the TECPLOT program; and GENERIC format is for those who use post-processing programs other than SMS, ArcGIS or TECPLOT. With the GENERIC format, a user may write their own translation program to convert the GENERIC format into the format of their choice. [APPENDIX B](#) provides a detailed description of the GENERIC file format.

## 2.2 Solution Procedure

It is noted that SRH-W solves all equations in SI units (e.g., distance and mesh coordinates in meters, elevation and water depth in meters, velocity in m/s, stress in  $\text{N/m}^2$ , etc.). For input and output, however, a user has the option of using either SI Units or the English Units. The specific unit requirements are clearly indicated during the model preprocessing stage. The solution procedure consists of four steps: mesh generation, preprocessing, model execution, and result post-processing. They are described below.

### 2.2.1 Mesh Generation

The first step in using SRH-W is to prepare a 2D mesh using a mesh generation program. By default, SMS is used for the mesh generation and it is described in [APPENDIX A](#). Once a mesh is generated, it is stored to a mesh file and will be used by the SRH-W preprocessor.

A mesh may be generated using units of meters (m) or feet (ft) or with any scale (e.g., mm or mile). The mesh scale (or unit) information will be an input to SRH-W.

### 2.2.2 Preprocessor Execution

Once a mesh is ready, *srhpre11* is started on a PC by clicking the executable. A SRH-W window will pop up that allows an interactive session to begin. The window may be resized to fit the monitor size. The *srhpre11* allows a user to set up the simulation through an interactive and menu-driven session; the command is entered one-by-one as directed by the preprocessor. At the begin, a case name is needed so that all input/output files for the simulation use this case name as the identifier. In this manual, “casename” is assumed as the case name unless otherwise stated. During the interactive preprocessing, all inputs are saved to a ‘script’ file named casename\_SOF.dat (Script Output File). This file may later be used to rerun *srhpre11* by renaming casename\_SOF.dat to casename\_SIF.dat

(Script Input File). The importance of \_SIF file cannot be over-emphasized and is described below:

- A user may stop *srhpre11* at any time during the preprocessing step; *srhpre11* execution may then be continued later from the stop point of last preprocessing using the \_SIF file. It is similar to the restart or hot-start procedure of the *srhw11* and it may be necessary so that a user may take a break or need to correct input errors.
- It allows a user to keep a permanent record of the simulation once completed. With \_SIF file saved, a simulation may be repeated later if necessary to reproduce the results.
- An experienced user may create and edit the \_SIF file directly for simulation setup. This is particularly useful when only minor changes are needed for carrying out a parametric study or input errors are to be corrected. Therefore, it is recommended that the script file casename\_SOF.dat be saved to casename\_SIF.dat immediately after it becomes available, as the \_SOF file may be over-written if *srhpre11* is executed again.

The casename\_SIF.dat is an ASCII file; each line is designated as either a COMMENT line or a COMMAND line. A comment line starts with '//', similar to the C/C++ language. A user may add lines of comments to the script file to assist the interpretation of the input file. The command line is the actual input text which is read and processed by *srhpre11*. A user may first run *srhpre11* with a sample session using the on-screen interactive option, and then examine casename\_SOF.dat to see the format of the script file.

After a successful *srhpre11* session, two files are created: casename\_OUT.dat and casename.dat, in addition to the \_SOF file. The \_OUT file provides information about the preprocessing execution, while the casename.dat serves as the input file to the main solver *srhw11*.

Sample execution of SRH-W is presented in Chapter 3: Tutorial.

### 2.2.3 Main Solver Execution

Once *srhpre11* is successfully completed, a file named casename.dat is created that is the input file to *srhw11*. A user may start executing the main solver by clicking *srhw11* in a PC window. A number of windows will pop up providing model solution progress and result monitoring. More detailed discussion may be found in Chapter 3: Tutorial.

## 2.3 SRH-W Output Files

During and after the execution of SRH-W, a number of output files are generated and some are described below:

### 2.3.1 \_RES File

A file, named casename\_RES.dat, will be created by SRH-W; this is the solution residual file that records the history of the solution process. Part of the information contained in the \_RES file is also plotted on screen with a pop-up window for a graphical viewing of the solution progress. For each iterative solution, residuals of each governing equation, normalized to order one, are recorded in the \_RES file. In addition to the on-screen plot, a user may also check the \_RES file directly to monitor the solution progress. For example, it provides information on the status of solution convergence/divergence. For a steady state simulation, the solution is probably diverging if residual keeps increasing. Note that residuals for turbulence equations are difficult to define and sometimes it may not be possible for them to drop to a low level. This mostly happens at a few points but the overall solution may have already been converged.

### 2.3.2 \_OUT File

The \_OUT.dat file is an informational file, named casename\_OUT.dat, that records some essential messages about the simulation run such as the cpu time consumed, problem definition, etc.

### 2.3.3 \_RST File

The \_RST.dat file is the restart or hot-start file, named casename\_RST.dat, that may be used to continue the simulation starting from a previous execution. Details have been discussed in [Section 2.1.2](#), and it is also discussed later in the command: *INITIAL CONDITION: CONSTANT FOR ENTIRE DOMAIN*.

### 2.3.4 Result Output File

Result output files are used for graphical post-processing. Several formats may be used as discussed in [APPENDIX B](#). Depending on the format selected, casename\_SMS.dat is generated if SMS format is used, casename\_TEC.dat file is created if TECPLOT format is selected, and casename\_GNR.dat is generated if GENERIC format is chosen.





# CHAPTER 3

## TUTORIAL

This chapter provides tutorial cases so that solution processes and procedures may be reviewed for using SRH-W and inputs and outputs may be familiar to a user. The primary purpose is to train a user to use SRH-W with simple examples. The solution process for more complex problems is similar. All tutorial cases come with SRH-W distribution package and a user is encouraged to run these tutorial cases to get hands-on experience. This chapter is recommended to read for a new user.

### 3.1 A Subcritical Flow in a Channel

Test case one of MacDonald (1996), a 1D subcritical flow, is used here to serve as a tutorial case to learn how to use the dynamic wave solver. Despite its simplicity, the case covers essential procedures to run SRH-W; it also trains a user getting familiar with the model. More details of the tutorial case may be found later in Section 8.3 1D Subcritical Flow.

Step 1 of the analysis is collection of data relevant to the flow simulated. For the case, these include the solution domain (1000m-by-10m size), bed elevation (provided in analytical form by MacDonald 1996), flow discharge at the inlet boundary ( $15 \text{ m}^3/\text{s}$ ), water elevation at the exit (0.7484 m), and Manning's roughness coefficient (0.03).

Step 2 involves the generation of a mesh for the solution domain. For the case, a simple 81-by-4 uniform Cartesian mesh is generated (Figure 5) using a structured mesh generator and stored as the PLOT3D format. The mesh file, named tutorial\_c1\_PFG.dat, comes with the SRH-W distribution package and may be used for the tutorial exercise.

Step 3 is to run the preprocessor, *srhpre11*, to develop an input file for the SRH-W solver. A sample snapshot of the window's session running *srhpre11* is shown in Figure 6. The case name used in this manual is "c1" and the time step of the simulation is 5 seconds. After completion of *srhpre11*, a script file named c1\_SOF.dat is created that may be renamed as c1\_SIF.dat. The c1\_SIF.dat script file may be used to run *srhpre11* again with the "Use a Script Input File" preprocessing mode instead of the interactive mode (a user is encouraged to try this!). The c1\_SIF script file has also been included in the distribution package and is not listed here. In addition to the script file, two additional files are generated: c1.dat and c1\_OUT.dat. The c1.dat file is an ASCII input file for use by *srhw11*. A user is encouraged to examine the file but does not have to

understand it. The c1\_OUT.dat file is intended to provide information to a user about the progress and potential setup errors. However, it currently does not provide much information.

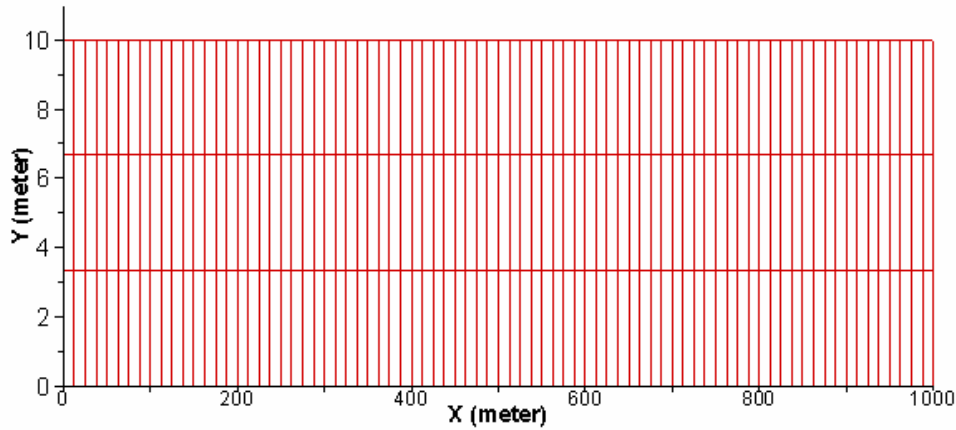


Figure 5. An 81-by-4 mesh used for simulation for test 1 of MacDonald (1996)

```

gswpre10
File Edit View State Window Help

Graphic1
the rest gives: Time(s) ~ Variable(SI-Unit)
Note that only SI unit is assumed for the variable!

==> STEADY-OR-UNSTEADY-SIMULATION
Enter: 1 --> Steady-State Simulation
      2 --> Unsteady Simulation

==> UNSTEADY-SIMULATION-PARAMETERS:
Enter: TSTART DT NTSTEP (space separated)
where:
TSTART: simulation starting time in second; 0 is used normally
DT:      time step in second
NTSTEP: total number of time steps used
NOTE: dt and ntstep may be changed during code execution through casename_DIP.dat f

==> MOLECULAR-VISCOSITY-FOR-WATER
Enter 1 or 2:
      1 --> Constant Value
      2 --> From a formula given the temperature (to be done)

==> CONSTANT-KINEMATIC-VISCOSITY
Enter kinematic viscosity in m^2/s (about 1.0e-6)

==> TURBULENCE-MODEL-SELECTION
1= Laminar Flow
2= Depth-Averaged Parabolic Model Vis=a*Vstar*h
   a=0.7 is used; use casename_DIP.dat is different a is used
3= Standard k-e model (unavailable currently)
end of file run.save reached. Start on-screen input !

==> TURBULENCE-MODEL-SELECTION
1= Laminar Flow
2= Depth-Averaged Parabolic Model Vis=a*Vstar*h
   a=0.7 is used; use casename_DIP.dat is different a is used
3= Standard k-e model (unavailable currently)

Running Input pending in Graphic1

```

Figure 6. A sample window session running *srhpre11* for the tutorial case 1

Before executing the solver *srhw11*, a user is encouraged to create the Dynamic Input (DIP) file, c1\_DIP.dat, as described in [Appendix C](#). The DIP file used for the tutorial case is included in the distribution package and may be used for other applications.

Step 4 is to run the solver, *srhw11*, by simply clicking the executable. Upon entering the case name (c1 for the tutorial case), a window will pop up and several sub-windows will be displayed so that the solution process may be monitored. Figure 7 shows these windows for the tutorial case. One window is the master window (called Graphic1) that displays the total cpu time for the simulation. The “Residual Monitoring” window may be used to check the solution process, e.g., the number of time steps that has been solved. It also provides residual reduction of the solver (residual may be interpreted as relative error of two velocity equations). In general, the residual should keep decreasing but it will stall at a constant value or will fluctuate around a value attributable to a number of causes. For the tutorial case, for example, the residual stalled due to the near zero lateral velocity component of the lateral velocity equation. The individual residual of u- and v-equations may be found in the output file: c1\_RES.dat. Note that the residual may not be a good indicator if a steady state solution has been achieved. A third window, Water Surface Elevation at Monitoring Point 1, displays the calculated water surface elevation at the user-specified monitoring point 1 if such a point is supplied. Note that only the water elevation at the monitoring point number 1 is displayed even if multiple points are supplied. This graph may provide a better indicator if steady state solution has been achieved. A good monitoring point is where the flow is hard to reach. Results at multiple monitoring points are stored in the output file: c1\_PT1.dat, c1\_PT2.dat, etc.

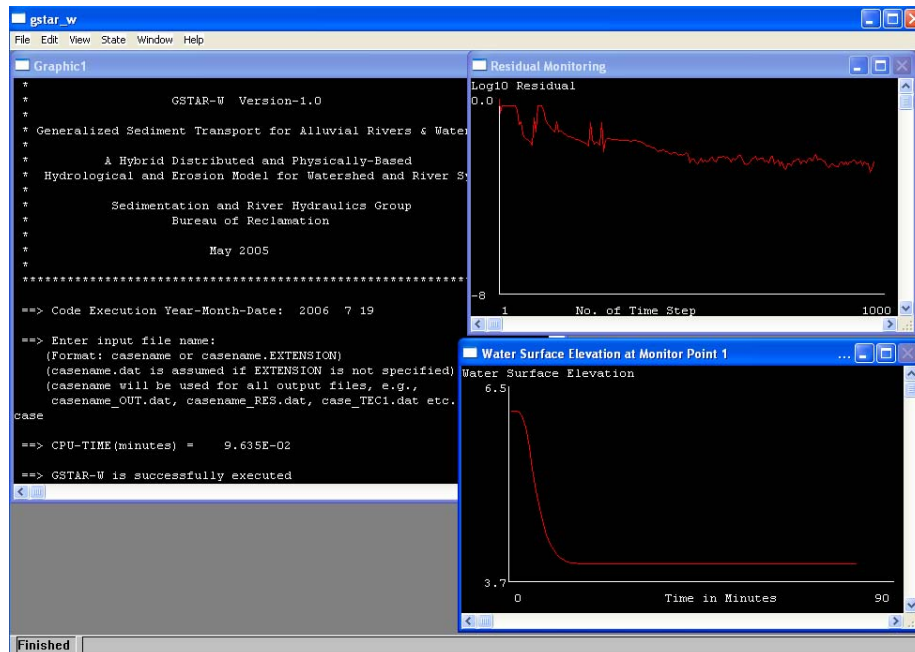


Figure 7. A sample window session running *srhw11* for the tutorial case 1

The final step is to post process the results. A number of output files are generated after completion of *srhw11* execution. They are discussed below for the tutorial case:

**c1\_DIA.dat:** This is the DIAGnostic file with potential errors and warnings about the execution. It helps to identify causes of execution error or failure. For the tutorial case, the file is almost empty indicating a successful run of the model.

**c1\_OUT.dat:** This is the OUTput file providing general model information such as input parameters, mesh size, list of restart file numbers and their corresponding time, cpu time of the simulation, ect.

**c1\_PT1.dat:** It provides time history of output variables at the user-specified monitoring point. The file is in column format and may be imported into Excel for plotting. Output from the file may be used to decide if a steady state solution has been obtained or to examine unsteady change of a variable.

**c1\_RES.dat:** It contains residuals of continuity and two velocity equations during the solution. Note that residuals are normalized. For example, the ResH is normalized by the maximum of the first three iterations. Therefore, residual of 1.0 is obtained for ResH if NITER is less than 4 in the c1\_DIP.dat file.

**c1\_RST1.dat:** This is the restart file in an unformatted binary form and its intended use has been discussed in CHAPTER 2.

**c1\_TEC1.dat:** It is the result output file with TECPLOT format (see [APPENDIX B](#) for more discussion on data format). The output file contains all output variables at the user-specified time and over all mesh points. It may be imported into the corresponding graphical software (TECPLOT for the tutorial case) for viewing and processing of the simulation results.

In general, only the result output file (e.g., c1\_TEC1.dat) is important. The restart file is also important if a user intends to continue the simulation from the point of last simulation. A simple way of restarting the run, say up to 1000 time steps, consists of three steps: (1) set IREST=1 and NTSTEP=1000 in the c1\_DIP.dat file; (2) rename c1\_RST1.dat to c1\_RST.dat; and (3) click the *srhw11*.

For the tutorial case, simulated water surface elevation and water depth are processed using TECPLOT and results are compared with the analytical solution of MacDonald (1996) in Figure 21 and Figure 22.

## 3.2 Water Runoff from a 2D Surface

A 2D surface runoff case is used next to serve as a tutorial case to learn how to use the diffusive wave solver to solve a watershed runoff problem. Details of this tutorial case may be found in Section 8.2 2D Surface Runoff.

Step 1 of the analysis is collection of data relevant to the case simulated, which includes the solution domain and bed elevation, rainfall duration (1.5 hr) and rainfall intensity (10.8 mm/hr), channel link information and associated nodes and nodal properties, Manning's roughness coefficient on the overland (0.015) and in the channel (0.15). Details of the tutorial case may be found in Section 8.2 2D Surface Runoff and the input file `c2_SIF.dat` may also be used to learn the exact inputs used for the simulation.

Step 2 involves the generation of a mesh for the solution domain. For the tutorial case, an unstructured mesh with 698 elements (cells) was used as shown in Figure 17. The mesh was generated with SMS software and stored as TABS format (not the GENERIC format!). Note that TABS format is not described by this manual but available from SMS, which may also be used by SRH-W v1. TABS format produces two files: a mesh file named `tutorial_c2.geo` and a boundary condition file named `tutorial_c2.bc`. Both files come with the SRH-W distribution package so that a user may use them directly.

Step 3 is to run the preprocessor, *srhpre11*, to develop an input file for SRH-W v1 solver. A sample snapshot of the window's session running *srhpre11* is shown in Figure 8. The case name used in this manual is "c2" and the time step used is one second. After completion of *srhpre11*, a script file named `c2_SOF.dat` is created that was renamed as `c2_SIF.dat`. The script file may be used to run *srhpre11* again with the "Use a Script Input File" preprocessing mode instead of the interactive mode. The script file has been included in the distribution package and is not listed here. In addition to the script file, two additional files are generated: `c2.dat` and `c2_OUT.dat`. The `c2.dat` file is an ASCII input file for use by *srhw11*. The `c2_OUT.dat` file provides information about the progress and potential setup errors. However, it currently does not provide much information.

Before executing the solver *srhw11*, users are encouraged to create the Dynamic Input (DIP) file, `c2_DIP.dat`, as described in [Appendix C](#). The DIP file used for the tutorial case is included in the distribution package and may be used for other applications.

Step 4 is to run the solver, *srhw11*, by simply clicking the executable. Upon entering the case name (c2 for the tutorial), a window will pop up and several sub-windows will be displayed so that the solution process may be monitored. Figure 9 shows these windows for the tutorial case. One window is the master window (called Graphic1) that displays the total cpu time for the simulation. The "Residual Monitoring" window may be used to check the solution process, e.g.,

the number of time steps that has been solved. It also provides residual reduction of the solver. The residual data may be found in the output file: c2\_RES.dat. A third window, Water Surface Elevation at Monitoring Point 1, displays the calculated water surface elevation at the user-specified monitoring point 1 if such a point is supplied.

```

gswpre10
File Edit View State Window Help

Graphic1
Enter: n hydrog Q unit OR CARRIAGE-RETURN
n_hydrog: the number of points where discharge is written to _QW.dat file
Q unit: the unit used for discharge: CMS CFS or MM/HR
CARRIAGE-RETURN: This is intended for probing in 1D channel network.
CARRIAGE-RETURN will ignore this input

==> HYDROGRAPH-GAGE-INFO-FOR-GAGE: 1
Enter: Icell AREA or Xgage Ygage AREA
where:
Icell: cell ID where hydrograph is output
Xgage,Ygage: coordinates in meter of the agge point
AREA: used only if QUNIT=mm/hr, UNIT=hecare; otherwise dummy

==> HYDROGRAPH-GAGE-INFO-FOR-GAGE: 2
Enter: Icell AREA or Xgage Ygage AREA
where:
Icell: cell ID where hydrograph is output
Xgage,Ygage: coordinates in meter of the agge point
AREA: used only if QUNIT=mm/hr, UNIT=hecare; otherwise dummy

*** Information about Monitoring Points:
Number of Monitoring Points = 1
X Y ELEMENT ID for each point:
Point: 1 X Y ELEMENT_ID = 5.000E+02 7.000E+02 544

==> GSWPre is successfully executed

Finished

```

Figure 8. A sample window session running *srhpre11* for the tutorial case 2

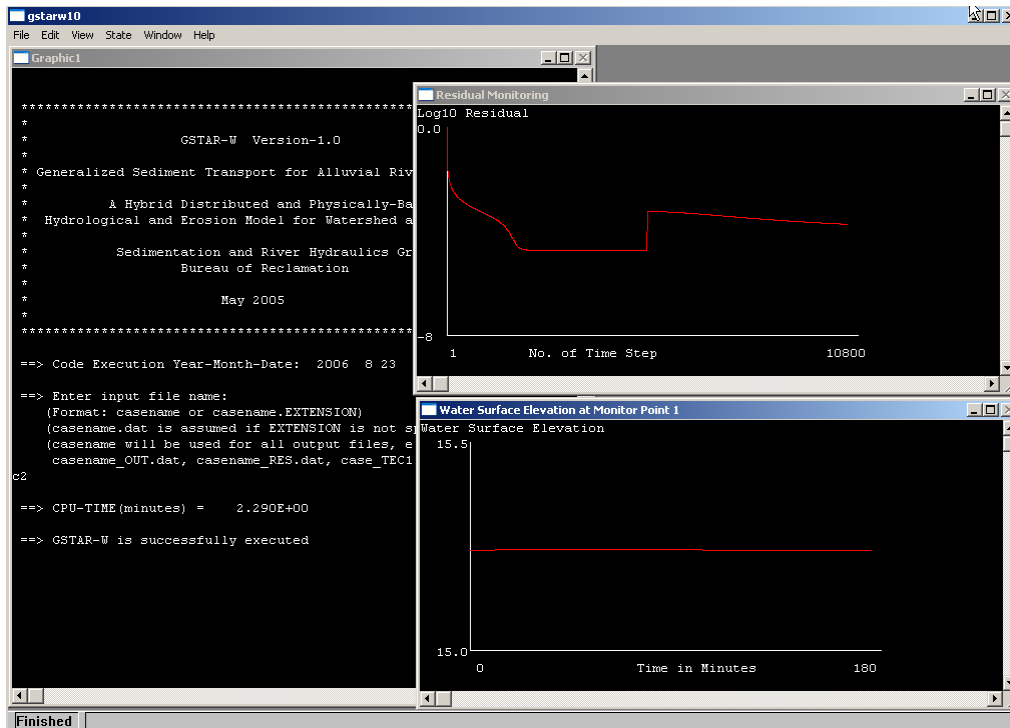


Figure 9. A sample window session running *srhw11* for the tutorial case 2

The final step is to post process the results. A number of output files are generated after completion of *srhw11* execution. They are discussed below for the tutorial case:

**c2\_DIA.dat:** This is the DIAGnostic file with potential errors and warnings about the execution. It helps to identify causes of execution error or failure.

**c2\_OUT.dat:** This is the OUTput file providing general model information such as input parameters, mesh size, list of restart file numbers and their corresponding time, cpu time of the simulation, ect.

**c2\_PT1.dat:** It provides time history of output variables at the user-specified monitoring point. The file is in column format and may be imported into Excel for plotting.

**c2\_RES.dat:** It contains residual of the diffusive wave equation during the solution.

**c2\_RST1.dat:** This is the restart file in an unformatted binary form and its intended use has been discussed in CHAPTER 2.

**c2\_TEC1.dat:** It is the result output file with TECPLOT format (see [APPENDIX B](#) for more discussion on data format). The output file contains all output

variables at the user-specified time and over all mesh points. It may be imported into the corresponding graphical software (TECPLOT for the tutorial case) for viewing and processing of the simulation results.

In general, only the result output file (e.g., c2\_TEC1.dat) is important. The restart file is also important if a user intends to continue the simulation from the point of last simulation.

For the tutorial case, simulated results were processed using TECPLOT and results are shown in Figure 18 and Figure 19.



# CHAPTER 4

## INPUT COMMANDS

This chapter lists all input commands used by *srhpre11* and serves as a complete reference of SRH-W input commands. Description of input commands is listed in the order of their appearances in *srhpre11*. Note that not all commands will appear during an actual session as only relevant commands are used. Remember that the casename\_SOF.dat file is created while running *srhpre11*. A user always has the option to terminate *srhpre11* at any time, rename the file to casename\_SIF.dat, and re-run *srhpre11* from last stop.

In the discussion below, some input parameters are mandatory while others are optional. Optional input parameters are put in brackets, e.g., [PARAM]; default values are assigned if optional parameters are not given.

### ***INPUT PREPROCESSING MODE***

Upon start of *srhpre11*, a user is prompted to select the “Input Preprocessing Mode”. Two options are available: enter integer 1 if the interactive input is used. This is a must if a user does not have the \_SIF.dat input file; enter integer 2 if a user already has the script input file named, e.g., casename\_SIF.dat. Note that *srhpre11* will always create a new script output file named, e.g., casename\_SOF.dat. It is recommended that the script output file be renamed to casename\_SIF.dat after completion of *srhpre11* so that it may be used as the script input file for future runs.

### ***CASE NAME***

One word is used to define the name of the simulation. For convenience of discussion, *CASENAME* is assumed as the case name and this convention is adopted throughout this manual. A user may use other words for the case name. Once entered, case name is used to identify all input and output files for the simulation by SRH-W v1. For example, the script input file should be named casename\_SIF.dat, the script output file is casename\_SOF.dat, the input file created by the preprocessor *srhpre11* is named casename.dat, and so forth.

### ***SIMULATION DESCRIPTION***

This provides a user the opportunity to describe the kind of simulation a user is carrying out. Description is limited to one line currently; *CARRIAGE-RETURN* may be entered if a user does not want to have any description. The description will appear in the casename\_SOF.dat file.

## ***FLOW SOLVER SELECTION***

This provides a selection of the flow solvers to be used for simulation. Two options are available: (1) Enter 2 if the implicit diffusive wave solver is selected; and (2) Enter 3 if the implicit dynamic wave solver is chosen. Note that only the diffusive wave solver should be selected if the application is for watershed runoff. The dynamic wave solver is limited to river system simulation.

## ***2D RESULT OUTPUT FORMAT AND UNIT***

This command specifies the result output file format and units for writing the 2D simulation results to output files. Three formats are currently available: SMS, TECPLOT, or GENERIC. SMS is a column-based format that may be imported into SMS or ArcGIS software for graphical viewing and processing; TECPLOT format may be imported into the TECPLOT graphical package for post-processing; and GENERIC format is the SRH-W specific format. A user may take the GENERIC file and convert it to other forms suitable to available post-processing packages. For specifics of these formats, a user is referred to [APPENDIX B](#).

Two unit systems are available to output the simulation results: (1) Enter 1 for SI unit system (e.g., meter for elevation and depth, m/s for velocity, and  $\text{N/m}^2$  for shear stress); and (2) Enter 2 for English unit system (e.g., ft, ft/s, and  $\text{lb/ft}^2$ ). The file name of the result output is dependent on the format chosen such as: casename\_SMS $n$ .dat, casename\_TEC $n$ .dat, or casename\_GNR $n$ .dat ( $n$  is a consecutive integer starting from 1).

## ***RESULT OUTPUT AT MONITORING POINTS***

This command allows a user to specify up to nine (9) monitoring points where simulated results will be recorded at each time step; that is, time series of output variables are available at monitoring points. X and Y coordinates of each point are given to define the points. Results at monitoring points may be used to check the solution convergence process. For a steady simulation, e.g., point results may be monitored to check if the solution is approaching to a steady state. For an unsteady simulation, point results may be plotted to show how variables are changing with time at the specified locations. The point files are named as casename\_PT $n$ .dat with  $n$  for the point number.

Note that the output variable list and the associated variable units at monitoring points are the same as those specified by the ***VARIABLE LIST FOR RESULT OUTPUT*** command and the ***2D RESULT OUTPUT FORMAT AND UNIT*** command. Also note that only the first monitoring point, PT1, is displayed in the monitoring window.

## ***COORDINATES OF MONITORING POINTS***

This command specifies the planview coordinates,  $X$  and  $Y$ , of all monitoring points. A total of  $2n$  real values are needed as inputs where  $n$  is the total number of monitoring points. The unit of  $(X,Y)$  should be the same as that of the mesh. If  $(X,Y)$  point is outside the solution domain, the preprocessor will issue a warning message and this point is ignored. It is recommended that the mesh generation program, such as SMS, be used to determine the coordinates of the monitoring points.

## ***VARIABLE LIST FOR RESULT OUTPUT***

This command allows a user to select a list of dependent or derived variables that may be the result output variables. Selected variables will appear in the 2D result output file in one of the three formats: SMS, TECPLOT, or GENERIC (casename\_SMS $n$ .dat, casename\_TEC $n$ .dat, or casename\_GNR $n$ .dat). They are also included in the monitoring point files, casename\_PT $n$ .dat.

Among all output variables, three variables are always included:  $X$   $Y$   $Z\_BED$

Additional variables that may be selected include the following:

***WSE WD U V VMAG FR SS RI TID***

where

<b><i>X Y:</i></b>	horizontal (planview) coordinates of a mesh point
<b><i>Z\_BED:</i></b>	bed elevation of a mesh point
<b><i>WSE WD:</i></b>	water surface elevation and water depth
<b><i>U V:</i></b>	depth averaged velocity components in $X$ and $Y$ directions, respectively
<b><i>VMAG FR:</i></b>	Velocity magnitude and Froude number
<b><i>SS:</i></b>	bed shear stress, as calculated in Equation (4)
<b><i>RI TID:</i></b>	Rainfall Intensity in mm/hr and total infiltration depth in mm

Note that ***RI*** and ***TID*** are for watershed applications only and their units are fixed.

## ***RESULT OUTPUT THROUGH MONITORING POLYLINES***

This command allows a user to specify up to nine (9) monitoring polylines through which flow discharges may be recorded at each time step. Flow discharge through each polyline may be used as a monitor to check the solution convergence process. The output file name will be casename\_LN $n$ .dat with  $n$  for the polyline ID.

The unit of the output discharge at the monitoring polylines is the same as that specified by the **2D RESULT OUTPUT FORMAT AND UNIT** command described above. That is, it is m<sup>3</sup>/s for SI unit and ft<sup>3</sup>/s for English unit.

### **INFO-OF-MESH-POINTS-ON-POLYLINES**

A monitoring polyline is defined with a list of nodal points of the mesh. This command specifies the number of nodal points and the list of nodal IDs of each polyline. It is required that two consecutive nodal points on the polyline should form a face of the mesh. A node is designated by its nodal ID that should be available from the mesh generation program, e.g., SMS. A wrong specification of the nodal points will lead to an error message; but the error will only be reported at the end of the *srhpre11* execution.

### **TIME-VARYING-FUNCTION (TVF) DEFINITION**

This command gives a user the opportunity to define a time series data set,  $y=f(t)$ , where  $t$  is time in second and  $y$  is any variable. For example,  $y$  can be discharge at an upstream boundary or stage (water surface elevation) at a downstream boundary. **TVF** is mainly used to define a time-dependent boundary condition. Two options are available:

#### Option-1: **CARRIAGE-RETURN**

This option is chosen if no more **TVF** is to be defined and a user needs to exit this command.

#### Option-2: **ID NPOINT FILE\_NAME**

This option allows a user to define the time series dataset using a discrete set of data stored in a file. In the above,

- ID:** a positive integer number identifying the **TVF**. **ID** is referenced when it is used to define the variable. A recommended way is to start **ID** from 1.
- NPOINT:** an integer specifying the total number of data pairs, ( $t_i$ ,  $y_i$ ) in the file ( $i$  ranges from 1 to **NPOINT**).
- FILE\_NAME:** a character string specifying the file name that stores the dataset. The format of the file should be as follows:

Line: 1	comments	
Line: 2	comments	
Line: 3	comments	
Line: 4	t(1)	y(1)
Line: 5	t(2)	y(2)

...

t(NPOINT)      y(NPOINT)

The first three lines are for comments about the dataset.

A user may define as many *TVF*s as necessary for the problem.

## UNSTEADY-SIMULATION-PARAMETERS

This command appears for the unsteady flow simulation. At present, unsteady simulation is always used even for steady state simulation. It requests the following input parameters:

*TSTART DT NTSTEP*

where:

**TSTART:** a real value for the simulation starting time in second (typically 0.0 is used unless there is a good reason).

**DT:** a real value for the time step in second for the simulation.

**NTSTEP:** an integer for the total number of time steps to be simulated.

Note that both ***DT*** and ***NTSTEP*** may be dynamically changed using the special `_DIP.dat` file during the SRH-W execution. See [APPENDIX C](#) for more information.

## MOLECULAR VISCOSITY FOR WATER

This command specifies the molecular viscosity for water and is needed only for the dynamic wave solver due to modeling of the diffusion process. Two options are provided: enter the integer 1 if a constant viscosity is used. The second option is unavailable presently. The molecular viscosity is insignificant for most applications as the flow process is assumed to be turbulent and turbulent viscosity is much higher than the molecular viscosity.

### CONSTANT-KINEMATIC-VISCOSITY

This command specifies the constant kinematic viscosity. For most applications, 1.0e-6 may be the input value as solution is not sensitive to it as explained above. Note that it is not the dynamic viscosity!

## ***TURBULENCE-MODEL-SELECTION***

This command specifies whether the flow is laminar or turbulent, and specifies the turbulence model to be used if turbulent. Enter an integer 1, 2 or 3 to select the following options:

- 1 → flow is laminar
- 2 → depth-averaged parabolic turbulent model
- 3 → standard k- $\epsilon$  two-equation model (to be done)

The depth-averaged parabolic turbulence model (Rodi, 1993) calculates the turbulent viscosity with  $\nu_t = \alpha V_* h$  where  $V_*$  is the frictional velocity and  $h$  is the water depth. Coefficient  $\alpha$  ranges from 0.3 to 1.0, and a default value of 0.7 is used by SRH-W. A user has the option to use a different  $\alpha$  using the `_DIP.dat` file. In general, final results may not be sensitive to  $\alpha$  for most applications and it should be regarded only as a secondary parameter for model calibration.

Other turbulent models have been added but are unavailable at present as they are to be tested fully before release. Also, usefulness of other models, in comparison with the depth-averaged parabolic model, is yet to be understood. We do not find the turbulence model critical in most applications and it is not recommended to be a primary calibration parameter.

## ***RAINFALL DURATION***

This command appears only for the diffusive wave solver and is used for watershed applications. If there is no rainfall (storm) event, SRH-W v1 will assume a non-watershed application and watershed-specific commands such as infiltration model, 1D channel network routing, etc., will not appear.

This command specifies the duration of a storm (rainfall) event for a watershed runoff simulation. It is assumed that a watershed application always has a storm event associated with it.

Two values, ***Rain\_Start*** and ***Rain\_End***, are the inputs and they are the times of rainfall start and rainfall end (the unit is hour).

Enter a *CARRIAGE-RETURN* or make ***Rain\_Start*** > ***Rain\_End*** if there is no storm event to be simulated.

## ***RAINFALL MODEL***

This command will appear if a rainfall event is specified and it will specify the type of rainfall model to be used. Two rainfall models are available. Enter integer 1 if rainfall is a constant rate during the rainfall period (from ***Rain\_Start*** to ***Rain\_End***) and is uniformly distributed in space. Enter integer 2 if rainfall is time

varying and spatially distributed and the data are based on a number of rainfall gages. For option 2, time series rainfall data files are needed as inputs, which is described next.

### ***CONSTANT RAINFALL INTENSITY***

This command will appear if option 1 is chosen in the ***RAINFALL MODEL*** command. The constant rainfall rate in the unit of mm/hr is the input.

### ***RAINFALL INTENSITY DATA***

This command will appear only if option 2 is selected in the ***RAINFALL MODEL*** command. It specifies the number of rain gages used to model the storm event and the number of rainfall data files. Usually each rainfall time series data is stored separately in a data file so the number of rainfall gages and the number of data files are the same. However, rainfall data at all gages may also be contained in one file. Each rainfall file must use the following data format:

```
LINE 1:
LINE 2:      first three lines are comments
LINE 3:
LINE 4:      Time1 Int_1 Int_2 ... Int_n
LINE 5:      Time2 Int_1 Int_2 ... Int_n
...
```

The unit of *Time* is hour and that of intensity is mm/hr and *n* stands for the number of rain gages included in the file. Only one intensity is needed (*n*=1) if rainfall gage data is stored separately.

### ***RAIN GAGE LOCATION***

This command specifies the (X,Y) coordinates of each rain gage location. With this information, SRH-W v1 will construct a spatially distributed rainfall over the simulated watershed using the bi-linear interpolation.

### ***RAINFALL INTENSITY DATA FILE NAME***

This command specifies the file names of all rainfall intensity data as determined by the ***RAINFALL INTENSITY DATA*** command.

### ***INFILTRATION MODEL***

This command appears if rainfall is specified in the ***RAINFALL DURATION*** command and is intended for watershed applications. It specifies if infiltration is modeled and which model is used if it is. At present, only the Green-Ampt (1911) infiltration model is available.

### ***1D-CHANNEL-NETWORK-MODEL***

This command appears only if rainfall is specified in the ***RAINFALL DURATION*** command and it is intended for watershed applications. It specifies if there is a channel network overlaid onto the simulated watershed. The option without the 1D channel network suggests that the channel is simulated by 2D mesh elements.

### ***CHANNEL COUPLING METHOD***

This command appears only if 1D channel network modeling is activated for a watershed application. It is intended for selection of methods for the coupling between the 1D channel network and the 2D watershed solution domain. At present, only explicit coupling based on mesh elements is available.

### ***TIME STEP FOR CHANNEL ROUTING***

This command appears only if a 1D channel network is simulated together with the 2D watershed solution domain. It specifies the time step, *dt\_chan*, used for the 1D channel network routing.

Note that another time step, *dt*, should have been selected in the previous ***UNSTEADY SIMUALTION PARAMETERS*** command for the 2D watershed simulation. As the 2D solution is implicit and the 1D channel network is explicit,  $dt\_chan \ll dt$  is usually used. It is recommended that  $dt = n * dt\_chan$  be used with  $n \gg 1$ .

### ***INITIAL-CONDITION-SETUP-METHOD***

An initial condition is needed for all simulations. For a steady state dynamic wave simulation, an initial condition for water surface elevation is important in obtaining convergence or for reduction of computer time. This command allows a user to choose one of the several methods to set up the initial condition and they are described below:

- **Constant Value Setup:** Select 0 if constant-value setup is used. This option allows constant values used for entire solution domain or different constants for different mesh zones. Constant water surface elevation or constant water depth may be specified. This option works well only for simple flows.
- **Dry Bed Setup:** Select 1 if the entire solution domain is dry initially. Zero velocity components and zero water depth are set up everywhere. This option works for almost all cases and is recommended for most applications. A longer computing time may be needed for problems with a long river reach, multiple side channels, or small flow discharge to a steady



state solution. Option 2 or 3 may be used to reduce the computing time if necessary.

- **Automatic Wet Bed Setup:** Select 2 if the water surface elevation is distributed automatically by SRH-W. This option sets the velocity components to zero and a majority of the solution domain will be wetted. Results with just one time step simulation may be used to examine the appropriateness of the initial setup. This option works for many problems, but it may leave wet ponds in the floodplain. If this option leads to divergence, return to option 1.
- **Restart Setup:** Select 3 if the initial condition is from another SRH-W solution with the same mesh. One use is to utilize a steady-state solution as the initial condition for an unsteady simulation; another usage is to select the diffusive wave water surface elevation as the initial condition for the dynamic wave solver. Often, results at other flow discharges may also be used as initial conditions for the steady state dynamic wave solver.

### ***INITIAL CONDITION: CONSTANT FOR ENTIRE DOMAIN***

This command appears if option 0 is selected for the ***INITIAL-CONDITION-SETUP-METHOD***. Under this option, SRH-W sets up initial conditions in two steps: (1) the first step is to use constant values in the entire solution domain. This may be sufficient for many problems; and (2) the second step is to over-write the constant-value setup in Step 1 with a different set of constant values in selected sub mesh blocks. The second step is, at present, limited to the structured mesh and is not available for an unstructured mesh such as that generated by SMS. Sub-domain setup is optional and it does not have to be used.

This command sets up constant initial values for the entire solution domain. For the dynamic waver solver, three values,  $U$ ,  $V$ ,  $HH$ , are needed; but  $TK$  and  $TD$  are also used if k- $\epsilon$  turbulence model is selected.  $U$  and  $V$  are velocity components along  $X$  and  $Y$  coordinate directions, respectively. Zero values may be assigned as they are found to be less critical.  $HH$  is the water surface elevation if it is positive and water depth if negative. Therefore, caution is needed if the water surface elevation is below sea level for the application as no negative water surface elevation may be specified as an initial condition. For a steady state simulation, it is found that convergence and cpu time are sensitive to the initial condition of water surface elevation. A small water depth, e.g., 10 mm, added to every element seems to work for many cases.  $TK$  and  $TD$  are turbulence kinetic energy and dissipation rate and they are needed only if k- $\epsilon$  turbulence model is selected.

### ***INITIAL-CONDITION: SUB-MESH SPECIFICATION***

This command is to setup constant-value initial conditions for selected sub-mesh blocks and is used only for structured meshes. Note that sub-mesh values will overwrite the previous setup with the ***INITIAL-CONDITION: CONSTANT-FOR-ENTIRE-DOMAIN*** command within the sub mesh.

Enter *CARRIAGE RETURN* to skip or exit the sub-mesh setup option. Otherwise enter the following for each sub-mesh:

***Iblock I1 I2 J1 J2***

where ***Iblock*** is the mesh block ID for a multi-block structured mesh, (***I1 I2***) and (***J1 J2***) are the element (or cell) index range for the sub-mesh block in the *I* and *J* coordinate directions, respectively.

#### ***INITIAL-CONDITION: CONSTANT FOR SUBMESH***

This command specifies constant initial conditions for the selected sub-mesh, similar to the ***INITIAL-CONDITION:CONSTANT-FOR-ENTIRE-DOMAIN*** command. Following five real values may be needed:

***U V HH [TK] [TD]***

See ***INITIAL-CONDITION:CONSTANT FOR ENTIRE DOMAIN*** command for the meaning of each variable.

#### ***INITIAL-CONDITION: RESTART FILE NAME***

This command is to specify the restart file name.

#### ***MESH-SCALE***

This command provides information about the mesh scale (or unit) used for the mesh to be imported into SRH-W. A mesh may be generated using any unit system and then be converted to the SI unit (i.e., meter) by ***srhpre11***. SRH-W uses the SI unit only for simulation. A real value, ***SCALE***, is specified and the (*X,Y,Z*) coordinates in the mesh file are divided by ***SCALE*** to convert to meter. For example, if a mesh is generated with millimeters (mm), the scale should be 1000.0.

#### ***IMPORT-MESH-FILE***

This command specifies the file name and the format of the mesh for importing the mesh into SRH-W. At present, two mesh formats are used: ***PLOT3D*** and ***SMS-2DM***. Read Chapter 2 of this manual for a detailed discussion of different mesh formats.

#### ***INITIAL WATER STORAGE INPUT METHOD***

This command appears only for watershed applications. It provides an option to specify an initial water storage depth on the simulated watershed. Water storage is to represent features such as ponds and lakes in the model. At present, the option is limited as only the zero depth option is available.

#### ***NUMBER OF SOIL/BED TYPES***

This command appears only for watershed applications and it specifies the total number of soil types used to characterize the watershed. Each soil type may be assigned to a number of soil properties such as the infiltration parameters and erosion and sediment related parameters. The default value is 1.

#### ***SOIL INFILTRATION PROPERTIES***

This command appears only for watershed applications and an infiltration model is used. It specifies the infiltration model related parameters for each soil type. At present, only the Green-Ampt model is used and three parameters are needed for each soil type. They are the hydraulic conductivity, suction head, and moisture content deficit.

#### ***SOIL TYPE DISTRIBUTION INPUT METHOD***

This command appears only if more than one soil type is specified in the ***NUMBER-OF-SOIL/BED-TYPES*** command and is used to specify how the soil/bed type is spatially distributed over the simulated watershed. Two choices are currently available: enter 1 if a file is available that gives the soil type for each mesh element; enter 2 if soil type is given at selected points over the simulated watershed.

#### ***NUMBER OF LAND USE CLASSES***

This command appears only for the diffusive wave solver and it specifies the total number of land use classes used to characterize the solution domain. Each land use class may be assigned a number of land use properties such as the Manning's roughness coefficient, rainfall interception depth, and other watershed related parameters.

#### ***LAND USE PROPERTIES***

This command specifies land use properties for each land use class. Properties include the following: Manning's roughness coefficient and water interception depth. Water interception depth is a dummy for non-watershed applications.

#### ***LAND USE CLASS DISTRIBUTION INPUT METHOD***

This command appears only if more than one land use class is specified in the **NUMBER-OF-LAND-USE-CLASSES** command and is used to specify how the land use class is spatially distributed over the simulated watershed. Three choices are currently available: enter 1 if a file is available that gives the land use class for each mesh element; enter 2 if land use class is given at selected points over the simulated watershed; and enter 3 if the land use class is specified with the material types of the **SMS-2DM** mesh generated using **SMS**.

### ***MANNING’S ROUGHNESS COEFFICIENT INPUT METHOD***

This command appears only for the dynamic wave solver and it decides the input method to be used to specify the distribution of Manning’s roughness coefficient over the solution domain. Two options are available: (1) enter 1 if a constant Manning’s coefficient is used over the entire solution domain; and (2) enter 3 if different Manning’s coefficients are specified over different material types of the **SMS-2DM** mesh generated using **SMS**.

### ***CONSTANT MANNING’S COEFFICIENT***

This command appears if option 1 is selected in the **MANNING’S-ROUGHNESS-COEFFICIENT-INPUT-METHOD** command. A constant Manning’s coefficient is provided over the entire solution domain.

### ***NUMBER OF MATERIAL TYPES USED***

This command appears only if option 3 is used in the **MANNING-ROUGHNESS-COEFFICIENT-INPUT-METHOD** command. The total number of material types is provided to specify the Manning’s coefficient.

### ***MANNING COEFFICIENT FOR MATERIAL TYPE***

This command appears only if option 3 is used in the **MANNING-ROUGHNESS-COEFFICIENT-INPUT-METHOD** command. It specifies the Manning’s roughness coefficient for each material type in the **NUMBER-OF-MATERIAL-TYPE** command.

### ***SPECIAL PROPERTIES WITHIN MESH ZONES***

This command is used if some special treatments are to be done over selected mesh blocks. Special applications are described in detail in [APPENDIX D](#). At present, the following special treatments are available:

- **Porous-Media-Model:** this option is to simulate the influence of porous media to the water flow. Porous media may be used to represent a number of features such as vegetation area, fish screens, etc (to be completed).

- **Cut-Away-Meshes:** this option is to cut away selected mesh cells such that they do not participate flow simulation.
- **Momentumless-Water-Sources/Sinks:** this option is to add to or withdraw from the solution domain a specified amount of water. It may be used to model a small amount of water flowing through a fish screen or culverts, etc.

### ***NUMBER OF MESH ZONES WITH MOMENTUMLESS SOURCES***

This command specifies the total number of mesh zones where momentumless water addition or withdrawal is to be simulated.

### ***MASS INFO FOR EACH ZONE***

This command specifies the momentumless source/sink info at each mesh zone. Following info is needed: total number of mesh elements within the zone, volumetric water flow rate (or discharge) through the zone, and the unit of the flow discharge.

### ***BOUNDARY-SEGMENT-DEFINITION***

With SRH-W v1, solution boundaries are divided into a number of segments and each boundary segment is assigned an integer ID. When SMS is used to generate the mesh (i.e., with ***SMS-2DM*** mesh type), boundary segments are created using the ***NODESTRING*** feature of SMS and the nodestring ID is used as the boundary segment ID (refer to [APPENDIX A](#)). A number of boundary types and associated boundary conditions are used to specify the type of each segment as well as necessary boundary conditions on it.

All boundaries of the solution domain have been automatically setup as a default boundary type within SRH-W v1. The default for watershed applications is ***FIX-H***, fixed water elevation at the boundary with zero water depth. The default for non-watershed applications is ***WALL***, a solid wall with zero velocities.

The above default setting should be adequate for most boundary segments. Any segments that are different from the default type should be defined using the ***BOUNDARY SEGMENT DEFINITION*** command and the default setting is then overwritten. This command requires the following inputs (variables in parentheses are optional):

***ID B-TYPE [Q] [UNIT]***

***ID*** is the boundary segment ID that was also the nodestring ID when the mesh was created by SMS. ***[Q]*** and ***[UNIT]*** are optional inputs and used only if the boundary segment is an upstream inlet (***INLET-Q*** or ***INLET-SC***). ***[Q]*** is the flow discharge through the boundary segment and ***[UNIT]*** is the unit for ***[Q]***. ***[UNIT]*** may be ***CFS*** for cubic feet per second or ***CMS*** for cubic meter per second. There

are two options to specify  $[Q]$ : (1) a constant real value; or (2) a time varying function (*TVF*) in the form of *TVFi* (*i* is the time varying function ID as discussed in the **TIME VARYING FUNCTION DEFINITION** command).

**B-TYPE** defines the type of the boundary and one of the following selections may be made:

***INLET-Q INLET-SC EXIT-H EXIT-EX FIX-H WALL SYMM***

where:

- ***INLET-Q***: an upstream inlet boundary with a subcritical flow. A flow discharge  $[Q]$  should be specified for such a boundary;
- ***INLET-SC***: an upstream inlet boundary with a supercritical flow. Both a flow discharge  $[Q]$  and a water surface elevation are specified at the boundary. This type is limited to non-watershed applications at present. Note that  $[Q]$  should be specified for such a boundary; but the water elevation at the boundary is specified separately later.
- ***EXIT-H***: a downstream exit boundary with a subcritical flow. A water surface elevation should be specified at this boundary and it is an input as described later. This boundary type is limited to non-watershed applications.
- ***FIX-H***: a downstream exit boundary where a fixed water depth is specified. The depth is specified as described later. Note that this boundary type is limited to watershed applications only.
- ***EXIT-EX***: a downstream exit boundary with a supercritical flow. No flow or water elevation is required at this boundary.
- ***WALL***: a solid wall boundary on which velocity is zero.
- ***SYMM***: a symmetry boundary. This boundary type may also be used as a slip wall boundary.

***SPATIALLY UNIFORM BOUNDARY CONDITIONS***

This command specifies spatially uniform (or constant) boundary values for selected boundary segments. Normally, only the water surface elevation or water depth may be specified on boundaries such as ***EXIT-H***, ***FIX-H*** and ***INLET-SC***. At present, SRH-W v1 does not allow spatially distributed (non-uniform) specification of water elevation or water depth. Uniform conditions work fine as far as the boundary is far away from the interested flow area.

It is recommended that a water surface elevation (or a water depth) be specified at ***INLET-Q*** boundary for a diffusive wave simulation for solution start-up stability. The elevation supplied is used only as an initial condition and should not influence or change the final solution.

Only the boundary segment ID is the input with this command, and a number of input selections will then appear depending on the type of the boundary segment selected as described below.

### ***SPATIALLY UNIFORM BC VALUES***

This command specifies spatially uniform boundary values at selected boundary segments.

Water surface elevation (*WSE*) is the most important variable to be specified at inlets and exits. For ***EXIT-H***, ***FIX-H***, and ***INLET-SC***, *WSE* should be provided and at present only a constant value may be specified with the units of meters always. At an ***INLET-Q*** boundary, flow discharge has already been specified with the ***BOUNDARY SEGMENT DEFINITION*** command. However, a user may also have the option to specify *WSE* at an ***INLET-Q*** boundary. If specified, *WSE* will be used as the initial condition which may help speeding up the convergence for a steady state simulation but does not change the final steady state solution.

If  $k$ - $\varepsilon$  turbulence model is used,  $k$  and  $\varepsilon$  values are also needed as boundary conditions at all inlets though they are less important. A user may use this command to specify constant  $k$  and  $\varepsilon$  values at inlets; or default values will be assigned by SRH-W if not specified (see 6.2 Inlet Boundary for details).

For other boundary segment types, no boundary conditions are needed.

### ***TIME INTERVAL FOR INTERMEDIATE RESULT OUTPUT***

This command is to specify the time interval, ***INTERVAL***, for intermediate result output. For every ***INTERVAL*** time, two files will be created by ***srhw11***: the restart file (casename\_RST*n*.dat) and the graphical result file (e.g., casename\_SMS*n*.dat or casename\_TEC*n*.dat (*n* is the integer indicating *n*-th output). If ***INTERVAL***<0, no intermediate output will be made and only the final results will be the output.

Intermediate output is recommended as it saves a copy of the restart file (\_RST*n*.dat file) so that simulation may be continued from a saved restart file in case of computer crash. In addition, it offers a user an opportunity to examine and view the results to monitor the solution progress.

Note that parameter ***INTERVAL*** also may be setup and changed dynamically using the \_DIP.dat file discussed in [APPENDIX C](#).

### ***NUMBER OF HYDROGRAPH GAGE POINTS***

This command appears only for watershed applications with a rainfall event. It specifies the number of gage points on the channel network where hydrographs may be the output.



# CHAPTER 5

## GOVERNING EQUATIONS

This chapter presents all governing equations used by SRH-W. It provides theoretical information and is intended for reference only.

### 5.1 Flow Equations

Most open channel and watershed overland flows are relatively shallow and the effect of vertical motions is negligible. As a result, the most general flow equations, the three-dimensional Navier-Stokes equations, may be vertically averaged to obtain a set of depth-averaged two-dimensional equations, leading to the following well known 2D St. Venant equations:

$$\frac{\partial h}{\partial t} + \frac{\partial hU}{\partial x} + \frac{\partial hV}{\partial y} = e \quad (1)$$

$$\frac{\partial hU}{\partial t} + \frac{\partial hUU}{\partial x} + \frac{\partial hVU}{\partial y} = \frac{\partial hT_{xx}}{\partial x} + \frac{\partial hT_{xy}}{\partial y} - gh \frac{\partial z}{\partial x} - \frac{\tau_{bx}}{\rho} \quad (2)$$

$$\frac{\partial hV}{\partial t} + \frac{\partial hUV}{\partial x} + \frac{\partial hVV}{\partial y} = \frac{\partial hT_{xy}}{\partial x} + \frac{\partial hT_{yy}}{\partial y} - gh \frac{\partial z}{\partial y} - \frac{\tau_{by}}{\rho} \quad (3)$$

In the above,  $x$  and  $y$  are horizontal Cartesian coordinates,  $t$  is time,  $h$  is water depth,  $U$  and  $V$  are depth-averaged velocity components in  $x$  and  $y$  directions, respectively,  $e$  is excess rainfall rate,  $g$  is gravitational acceleration,  $T_{xx}$ ,  $T_{xy}$ , and  $T_{yy}$  are depth-averaged turbulent stresses,  $z = z_b + h$  is the water surface elevation,  $z_b$  is the bed elevation,  $\rho$  is the water density,  $\tau_{bx}, \tau_{by}$  are the bed shear stresses (friction) that may be obtained using the Manning's resistance equation:

$$(\tau_{bx}, \tau_{by}) = \rho U_*^2 \frac{(U, V)}{\sqrt{U^2 + V^2}} = \rho C_f \sqrt{U^2 + V^2} (U, V); C_f = \frac{gn^2}{h^{1/3}} \quad (4)$$

where  $n$  is Manning's roughness coefficient and  $U_*$  is bed frictional velocity. Turbulence stresses are from the Boussinesq's assumption as:

$$T_{xx} = 2(\nu + \nu_t) \frac{\partial U}{\partial x} - \frac{2}{3} k$$

$$T_{xy} = (\nu + \nu_t) \left( \frac{\partial U}{\partial y} + \frac{\partial V}{\partial x} \right) \quad (5)$$

$$T_{yy} = 2(\nu + \nu_t) \frac{\partial V}{\partial y} - \frac{2}{3} k$$

where  $\nu$  is kinematic viscosity of water;  $\nu_t$  is turbulent eddy viscosity; and  $k$  is turbulent kinetic energy.

A turbulence model is needed in order to obtain the turbulent eddy viscosity. Two turbulence models may be used (Rodi 1993): the depth-averaged parabolic model (a zero-equation model) and the two-equation  $k-\varepsilon$  model. With the parabolic model,  $\nu_t = C_t U_* h$  with  $U_*$  the frictional velocity defined in Equation (4). The model constant  $C_t$  ranges from 0.3 to 1.0. At present,  $C_t = 0.7$  is the default value used by SRH-W v1; but its value may be changed using the \_DIP.dat file described in [APPENDIX C](#). Note that terms with  $k$  are dropped in Equation (5).

If the standard two-equation  $k-\varepsilon$  model is used (under development but not yet available), turbulent viscosity is calculated with  $\nu_t = C_\mu k^2 / \varepsilon$ . Two additional equations are solved as follows:

$$\frac{\partial hk}{\partial t} + \frac{\partial hUk}{\partial x} + \frac{\partial hVk}{\partial y} = \frac{\partial}{\partial x} \left( \frac{h\nu_t}{\sigma_k} \frac{\partial k}{\partial x} \right) + \frac{\partial}{\partial y} \left( \frac{h\nu_t}{\sigma_k} \frac{\partial k}{\partial y} \right) + P_h + P_{kb} - h\varepsilon \quad (6)$$

$$\frac{\partial h\varepsilon}{\partial t} + \frac{\partial hU\varepsilon}{\partial x} + \frac{\partial hV\varepsilon}{\partial y} = \frac{\partial}{\partial x} \left( \frac{h\nu_t}{\sigma_\varepsilon} \frac{\partial \varepsilon}{\partial x} \right) + \frac{\partial}{\partial y} \left( \frac{h\nu_t}{\sigma_\varepsilon} \frac{\partial \varepsilon}{\partial y} \right) + C_{\varepsilon 1} \frac{\varepsilon}{k} P_h + P_{\varepsilon b} - C_{\varepsilon 2} h \frac{\varepsilon^2}{k} \quad (7)$$

The follow definitions and coefficients are used (Rodi 1993):

$$P_h = h\nu_t \left[ 2 \left( \frac{\partial U}{\partial x} \right)^2 + 2 \left( \frac{\partial V}{\partial y} \right)^2 + \left( \frac{\partial U}{\partial y} + \frac{\partial V}{\partial x} \right)^2 \right] \quad (8)$$

$$P_{kb} = C_f^{-1/2} U_*^3; \quad P_{\varepsilon b} = C_{\varepsilon \Gamma} C_{\varepsilon 2} C_\mu^{1/2} C_f^{-3/4} U_*^4 / h \quad (9)$$

$$C_\mu = 0.09, C_{\varepsilon 1} = 1.44, C_{\varepsilon 2} = 1.92, \sigma_k = 1, \sigma_\varepsilon = 1.3, C_{\varepsilon \Gamma} = 1.8 \sim 3.6 \quad (10)$$

The terms  $P_{kb}$  and  $P_{\varepsilon b}$  are added to account for the generation of turbulent energy and dissipation due to bed friction in case of uniform flows.

Some discussion of the Manning's roughness coefficient is in order. With SRH-W, the Manning's coefficient is a local constant that does not change with flow; but it may be spatially distributed depending on bed types. In addition to the Manning's coefficient, another representation of flow roughness is also convenient with the equivalent roughness height  $k_s$  of the bed. For a loose bed, the equivalent roughness height and Manning's coefficient should include both effects of the bed material grain size and bed form. These two parameters may be converted from each other using the Strickler's formula:

$$n = \frac{k_s^{1/6}}{A} \quad (11)$$

where  $A$  is in the neighborhood of 26 depending on sediment size, bed form, vegetation, and channel morphology. For flat beds,  $k_s$  may take  $2d_{90}$ , based on the diameter of the bed material. A somewhat higher value, e.g.,  $3d_{90}$ , was used by van Rijn (1987). For sand-wave beds,  $k_s$  is related to the wave height.

## 5.2 Equations with Diffusive Wave Approximation

The flow equation set described above is also called the dynamic wave approximation. The dynamic wave equations are mainly used to solve hydraulic flows for river applications with SRH-W. The equation set, however, is still too complex and computation-intensive for applications with a large spatial extent. For watershed and other large scale applications, therefore, further simplification is used. Further simplification may be achieved by assuming that the convective and diffusive transports of water are in equilibrium which leads to the so-called diffusive wave equation. Or, the diffusive wave assumption leads to the following from equations (1) to (3):

$$\frac{\tau_{bx}}{\rho} = -gh \frac{\partial z}{\partial x} \quad \text{or} \quad S_{fx} = S_{ox} - \frac{\partial h}{\partial x} \quad (12)$$

$$\frac{\tau_{by}}{\rho} = -gh \frac{\partial z}{\partial y} \quad \text{or} \quad S_{fy} = S_{oy} - \frac{\partial h}{\partial y} \quad (13)$$

where  $S_{ox}, S_{oy}$  are bed slopes in the x and y direction, respectively;  $S_{fx}, S_{fy}$  are friction slopes in the x and y direction, respectively. Resistance law can be expressed as:

$$q_i = hV_i = \alpha_i h^\beta \quad (i = x \text{ or } y) \quad (14)$$

where  $\alpha_x, \alpha_y$  depend on friction slopes ( $S_{fx}, S_{fy}$ ) and  $\beta$  is usually a constant. With the Manning's roughness equation one may obtain:

$$\alpha_i = \frac{S_{fi}}{n\sqrt{S}}, S = (S_{fx}^2 + S_{fy}^2)^{1/2} \quad \text{and} \quad \beta = \frac{5}{3} \quad (i=x \text{ or } y) \quad (15)$$

where  $n$  is the Manning roughness coefficient. Note that if bed slope is used, instead of friction slope, in equation (14), the kinematic wave equation is obtained.

The final diffusive wave equation may be derived from the continuity equation in equation (1) and may be written as:

$$\frac{\partial h}{\partial t} + \frac{\partial}{\partial x}(\alpha_x h^\beta) + \frac{\partial}{\partial y}(\alpha_y h^\beta) = e \quad (16)$$

Or, it may be written in the following form:

$$\frac{\partial h}{\partial t} = \frac{\partial}{\partial x} \left( \frac{h^\beta}{n\sqrt{S}} \frac{\partial z}{\partial x} \right) + \frac{\partial}{\partial y} \left( \frac{h^\beta}{n\sqrt{S}} \frac{\partial z}{\partial y} \right) + e \quad (17)$$

## 5.3 Sub-Models for Watershed Runoff Simulation

The rainfall-runoff module, for watershed simulation, needs additional sub-models such as precipitation, rainfall interception, infiltration, channel network routing, and evaporation and transpiration. Those used in SRH-W are discussed below.

### 5.3.1 Introduction

Development of rainfall-runoff numerical models for watersheds has received much attention since the early 1970s due to the advancement of computing technologies. Earlier models used simple methods to quantify various hydrological components such as the unit hydrograph method, empirical/statistical relations, lumped method and analytical equations. As computer processor power has increased exponentially, more complex multi-dimensional models have been developed.

Rainfall-runoff models can be classified into three types: lumped, semi-lumped and distributed models.

Lumped or semi-lumped models are simpler to use and require fewer input parameters. In addition, these models need less computing time so that larger spatial scale and longer time duration problems may be simulated. Lumped and semi-lumped models often use parameterization to represent physical processes and, therefore, success of these models hinges on the applicability range of the models as well as the availability of data for model calibration. Most models are based on regression relationships between rainfall and runoff - their parameters have no physical meanings and depend on the availability of sufficiently long meteorological and hydrological records for the calibration. Such records are often unavailable. Even if historical flow data are available, they only represent past states. The calibration is often not extendable to future conditions and therefore the models are often not predictive.

Distributed models are usually based on multi-dimensional representation of a watershed. They are better suited for problems involving the prediction of future hydrologic trends produced by changes in land use or climate; for such cases no data are available for calibration. The input parameters for such models have physical meaning (e.g., soil conductivity and sediment size distribution) and may be measured in the field easily. Model validation can be done on a relatively short period of meteorological and hydrological record. Once validated, such models have great potential for prediction of future changes. Distributed models also have advantages in using the sophisticated GIS, remote sensing, and advanced visualization tools to process spatial data such as NEXRAD rainfall and AVHRR snow cover, and use of real time point measurement (such as soil moisture). As more advanced remote sensing technologies become available, distributed models will be more advantageous. The stated disadvantages of distributed models are high computational cost and high demand of distributed input data.

There is tremendous potential and utility for physically-based numerical models. Distributed multi-dimensional models have undergone extensive development ranging from the simple kinematic wave model to the full dynamic wave model, as pointed out by Woolhiser (1996). There seems to be little disagreement regarding the usefulness of physically-based models for understanding hydrologic systems. Models of this type are widely considered to hold the greatest opportunity to examine hydrologic impact of land use change and climate change (Sharika et al. 2000). Distributed hydrologic models also have immense potential and utility for forecasting the movement of pollutants and sediments (Beven 1985).

Singh (1995) compiled a number of rainfall-runoff models. These models include, but are not limited to, the Precipitation-Runoff Modeling System (PRMS) by Leavesley et al. (1983) and the Hydrological Simulation Program - FORTRAN (HSPF) by Johanson et al. (1984). These models are modular and interactive programs. Input data include meteorological, hydrologic, snow, and watershed descriptions. The outputs are runoff hydrographs, maximum discharge, flow volume, and flow duration.

Singh and Frevert (2002a, b) provided an updated listing of available hydrological models in which six distributed models were described including the Distributed Hydrology Soil vegetation Model (DHSVM), SHETRAN, CASC2D, and the Dynamic Watershed Simulation Model (DWSM).

It is recognized that solving overland flows by a fully dynamic 2D model accounting for micro-topographic characteristics is computationally very intensive. Attempts were made to adopt simplified equations. A first practical method was based on the approximate kinematic wave theory by Lighthill and Whitham (1955) and Iwagaki (1955). It was Henderson and Wooding (1964) who first applied the kinematic wave theory to simulate overland flows in which the runoff from a V-shaped catchment was considered. Later, a detailed analysis was carried out by Woolhiser and Liggett (1967) on the kinematic wave criteria. Since then, the kinematic model has been popular and received much attention. The kinematic model is still widely used (e.g., Jaber and Mohtar 2003).

In addition, the concept of kinematic cascades was introduced by Brakensiek (1967) and it was used in models such as KINEROS. This method is based on the kinematic wave theory but it overcomes geometric restrictions in modeling complete watersheds. This type of model represents the first of its kind to combine a physically-based approach with an operational method as well as offering certain flexibility to varying overland shapes.

Despite much progress, the kinematic model still has many limitations in its ability to simulate watershed rainfall-runoff processes. Some of the recent models focused on the diffusive wave approximation of overland flows. For example, di Giammarco et al. (1996), CASC2D (Julien et al. 1995; Johnson et al. 2000), and GSHSHA (Downer 2002) all solved the diffusive wave equations. Diffusive wave model is more accurate in taking the backwater effect into account while the added computational complexity and cost remain relatively low in comparison with the full dynamic model. This advantage makes the diffusive model also suitable for problems with flatter terrains.

### **5.3.2 Rainfall Component**

Rainfall intensity, duration and distribution in a watershed are important to determine the surface runoff. The precipitation information may be obtained through a number of standard means such as rain gauges and radar-rainfall data. Other existing weather generation methods may be used in conjunction with the SRH-W model such as those of EPIC (Williams et al., 1984) and SWRRB (Williams et al., 1985). The rainfall information may be specified for each watershed zone or is interpolated directly from rain gage or radar-rainfall data.

When rainfall intensity time series are available at a number of rain gages covering the watershed, an interpolation scheme is used to distribute the intensity

to all elements of the watershed. Two schemes are available: the bi-linear interpolation or the inverse distance squared method. For example, the inverse distance squared method uses the following formula for rainfall intensity redistribution:

$$I(x, y) = \frac{\sum_{i=1}^{Nr} I_i / d_i^2}{\sum_{i=1}^{Nr} 1 / d_i^2} \quad d_i^2 = (x - x_i)^2 + (y - y_i)^2 \quad (18)$$

where  $x, y$  are the Cartesian coordinates of a watershed point,  $I(x, y)$  is the rainfall intensity at  $(x, y)$ ,  $Nr$  is the total number of rain gages,  $I_i$  is the intensity at rain gage  $i$ , and  $(x_i, y_i)$  is the Cartesian coordinates of the  $i$ -th rain gage.

### 5.3.3 Interception Component

As rain falls on a watershed, a portion of it is “intercepted” by the vegetation cover and is held on the foliage by the surface tension force; the remaining rainfall goes to the ground directly. The split depends on the percentage of vegetation cover. The intercepted rainfall usually evaporates and does not fall to the ground. Thus, this portion of the rain does not take part in the runoff and should be subtracted out of the rainfall (Eagleson, 1970). This interception is also called the retention (Chow et al., 1988).

Several interception models may be used. Currently a simple approach adopted by CASC2D and KINEROS is used. An interception depth is prescribed by a user over the watershed which is one of the properties of the land use, i.e., different land use classes may be assigned different interception depths. Measured values of interception depth for a number of vegetative covers can be found in Woolhiser *et al.* (1990) and Bras (1990). During the rainfall-runoff simulation, the rainfall depth is reduced first by the amount of interception depth. Once the interception depth is satisfied, surface infiltration and runoff start.

The simple interception model should work, particularly for medium to large watersheds and for continuous simulation. For field and small watersheds with event-based simulation, dynamic models may be incorporated. One such model is used by SHESED (Bathurst et al. 1995). The accounting procedure for the rate of change of interception is calculated by:

$$\frac{\partial h_{int}}{\partial t} = p_1 p_2 (I - \alpha E_p) - k e^{b(h_{int} - S)} \quad (19)$$

where  $h_{int}$  is water depth stored on the canopy,  $t$  is time,  $p_1$  is percentage of plan view ground covered by vegetation,  $p_2$  is ratio of total leaf area to ground area

covered by vegetation ( $p_2 \leq 1$  is required),  $I$  is rainfall rate,  $E_p$  is potential evaporation rate,  $\alpha = \min(1.0, C/S)$ ,  $S$  is canopy storage capacity (the minimum depth of water required to wet all canopy surfaces),  $k$  and  $b$  are drainage parameters.

Another model was proposed by EROSEM as follows:

$$h_{int} = h_{max} (1 - e^{-R/h_{max}}) \quad (20)$$

where  $h_{max}$  is the maximum interception depth dependent on vegetation properties and  $R$  is the accumulated rainfall depth from the start of the rainfall.  $(I - h_{int})$  is the amount of rainfall reaching the ground.

### 5.3.4 Infiltration Component

Once the rainfall interception depth is satisfied, continued rainfall is available for infiltration and runoff; an infiltration model is needed. In this regard, one has to distinguish the relative strength of rainfall intensity and the potential infiltration rate. Whenever the rainfall rate exceeds the infiltration rate in the absence of a near-surface water table, runoff is due to the Hortonian mechanism (Horton 1933). Hortonian runoff is most likely to occur on watersheds where the relief is high and the water table is deep. In general, Hortonian runoff is a valid assumption in arid and semi-arid regions such as many regions of the western, mid-western and southern US when the rainfall rate exceeds 30 mm/hr (Downer et al. 2002).

The main non-Hortonian runoff mechanism is the so-called saturation excess runoff that is due to the rising water table leading to saturated surfaces (Dunne and Black 1970). This process happens in humid and sub-humid regions. Under saturation excess runoff, waters are contributed from both the rainfall and the return flow from the groundwater exfiltration. Simulation due to saturation excess runoff is much more involved as the subsurface is part of the overall simulation and it strongly depends on properties of subsurface soil hydraulic and groundwater conditions. Extra parameters, in comparison with the Hortonain runoff model, are needed. They may include soil stratigraphy, aquitard and aquiclude locations, initial water table, hydraulic conductivities, and soil-water retention curves, etc.

SRH-W v1 offers the Green-Ampt (1911) model only at present that is suitable for Hortonian runoff. Other model based on TOPMODEL approach (Beven and Kirkby 1979; Beven 1981) may be used for more general mixed-mode use but is not currently available. Both models are presented below.

The Green-Ampt model assumes that there are two zones in the subsurface: a saturated zone on the top and an initial “dry” zone (but with an initial water



content) at the bottom, separated by a sharp wetting front (Bras, 1990). The wet zone increases in length as infiltration progresses as depicted in Figure 10. Neglecting the level of ponding on the surface, the general equation of the Green-Ampt relationship is expressed as (Bras, 1990):

$$f = K_s \left( 1 + \frac{\Psi_f (\theta_s - \theta_i)}{F} \right) \quad (21)$$

where  $f$  is infiltration rate [ $m/s$ ] (or the infiltration capacity),  $K_s$  is saturated hydraulic conductivity [ $m/s$ ],  $\Psi_f$  is capillary pressure head at the wetting front [ $m$ ],  $\theta_s$  is the saturated moisture content [dimensionless],  $\theta_i$  is initial moisture content [dimensionless] present in the “dry” zone, and  $F$  is total infiltrated depth [ $m$ ].

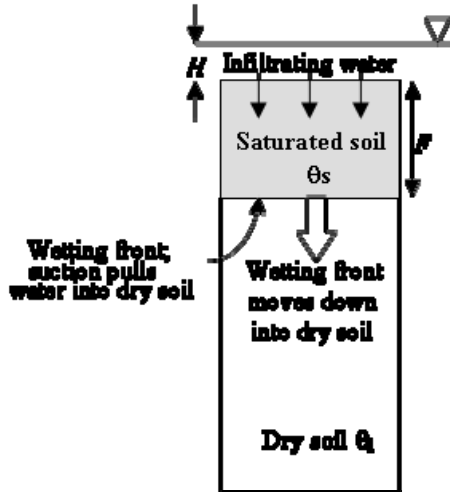


Figure 10. Illustration of the Green-Ampt infiltration model

The Green-Ampt model has been implemented in a manner as suggested by Mein and Larson (1973) and by Ogden and Saghafian (1997) in SRH-W v1. It is noted that four physical characteristic parameters are needed as inputs to the model: the hydraulic conductivity, the capillary pressure head, the saturated moisture content (from the effective soil porosity), and the initial soil moisture content. The experimental data of Rawls *et al.* (1983) may be consulted for their values for different soil textures. Chow *et al.* (1988) also listed some of the data.

TOPMODEL was proposed and developed by Beven and Kirkby (1979) and Beven (1981) and has been widely used for various water resource applications. The model may be used for mixed mode cases where saturation excess runoff plays a role. Beven (1981) examined ways to predict water table profiles and subsurface flow hydrographs. By assuming the subsurface saturated flow and

water table parallel to the ground surface in a thin soil mantle, the steady subsurface flow may be expressed in the kinematic wave form as:

$$q(\vec{r}) = K_s h_w \tan \theta \quad (22)$$

where  $q(\vec{r})$  is the saturated subsurface flow rate per unit contour length (specific discharge) at a point  $\vec{r}$  in the catchment [ $m^2/s$ ],  $K_s$  is the saturated hydraulic conductivity [ $m/s$ ],  $h_w$  is the subsurface water depth ( $L$ ) perpendicular to the slope, and  $\theta$  is the slope angle (Wu and Siddle 1995). When a lateral water flux occurs during precipitation, the soil water content increases in the down slope direction. Topographic divergence and convergence also affects the lateral movement of water and the soil water content. The  $K_s h_w$  term is called the transmissivity and its distribution with depth is assumed to be:

$$T = K_s h_w = T_0 e^{-fz} \quad (23)$$

with  $T_0$  the lateral transmissivity when the soil is just saturated [ $m^2/s$ ],  $z$  is local water table depth from ground surface [ $m$ ], and  $f$  is a scaling parameter [ $1/m$ ].

On the other hand, the specific discharge can be represented as a function of the average vertical recharge rate  $R$  [ $m/s$ ] under quasi-steady state condition. That is, the subsurface flow rate is expressed as (Barling et al. 1994):

$$q(\vec{r}) = R a_i \quad (24)$$

with  $a_i$  the upslope area draining through point  $\vec{r}$  per unit contour length. Dietrich et al. (1992) stated that, for steady state shallow subsurface flows,  $R$  can be considered as a "precipitation - evaporation - deep drainage" term.  $R$  can also be called short term precipitation.

Depth of water table can be estimated by combining equation (22) and (24) as:

$$h_w = \frac{R a_i}{K_s \sin \theta}, \text{ when } h_w = h \quad (25)$$

where  $h$  is the soil thickness perpendicular to slope. At any point where  $h_w$  exceeds  $h$ , the ground is saturated and the amount of precipitation causing runoff at that point is:

$$Q_i = R a_i - K_s h_i \sin \theta \quad (26)$$

where  $K_s h_i$  can be written as a function of transmissivity  $T_i$  [ $m^2/s$ ]. Due to differences in the specific catchment area from which the subsurface water drains,

the rainfall amount to saturate the ground would be spatially distributed in a watershed. The amount of precipitation required for ground saturation can be estimated by setting  $Q_i$  to 0 and solving for  $R_i$ , i.e.,

$$R_i = \frac{T_i \sin \theta}{a_i} \quad (27)$$

A precipitation rate greater than  $R_i$  will produce runoff at that point. Also, the local water table depth may be obtained as:

$$z = -\frac{1}{f} \ln \frac{Ra_i}{T_0 \tan \theta} \quad (28)$$

The steady state assumption implies that the specific upslope area is an appropriate surrogate for the subsurface flow rate. This is true only if recharge rate to a perched water table occurs at a constant rate for the length of time required for every point on a catchment to reach subsurface drainage equilibrium. In most cases, the velocity of subsurface flow is so small that most points on a catchment only receive contributions from a small portion of their total upslope contributing area and the subsurface flow regime is in a state of dynamic nonequilibrium (Barling et al., 1994). This concept may be important to the evaluation of the effect of seasonal precipitation on slope stability, landslide and erosion.

### 5.3.5 Diffusive Wave Channel Network Solver

SRH-W currently offers the option of the diffusive wave channel network solver. The diffusive wave channel network solver is similar to that of Julien and Saghafian (1991), and has the following assumptions and limitations:

- Diffusive wave approximation is introduced;
- Channel cross-sectional shape is limited to trapezoid or rectangular;
- Only explicit time stepping method is used; and
- The network is assumed to be dendritic with one downstream watershed outlet.

For many applications, the kinematic wave number of the channel flow is moderately high (e.g.,  $>5$ ) or the Froude number is not high (e.g.,  $<0.5$ ). For such cases, the diffusive wave channel model is an accurate representation. Even for flows with high Froude number, the diffusive wave model is still accurate if the flow is relatively uniform. For other applications, detailed channel cross-sectional data are not available and can only be estimated. Then the diffusive wave channel network model may provide a quick, yet reasonable, solution. Another advantage of the diffusive wave model is that it is applicable to both subcritical and supercritical flows.

The one dimensional channel routing equations are the standard dynamic wave model for open channels, i.e., the St. Venant equations as follows:

$$\frac{\partial A}{\partial t} + \frac{\partial Q}{\partial x} = q_l \quad (29)$$

$$\frac{\partial Q}{\partial t} + \frac{\partial}{\partial x} \left( \frac{\beta Q^2}{A} \right) = gA(S_0 - S_f - \frac{\partial h_{ch}}{\partial x}) \quad (30)$$

where  $A$  is the channel flow cross-sectional area occupied by water [ $m^2$ ],  $t$  is time [ $s$ ],  $x$  is streamwise flow axis [ $m$ ],  $Q$  is flow discharge [ $m^3/s$ ],  $q_l$  is the lateral inflow rate per unit channel length [ $m^2/s$ ],  $\beta$  is flow momentum coefficient,  $g$  is gravitational acceleration [ $m/s^2$ ],  $S_0$  is bed slope [ $m/m$ ],  $S_f$  is friction slope [ $m/m$ ], and  $h_{ch}$  is flow depth [ $m$ ].

If the two terms on the left hand side of equation (30) are negligible, i.e., the diffusive wave approximation is assumed, the following equation is derived:

$$\frac{\partial h_{ch}}{\partial x} = S_0 - S_f \quad (31)$$

By assuming the flow is completely turbulent, the Manning's equation may be used to relate the friction slope to the discharge as:

$$Q = \frac{A}{n} R^{2/3} S_f^{1/2} \quad (32)$$

where  $R$  is the hydraulic radius [ $m$ ] of the channel, and  $n$  is the Manning roughness coefficient. Because the channel cross-section shape is not allowed to change currently, the above two equations may be combined to solve the channel cross-sectional area,  $A$ , and it is the only dependent variable.

An explicit time marching scheme is used to solve equation (29) and it may be expressed as:

$$A^{k+1} = A^k - \frac{\delta t}{\delta x} \{Q_{up} - Q_{dn}\} + \delta t q_l \quad (33)$$

where  $\delta t$  is the time step used for channel time advancement that may be specified independent of the time step used for the overland,  $\delta x$  stands for the longitudinal distance between two cross sections of the channel,  $Q_{up}$  and  $Q_{dn}$  are flow discharges at the upstream and downstream cross sections, respectively.

The diffusive wave channel network solver is coupled to the overland solver through the mesh and the lateral flow flux term  $q_l$ . The lateral flux,  $q_l$ , is from the solution of overland rainfall-runoff model while the solution on overland is influenced by the channel water surface elevation. The banklines of the channel network may be aligned with the overland zonal interfaces for a tight and more flexible coupling. But the solver also offers the option to use the overland mesh cells to represent the channel network similar to the approach of CASC2D. The later approach has the limitation that the mesh cell size may not be smaller than the channel width and the solution will be dependent on the mesh size.



# CHAPTER 6

## INITIAL AND BOUNDARY CONDITIONS

SRH-W needs proper initial and boundary conditions for simulation. This chapter discusses the type of initial and boundary conditions used.

### 6.1 Initial Conditions

Initial conditions, i.e., values of velocity components ( $U$  and  $V$ ), water surface elevation ( $Z$ ), and turbulence kinetic energy and dissipation rate ( $k$  and  $\varepsilon$ ) if  $k - \varepsilon$  model is used, are needed to start the SRH-W simulation. Several ways are offered by SRH-W to set up the initial conditions.

If only steady state solutions are sought, initial water surface elevation is the only initial variable to be set up, as zero velocity components and small values of  $k$  and  $\varepsilon$  values may be automatically set up by SRH-W. Initial water surface elevation may be set up in several ways including: constant value setup, dry bed setup, distributed setup, and restart setup. Readers are referred to [Chapter 4](#) for more information for each setup method.

For unsteady simulation, restart setup is recommended. For example, the initial conditions are from a SRH-W steady state solution.

### 6.2 Inlet Boundary

An inlet boundary is defined as a boundary segment on the solution domain where flow is expected to move into the domain. Multiple inlets may be specified for a solution domain. At an inlet, velocity is specified by a user. If sediment transport is also simulated, sediment concentrations at the inlet are also needed.

At present, a total discharge,  $Q$  in  $\text{m}^3/\text{s}$ , through an inlet is specified. This discharge may be a constant value for steady state simulation or a hydrograph ( $Q$  versus time) for an unsteady simulation. SRH-W calculates a distribution of the velocity vector along the inlet in such a way that the total discharge is satisfied. Three approaches may be used for the velocity distribution at the inlet such that the total specified discharge is satisfied.

**Uniform-v Approach:** A constant velocity magnitude is imposed at the inlet with flow direction normal to the inlet boundary.

**Uniform-q Approach:** A constant unit discharge,  $q=vh$ , is assumed with flow direction normal to the inlet boundary ( $v$  is velocity magnitude and  $h$  is water depth at inlet).

**Conveyance Approach (to be completed):** A conveyance parameter is calculated first such that  $K = Q / \sum_i \frac{h_i^{5/3}}{n_i} \Delta s_i$  with  $i$  = the  $i$ -th boundary face of the inlet,  $h_i$  = the water depth,  $n_i$  = the Manning's coefficient, and  $\Delta s_i$  =  $i$ -th boundary face distance. The velocity at each face  $i$  is then calculated as  $v_i = Kh_i^{2/3} / n_i$ . The flow direction is assumed to be normal to the inlet boundary.

Currently, flow direction not normal to the inlet boundary is not available.

If flow is subcritical at an inlet, water surface elevation at the inlet is not needed and is calculated by SRH-W assuming that the water surface slope normal to the inlet is constant.

If flow is supercritical at an inlet, water surface elevation at the inlet is also needed as the boundary condition. Currently, only a constant water surface elevation may be specified.

If the  $k$ - $\varepsilon$  turbulence model is used,  $k$  and  $\varepsilon$  values are needed at an inlet. For most applications, they are not important and have negligible impact on the flow pattern (Rodi, 1980). SRH-W offers two options: (1) a user may specify constant  $k$  and  $\varepsilon$  values at an inlet with the ***SPATIALLY UNIFORM BC VALUES*** command; or (2) default values are setup by SRH-W automatically if there are no inputs. Default values are based on the relationships proposed by Rastogi and Rodi (1978) at an inlet:  $\nu_t = 0.0765 U_* h$  and  $\varepsilon = g U_* S$ , in which  $S$  is energy slope and  $U_*$  is the friction velocity. Or, the following  $k$  and  $\varepsilon$  values are specified at an inlet:  $k = 0.922 U_*^2$  and  $\varepsilon = U_*^3 / h$  with  $U_*^2 = gn^2 (U^2 + V^2) / h^{1/3}$ .

## 6.3 Exit Boundary

An exit boundary is defined as a boundary segment on the solution domain where flow is expected to move out of the domain. Multiple exits may be specified for a problem.

At an exit where the flow is expected to be subcritical, only the water surface elevation is needed as the boundary condition. No boundary conditions are needed if the flow at the exit is supercritical. SRH-W will automatically calculate the variables at the exit assuming that derivatives of variables normal to the boundary are constant.



Several ways may be used to supply the water surface elevation condition at a subcritical exit and they are discussed below.

**User-Specified Water Surface Elevation:** A user may specify the water surface elevation (stage), steady or a time series, directly at an exit. The elevation may be constant or a function of time. Often, the water surface elevation at the exit is either from measured data or from a 1D model such as HEC-RAS or SRH-1D that includes a much larger spatial area of the simulation river reach.

**Rating Curve Approach (to be completed):** A user may provide rating curve data that gives the water surface elevation at the exit as a function of the flow discharge. SRH-W will calculate the water surface elevation at the exit automatically based on the flow discharge through the exit.

**Free Surface Elevation (to be completed):** For unsteady simulation such as flood propagation, the free surface elevation condition may be used in which the water surface elevation at the exit is calculated by SRH-W using the kinematics condition, i.e.,  $\frac{\partial h}{\partial t} + \sqrt{gh} \frac{\partial h}{\partial n} = 0$  ( $n$  here refers to the unit normal at the boundary).

Exit-averaged quantities are used to obtain the average water surface elevation across the exit.

## 6.4 Solid Wall Boundary

Solid wall boundaries may represent banks and islands. No-slip condition is assumed at solid walls for the dynamic wave solver. However, a solid wall is equivalent to symmetry boundary for the diffusive wave solver. Therefore, only no-slip wall condition for the dynamic waver solver is described below.

The wall function approach is employed at a solid wall. With this approach, the flow shear stress vector at a wall boundary face is calculated as follows:

$$(\tau_{wx}, \tau_{wy}) = \rho C_\mu^{1/4} k_p^{1/2} \frac{\kappa(U, V)}{\ln(Ey_p^+)} \quad (34)$$

with  $y_p^+ = C_\mu^{1/4} k_p^{1/2} y_p / \nu$  for  $k - \varepsilon$  model; and

$$(\tau_{wx}, \tau_{wy}) = \rho U_* \frac{\kappa(U, V)}{\ln(Ey_p^+)} \quad (35)$$

with  $y_p^+ = U_* y_p / \nu$  for depth-averaged parabolic model (zero-equation model).

In the above,  $C_\mu$  is defined in equation (10),  $k_p$  is turbulent kinetic energy at cell P that contains the wall boundary face,  $\kappa = 0.41$  is the von Karman constant,  $y_p$  is normal distance from cell center P to a wall, and E is a constant.

For the  $k - \varepsilon$  model,  $P_h$  and  $\varepsilon$  at cell P are fixed and calculated as:

$$P_h = \tau_w^2 / (\kappa \mu y_p^+) \text{ and } \varepsilon = C_\mu^{3/4} k_p^{3/2} / (\kappa y_p) \quad (36)$$

At solid walls, the gradient of sediment concentration in the direction normal to a wall is set to zero.

## 6.5 Symmetry Boundary

Symmetry boundary is defined as a boundary where all dependent variables are extrapolated assuming the gradient of the variable in a direction normal to the boundary is zero except the velocity component normal to the boundary. The velocity component normal to the boundary is set to zero.

Note that the symmetry boundary acts the same as the slip wall boundary condition within SRH-W.

# CHAPTER 7

## NUMERICAL METHODS

This chapter provides the numerical methods and algorithms used to solve the governing equations in Chapter 5.

### 7.1 Diffusive Wave Solver for Flow

Equation (17) with the Manning's roughness equation may be rewritten as:

$$\frac{\partial h}{\partial t} = \frac{\partial}{\partial x} \left( \frac{h^\beta}{n\sqrt{S}} \frac{\partial z}{\partial x} \right) + \frac{\partial}{\partial y} \left( \frac{h^\beta}{n\sqrt{S}} \frac{\partial z}{\partial y} \right) + e \quad (37)$$

where  $z = z_b + h$  is the water surface elevation and  $z_b$  is the bed elevation. Numerical solution of (37) involves the use of a mesh covering the solution domain, as well as discretization of the equation on the mesh. SRH-W adopts the arbitrarily shaped element method of Lai (1997, 2000) and Lai et al. (2003a,b), and a mesh cell is a polygon with arbitrary number of sides. The cell-centered scheme is utilized versus an alternative possibility of cell-vertex scheme. This means that all dependent variables are located at the center of a cell instead of cell vertices.

Discretization of the governing equation is carried out using the finite volume approach so that conservation property of the governing equation may be preserved locally and globally. A sample polygon is shown in Figure 11 where a neighboring cell is also sketched. Integration of Eq.(37) on a polygonal cell, say polygon  $P$ , leads to the following:

$$\frac{(h^{n+1} - h^n)A}{\Delta t} = \theta \sum_{all-faces} D_f^{n+1} \frac{\partial z^{n+1}}{\partial n} \delta l + (1 - \theta) \sum_{all-faces} D_f^n \frac{\partial z^n}{\partial n} \delta l + eA \quad (38)$$

where  $\Delta t$  is time step,  $A$  is the polygonal cell area,  $\delta l$  is the cell side distance,  $\vec{n}$  is cell side unit normal vector,  $\theta$  is the time implicitness factor (0=explicit, 1=full implicit, 0.5=2<sup>nd</sup>-order Crank-Nicolson),  $D = \frac{h^\beta}{n\sqrt{S}}$ , and subscript  $f$  indicates value evaluated at cell side center.

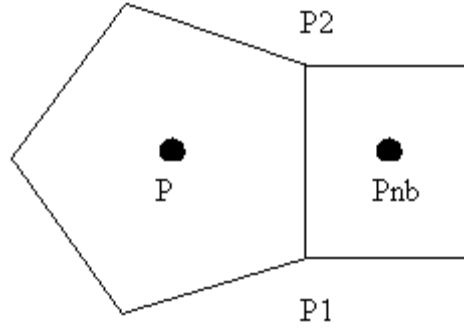


Figure 11. Schematic illustrating two neighboring cells with a common side

Further,  $\frac{\partial z}{\partial n} = \nabla z \bullet \vec{n} = \frac{z_{nb} - z}{\delta} + C$ , sum of a normal term plus a cross term ( $C$ ).

Details of the diffusive term, expressions for normal and cross terms, may be found in Lai and Yang (2004).

Equation (38) may be finalized as:

$$h^{n+1} = \left(\frac{\theta \Delta t}{A}\right) \sum_{all-faces} \left(\frac{\delta l}{n\sqrt{S}}\right)_f^{n+1} (h_f^{n+1})^\beta \left\{ \frac{z_{nb}^{n+1} - z^{n+1}}{\delta} + C_f^{n+1} \right\} + S \quad (39)$$

The source term  $S$  is treated explicitly and is written as:

$$S = h^n + \frac{(1-\theta)\Delta t}{A} \sum_{all-faces} \left(\frac{\delta l}{n\sqrt{S}}\right)_f^n (h_f^n)^\beta \left\{ \frac{z_{nb}^n - z^n}{\delta} + C_f^n \right\} + e\Delta t \quad (40)$$

Eq.(39) is a non-linear algebraic equation for water depth (or water surface elevation) at each mesh cell, and a collection of equations for all mesh cells are solved iteratively in SRH-W. The semi-Newton method is applied as described below.

The iterative solution procedure of Eq.(39) is performed as follows:

$$h^{k+1} = \sum_{all-faces} B_f^k (h_f^\beta)^{k+1} (z_{nb}^{k+1} - z^{k+1}) + b^k \text{ with } B_f^k = \frac{\theta \Delta t}{A} \bullet \left(\frac{\delta l}{n\sqrt{S}\delta}\right)_f^k \quad (41)$$

Further, equation (41) is linearized and then solved according to the following:

$$\left\{ 1 + \sum_f B_f^k \left[ (h_f^\beta)^k - (z_{nb}^k - z^k) \left( \frac{\partial h_f^\beta}{\partial z} \right)^k \right] \right\} \delta z = \sum_f B_f^k \left[ (h_f^\beta)^k + (z_{nb}^k - z^k) \left( \frac{\partial h_f^\beta}{\partial z_{nb}} \right)^k \right] \delta z_{nb} + f \quad (42)$$

where  $f = -h^k + \sum_{all-faces} B_f^k (h_f^k)^\beta (z_{nb}^k - z^k) + b^k$  that represents the residual (error) of the equation at k-th iteration,  $\delta z = z^{k+1} - z^k$  and  $\delta z_{nb} = z_{nb}^{k+1} - z_{nb}^k$  are the increments, and  $h_f^\beta$  is a function of  $z$  and  $z_{nb}$  depending on the convective scheme used.

In the above equations  $h_f^\beta$  is the value at a cell face and an interpolation scheme (a convective scheme such as the upwind scheme) is used to obtain the value. If the second order central difference scheme is applied directly, spurious oscillation may occur for flows with sufficiently high cell Peclet number. Therefore, damping is added to the second order scheme similar to the concept of artificial viscosity. The damped convective scheme is derived as follows:

$$h_f = h_f^{CN} + d (h_f^{UP} - h_f^{CN}) \quad (43)$$

with  $h_f^{UP} = \frac{1}{2} (h_1 + h_2) - \frac{1}{2} \text{sign}(V_f) (h_2 - h_1)$  and  $h_f^{CN} = \frac{\delta_1 h_2 + \delta_2 h_1}{\delta_1 + \delta_2}$  (current implementation used  $\delta_1 = \delta_2$ ).  $h_f^{CN}$  is the second-order interpolation scheme and  $d$  represents the amount of damping used ( $d=0$  means pure central scheme, 1 means pure 1<sup>st</sup>-order upwind scheme).

The above can be combined to give:

$$h_f = h_f^{UP} + (1-d) \frac{(\delta_1 - \delta_2) + \text{sign}(V_f)(\delta_1 + \delta_2)}{2(\delta_1 + \delta_2)} (h_2 - h_1) \quad (44)$$

Equation set (42) is a system of linear equations and has the property of a hyperbolic equation. It may be organized concisely as the following linear equation:

$$A_P \delta z = \sum_{nb} A_{nb} \delta z_{nb} + f \quad (45)$$

where “nb” refers to all neighbor cells that share the same sides with element P. A collection of equations (45) for all mesh cells, along with boundary conditions, form a matrix that is solved with the ILU preconditioned Conjugate Gradient

Squared (CGS) solver. The CGS solver is appropriate for both structured and unstructured meshes. Note that if derivatives of  $h$  are set to zero, equation set (42) is reduced to the type of Poisson equation with elliptic property.

In order to establish convergence criterion, the residual is computed as follows:

$$R_{\Phi} = \frac{\sum_{all\ elements} \left| A_p \delta z - \sum_{nb} A_{nb} z_{nb} + f \right|}{\sum_{all\ elements} |A_p \delta z|} \quad (46)$$

The above definition guarantees that the conservation equation is satisfied to the preset convergence criterion.

## 7.2 Dynamic Wave Solver for Flow

### 7.2.1 Discretization

The 2D depth-averaged equations in (1) to (3) may be written in tensor form as

$$\frac{\partial h}{\partial t} + \nabla \bullet (h \vec{V}) = 0 \quad (47)$$

$$\frac{\partial (h \vec{V})}{\partial t} + \nabla \bullet (h \vec{V} \vec{V}) = -gh \nabla z + \nabla \bullet \left( h \vec{\vec{T}} \right) - \frac{\vec{\tau}_b}{\rho} \quad (48)$$

where  $\vec{V}$  is the mean velocity vector,  $\vec{\vec{T}}$  is the 2<sup>nd</sup>-order tensor of turbulence stress with its component defined in equation (5),  $\vec{\tau}_b$  is the bed shear stress vector, and  $\rho$  is the fluid density. Note that rainfall is omitted as it is used only for the diffusive wave equation.

The governing equations are discretized using the finite-volume approach, following the work of Lai (1997, 2000) and Lai et al. (2003a). The solution domain is covered with an unstructured mesh with each mesh element assuming arbitrarily shaped polygons. Most commonly used polygons are triangles and quadrilaterals. All dependent variables are stored at the geometric center of a polygon. The governing equations are integrated over a polygon using the Gauss theorem. As an illustration, consider the general convection-diffusion equation representative of all governing equations:

$$\frac{\partial h \Phi}{\partial t} + \nabla \bullet (h \vec{V} \Phi) = \nabla \bullet (\Gamma \nabla \Phi) + S_{\Phi}^* \quad (49)$$

Here  $\Phi$  denotes any dependent variable, a scalar or a component of a vector,  $\Gamma$  is the diffusivity, and  $S_\phi^*$  is the source/sink term. Integration over an arbitrarily shaped polygon P shown in Figure 12 leads to:

$$\frac{(h_P^{n+1}\Phi_P^{n+1} - h_P^n\Phi_P^n)A}{\Delta t} + \sum_{all-sides} (h_C V_C |\vec{s}|)^{n+1} \Phi_C^{n+1} = \sum_{all-sides} (\Gamma_C^{n+1} \nabla \Phi^{n+1} \cdot \vec{n} |\vec{s}|) + S_\phi \quad (50)$$

In the above,  $\Delta t$  is time step,  $A$  is polygon area,  $V_C = \vec{V}_C \cdot \vec{n}$  is the velocity component normal to the polygonal side (e.g.,  $P_1P_2$  in Figure 12) and is evaluated at the side center  $C$ ,  $\vec{n}$  is polygon side unit normal vector,  $\vec{s}$  is the polygon side distance vector (e.g., from  $P_1$  to  $P_2$  in Figure 12), and  $S_\phi = S_\phi^* A$ . Subscript  $C$  indicates a value evaluated at the center of a polygon side and superscript,  $n$  or  $n+1$ , denotes the time level. In the remaining discussion, superscript  $n+1$  will be dropped for ease of notation. Note that the first-order Euler implicit time discretization is adopted. The main task of the discretization is to obtain appropriate expressions for the convective and diffusive fluxes at each polygon side.

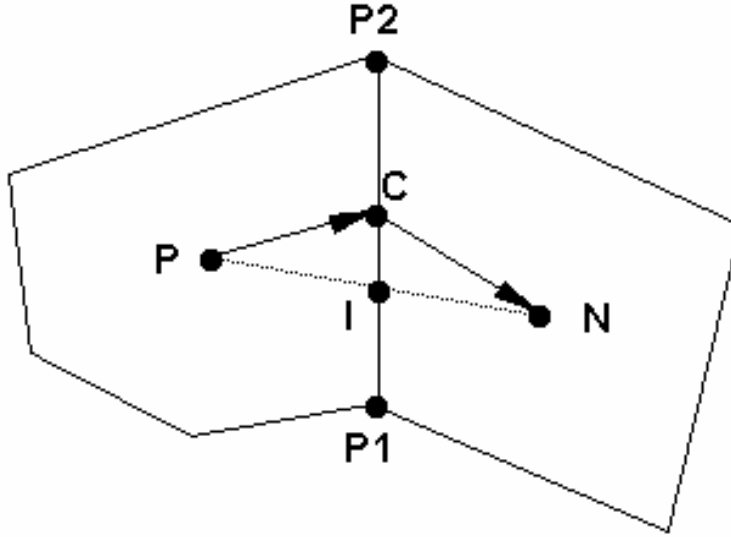


Figure 12. Schematic illustrating a polygon P along with one of its neighboring polygons N

Discretization of the diffusion term, the first term on the right hand side of equation (50), needs further attention. The final expression for  $\nabla \Phi \cdot \vec{n}$  can be written as:

$$\nabla \Phi \bullet \vec{n} |\vec{s}| = D_n (\Phi_N - \Phi_P) + D_c (\Phi_{P2} - \Phi_{P1}) \quad (51)$$

where

$$D_n = \frac{|\vec{s}|}{(\vec{r}_1 + \vec{r}_2) \bullet \vec{n}}; \quad D_c = - \frac{(\vec{r}_1 + \vec{r}_2) \bullet \vec{s} / |\vec{s}|}{(\vec{r}_1 + \vec{r}_2) \bullet \vec{n}} \quad (52)$$

In the above,  $\vec{r}_1$  is the distance vector from P to C and  $\vec{r}_2$  is from C to N. The normal and cross diffusion coefficients,  $D_n$  and  $D_c$ , at each polygon side involve only geometric variables; they are calculated only once in the beginning of the computation.

Calculation of a variable, say  $Y$ , at the center C of a polygon side is discussed next. This is an interpolation operation used frequently for a number of variables. In the next, a second-order accurate expression is derived. As shown in Figure 12, a point I is defined as the intercept point between line PN and line  $P_1P_2$ . A second-order interpolation for point I gives:

$$Y_I = \frac{\delta_1 Y_N + \delta_2 Y_P}{\delta_1 + \delta_2} \quad (53)$$

in which  $\delta_1 = \vec{r}_1 \bullet \vec{n}$  and  $\delta_2 = \vec{r}_2 \bullet \vec{n}$ .  $Y_I$  may be used to approximate the value at the side center C. This treatment, however, does not guarantee second-order accuracy unless  $\vec{r}_1$  and  $\vec{r}_2$  are parallel. A truly second-order expression is derived as:

$$Y_C = Y_I - C_{side} (Y_{P2} - Y_{P1}) \quad (54a)$$

$$C_{side} = \frac{(\delta_1 \vec{r}_2 - \delta_2 \vec{r}_1) \bullet \vec{s}}{(\delta_1 + \delta_2) |\vec{s}|^2} \quad (54b)$$

The extra term in the above is similar in form to the cross diffusion term in equation (51).

$\Phi_C$  in the convective term in equation (50) needs further discussion. If the second-order scheme is applied directly, spurious oscillations may occur for flows with a high cell Peclet number (Patankar 1980). Therefore, a damping term is added to the second-order scheme similar to the concept of artificial viscosity. The damped scheme is derived by blending the first-order upwind scheme with the second-order central difference scheme and can be expressed as

$$\Phi_C = \Phi_C^{CN} + d(\Phi_C^{UP} - \Phi_C^{CN}) \quad (55)$$

where



$$\Phi_C^{UP} = \frac{1}{2}(\Phi_P + \Phi_N) + \frac{1}{2} \text{sign}(V_C)(\Phi_P - \Phi_N) \quad (56)$$

and  $\Phi_C^{CN}$  is the second-order interpolation scheme, equation (54a). In the above expression,  $d$  defines the amount of damping used. In most applications,  $d = 0.2 \sim 0.3$  is used.

With expressions for the diffusion and convection terms, the final discretized governing equation for an element P can be organized as the following linear equation

$$A_P \Phi_P = \sum_{nb} A_{nb} \Phi_{nb} + S_{diff} + S_{conv} + S_\Phi \quad (57)$$

where “nb” refers to all neighbor polygons surrounding the polygon P. The coefficients in this equation are:

$$A_{nb} = \Gamma_C D_n + \text{Max}(0, -h_C V_C |\vec{s}|) \quad (58a)$$

$$A_P = \frac{h_P^n A}{\Delta t} + \sum_{nb} A_{nb} \quad (58b)$$

$$S_{diff} = \frac{h_P^n A}{\Delta t} + \sum_{all \ sides} \Gamma_C D_c (\Phi_{P2} - \Phi_{P1}) \quad (58c)$$

$$S_{conv} = \sum_{all \ sides} (h_C V_C |\vec{s}|) \left\{ (1-d) \left[ \frac{\delta_1}{\delta_1 + \delta_2} - \frac{1 - \text{sign}(V_C)}{2} \right] (\Phi_N - \Phi_P) \right\} \\ - \sum_{all \ sides} (h_C V_C |\vec{s}|) [(1-d) C_{side} (\Phi_{P2} - \Phi_{P1})] \quad (58d)$$

### 7.2.2 Side Normal Velocity Calculation and Elevation Correction Equation

For a non-staggered mesh, a special procedure is required to obtain the polygon side normal velocity that is used to enforce the continuity equation. Otherwise the well-known checkerboard instability may appear (Rhie and Chow 1983). Here the procedure proposed by Rhie and Chow (1983) and Peric et al. (1988) is adopted. That is, the normal velocity is obtained by averaging the momentum equation from element centers to element sides. A detailed derivation is omitted, but interested readers are referred to the previous work (e.g., Rhie and Chow 1983, Peric et al. 1988, and Lai et al. 1995). It is sufficient to express the final side normal velocity as follows:

$$V_c = \langle \vec{V} \rangle \bullet \vec{n} + \left\langle \frac{A}{A_p} \right\rangle \langle gh \nabla z \rangle \bullet \vec{n} - \left\langle \frac{A}{A_p} \right\rangle gh \nabla z \bullet \vec{n} \quad (59)$$

where “ $\langle \rangle$ ” stands for the interpolation operation from mesh element center to side as expressed in (54a). When a vector appears in the interpolation operation, the interpolation is applied to each Cartesian component of the vector.

The velocity-water surface elevation coupling is achieved using a method similar to the SIMPLEC algorithm (Patankar 1980). In essence, if the elevation from a previous time step or iteration,  $z^n$ , is known, an intermediate velocity field, may be obtained by solving the linearized momentum equation:

$$A_p \vec{V}_p^* = \sum_{nb} A_{nb} \vec{V}_N^* - a \nabla z^n + \vec{S}_v \quad (60)$$

where  $a$  is a constant. Next, we seek corrections of velocity  $\vec{V}' = \vec{V}^{n+1} - \vec{V}^*$  and elevation  $z' = z^{n+1} - z^n$  such that the momentum equation is satisfied, i.e.,

$$A_p \vec{V}_p^{n+1} = \sum_{nb} A_{nb} \vec{V}_N^{n+1} - a \nabla z^{n+1} + \vec{S}_v \quad (61)$$

Or, the following correction equation is obtained:

$$A_p \vec{V}_p' = \sum_{nb} A_{nb} \vec{V}_N' - a \nabla z' \quad (62)$$

With the SIMPLEC algorithm, the above may be approximated as

$$\vec{V}_p' = - \frac{a}{A_p - \sum_{nb} A_{nb}} \nabla z' \quad (63)$$

Substitution of the above into the continuity equation (47) leads to the following elevation correction equation:

$$\frac{z'}{\Delta t} + \nabla \cdot (\vec{V} z') = \nabla \cdot \left( \frac{ah}{A_p - \sum_{nb} A_{nb}} \nabla z' \right) - \nabla \cdot (h^n \vec{V}^*) \quad (64)$$

The above elevation correction equation may be solved to obtain  $z'$  and then (63) is used to obtain the velocity correction. A number of iterations are usually needed within each time step if the flow is unsteady; but one iteration is used for a steady state simulation.

### 7.2.3 Summary of Solution Procedure

Governing equations are solved in an equation-by-equation manner. In a typical iterative solution process, momentum equations are solved first assuming known water surface elevation and turbulent viscosity given at the previous time step. The newly obtained velocity is used to calculate the normal velocity at mesh element sides in equation (59). This side velocity will usually not satisfy the continuity equation. Therefore, the pressure correction equation (64) is solved and (63) is used to obtain a new elevation and new velocity. After the elevation correction equation, other scalar equations, such as turbulence and sediment equations, may be solved. This completes one iteration of the solution cycle. The above iterative process may be repeated within one time step until a preset residual criterion for each equation is met. Then the solution would advance to the next time step. For a steady state simulation, one iteration is usually used as time-accurate intermediate solutions are usually not sought. In this study, the residual of a governing equation is defined as the sum of absolute residuals at all mesh elements.

The implicit solver requires the solution of non-symmetric sparse matrix linear equations in (57). Direct solvers are impractical for calculations with a lot of mesh elements because of excessive demand for computer memory and CPU time. ON the other hand, the choice of iterative solvers is limited for the unstructured mesh. In SRH-W, the standard conjugate gradient solver with ILU preconditioning is used (Lai 2000).



# CHAPTER 8

## VERIFICATION CASES

This chapter focuses on verification of SRH-W, as a numerical technique or model has to be tested to lend credence to its validity and application range. A number of verification and test cases are presented, from simple cases with analytical solutions to those with experiment data, and some are compared with published numerical results of other models. The next chapter presents application and validation cases when SRH-W is applied to practical projects.

### 8.1 1D Surface Runoff

A simple one-dimensional (1D) surface runoff study was carried out by Govindaraju et al. (1988). This case was also simulated by Therrien et al. (2003) with the HYDROSPHERE model. It is chosen here to test SRH-W for two reasons: semi-analytical solutions of the diffusive wave equation, as well as previous numerical results, are available for comparison; and a wide range of conditions from subcritical to supercritical flows with a range of kinematic wave numbers are covered. Such a test helps to ensure the correct programming and implementation of the diffusive wave governing equation.

The schematic of the problem is depicted in Figure 13. The flat plate has a slope  $S_0=0.01$  and length  $L=100m$ . Two cases are simulated and their parameters are listed below:

#### Case I:

- Froude number  $F_0 = \frac{u_0}{\sqrt{gd_0}} = 0.5$
- kinematic wave number  $K = \frac{S_0 L}{d_0 F_0^2} = 10$
- Rainfall intensity  $I_0 = 4.0 \text{ mm/s}$
- Manning's Coefficient  $n = 0.0548 \text{ s/m}^{1/3}$

#### Case II:

- Froude number  $F_0 = \frac{u_0}{\sqrt{gd_0}} = 1.5$
- kinematic wave number  $K = \frac{S_0 L}{d_0 F_0^2} = 3$
- Rainfall intensity  $I_0 = 2.7 \text{ mm/s}$

- Manning's Coefficient  $n = 0.0155 \text{ s/m}^{1/3}$

In the above,  $u_0$  and  $d_0$  are the steady-state final velocity and water depth, respectively, at  $x = L$ , and  $g$  is the gravitational acceleration.

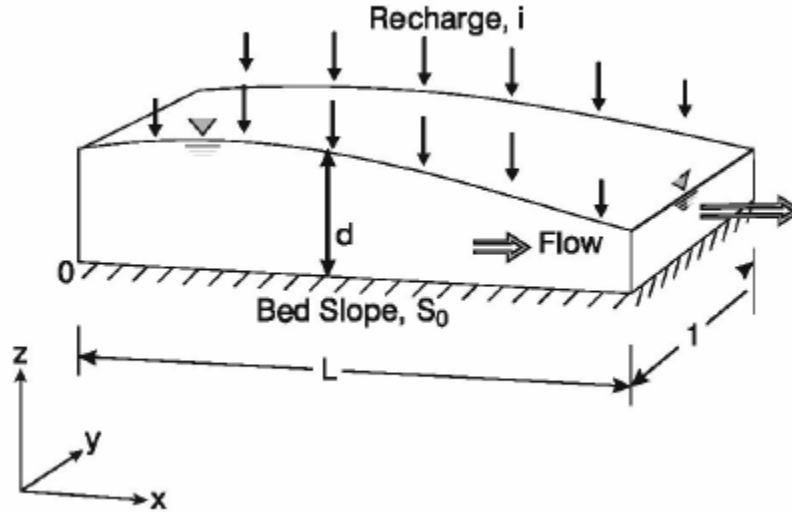


Figure 13. Schematic of the 1D Surface Runoff Case (Therrien et al., 2003)

Under constant rainfall and zero infiltration, simulation starts at  $t = 0$  with the initial condition of zero depth. A zero depth condition is maintained at  $x = 0$  (upstream) and a zero depth gradient condition is assumed at  $x = L$  end (downstream). The setting of the above conditions is the same as Govindaraju et al. (1988) and Therrien et al. (2003). The 100 meter slope is divided into 100 cells with cell size of 1m by 1m. Both explicit and implicit schemes are used for the simulation. The simulation results are discussed below in terms of comparisons with previous studies, as well as implicit versus explicit solvers.

**Comparison of Results with Semi-Analytical and Previous Solutions:** Results of two simulated cases are compared with previous semi-analytical and numerical solutions first in order to ensure that SRH-W solves the right equations. The predicted hydrograph at the downstream end of the slope is compared with previous results in Figure 14 and Figure 15 for both cases. In these figures, solutions from the kinematic wave and dynamic wave (i.e., the full St. Venant equations) are also shown. The SRH-W solution of the diffusive wave equation compares very well with the diffusive wave results of Govindaraju et al (1988) and Therrien et al. (2003), indicating the correct implementation of the governing equations. Overall, the diffusive wave equation is found to be a good approximation to the full St. Venant equations if the kinematic wave is not too small (e.g.,  $K > 5$ ), while the kinematic wave is good only if  $F_0 > 0.5$  and  $K > 15$  (based on Woolhiser and Liggett, 1967).

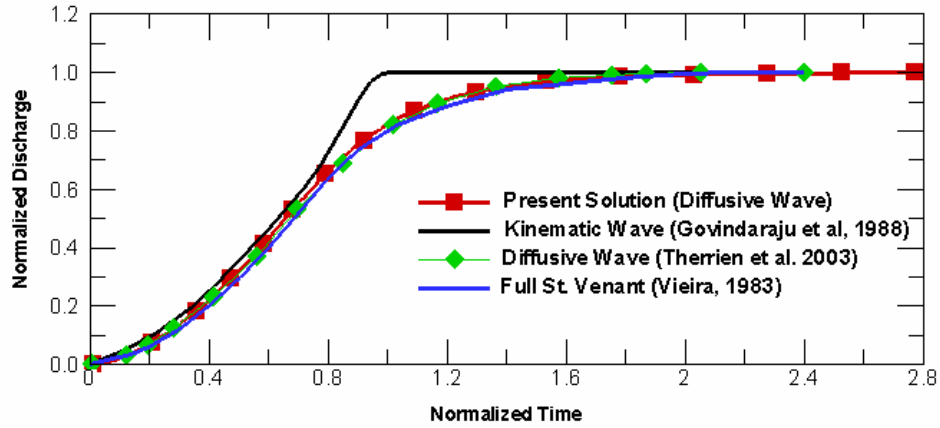


Figure 14. Comparison of Hydrographs for Case I with  $F_0 = 0.5$   $K = 10$

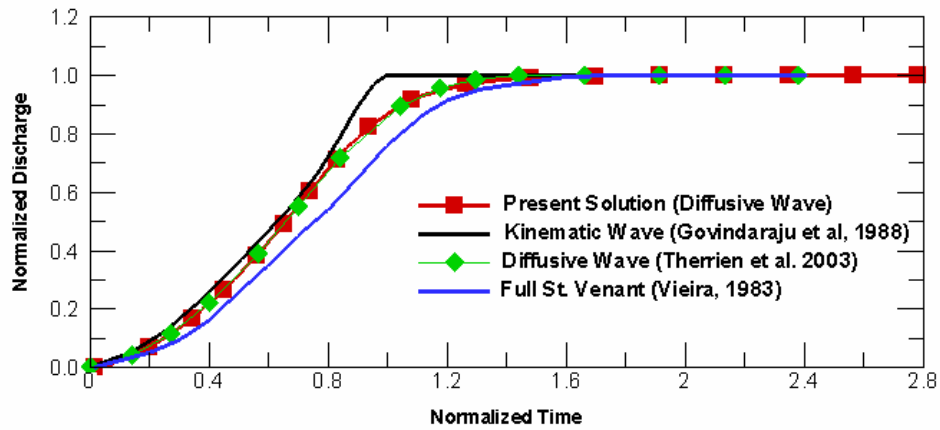


Figure 15. Comparison of Hydrographs for Case II with  $F_0 = 1.5$   $K = 3$

**Comparison of Implicit and Explicit Solvers:** SRH-W offers options of both implicit and explicit solvers. Simulations have been carried out to investigate the stability range of each solver for the two cases. For case I, it was found that the explicit scheme needs to use a time step as small as 0.01 second to obtain a stable solution. A time step of 0.015 second and above leads to divergence. With the implicit scheme, however, stable solutions may be obtained for up to a time step of 5.0 seconds. If the time step is larger than 5 seconds, the solution is not accurate anymore as solution accuracy is dependent on the appropriate time step. For case II, a stable solution may be obtained if the time step is less than 0.015

second for the explicit scheme while up to a one second time step may be used with the implicit solver.

In both cases, the results obtained from the explicit and implicit schemes are almost identical, as expected. The implicit scheme is a better choice, at least for the cases studied, as it offers not only a more robust and stable solution but also savings in computing time. Due to wider stability range of the implicit scheme, a user has much more freedom in choosing the time step for simulation.

## 8.2 2D Surface Runoff

A two-dimensional surface runoff case is simulated next which also has an approximate analytical solution and previous numerical results for comparison. This case was analyzed in detail by diGiammarco et al. (1996) and Vanderkwaak (1999), and is used to test the 2D aspect of the diffusive wave solver.

The geometry of the simulated case is displayed in Figure 16 in which a V-shaped overland is connected to a channel. Due to symmetry of the problem, only half of the domain needs to be simulated. The overland plane has a single slope of 0.05 and the channel has a single slope of 0.02 and a width of 20 m. The depth of the channel varies linearly from 1 m at the upstream end to 20 m at the downstream end. Two meshes are developed to represent the overland and the channel, one with a structured mesh while the other is an unstructured mesh, and they are shown in Figure 17. The edge of the cell size is maintained at 50 m for the structured mesh and approximately 50 m for most of the unstructured mesh cells.

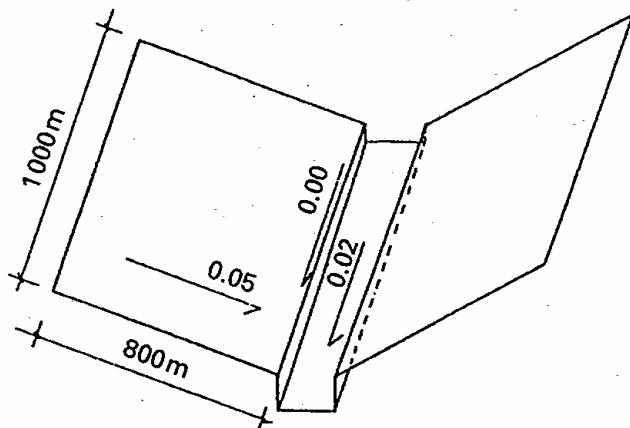


Figure 16. Geometry of the V-Shaped Catchment (diGiammarco et al., 1996)



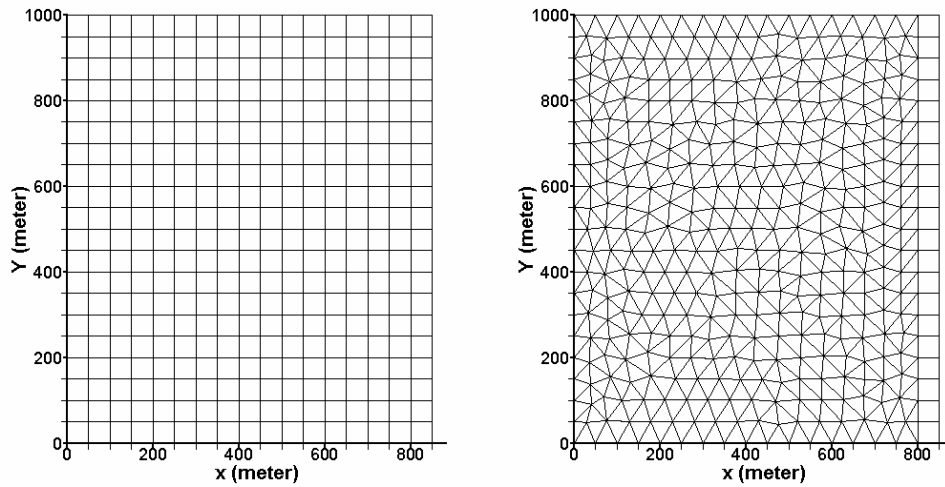


Figure 17. Structured mesh (on the left) and unstructured mesh (on the right) used for simulation of the 2D V-Catchment Case

The initial and boundary conditions are set up as follows: zero depth is assumed at the beginning of the simulation. The upstream side of the overland has a zero water depth condition and the two sides of the overland are treated as the symmetry boundary condition. At the discharge side of the overland, a zero depth gradient condition is applied as the channel depth of 1 m avoids the back water effect. At the channel exit, a zero depth gradient condition is imposed. Simulation has been carried out under a constant rainfall intensity of 10.8 mm/hr and zero infiltration with the rainfall duration of 1.5 hr. The Manning's roughness coefficient is 0.015 for the overland and 0.15 for the channel. These coefficients are not very realistic but were chosen to match the analytical solutions.

**Comparison with Previous Results:** A number of simulations have been carried out using SRH-W with structured or unstructured meshes (Figure 17), and explicit or implicit schemes. Essentially identical solutions are obtained and they are compared with previous results in Figure 18 and Figure 19. In the figures, the analytical solution is the kinematic wave solution of Overton and Brakensiek (1973) and Stephenson and Meadows (1986). diGiammarco et al. (1996) and CASC2D (Sanchez, 2002) are numerical solutions of the diffusive wave equation for the problem. diGiammarco et al. (1996) used a central difference scheme that leads to an 'overshoot' of the solution during the rising limb of the hydrograph; while CASC2D used a first-order upwind scheme that is too dissipative. Overall, it is shown that SRH-W agrees with the analytical and previous numerical results quite well, indicating that the right equation has been solved. In addition, both explicit and implicit schemes, plus both structured and unstructured meshes, produced the same solution. This proves that the discretization formulation for the arbitrarily shaped elements is consistent and has been correctly implemented.

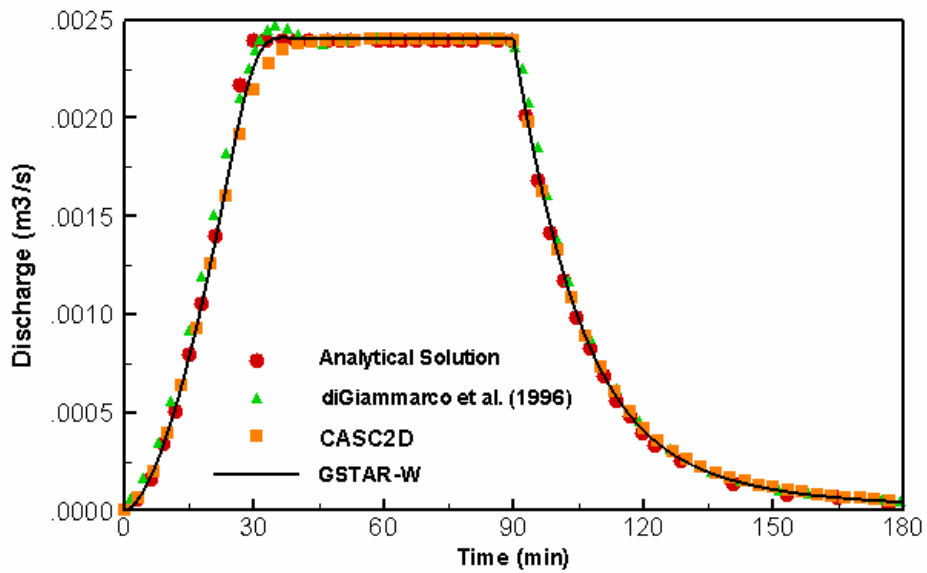


Figure 18. Comparison of Discharges at the Overland Exit into the Channel (GTAR-W is the former name of SRH-W)

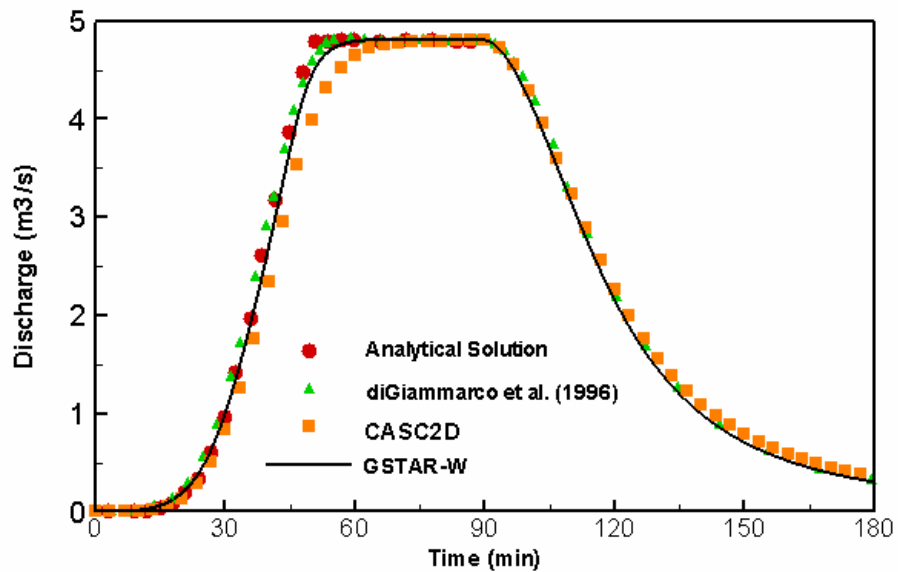


Figure 19. Comparison of Discharges at the Channel Exit (GTAR-W is the former name of SRH-W)

**Stability Range of Different Solvers:** SRH-W has both explicit and implicit solvers and their stability range can be studied further for this simple 2D case. A parametric study has been carried out which indicated that up to a 30-second time step may be used with the explicit scheme. Larger time steps lead to oscillatory

hydrographs. For the implicit scheme, a time step as large as 5 minutes may be used with the results similar to those shown in Figure 18 and Figure 19. Larger time steps do not make sense even though there is no stability problem as loss of accuracy leads to results in error.

### 8.3 1D Subcritical Flow in a Channel

MacDonald (1996) presents a number of non-trivial analytical test cases for 1D steady St. Venant equations. Test case 1 is a subcritical flow that is selected to test the dynamic wave solver of SRH-W. Case 1 has a horizontal extent of 1000m by 10m with a variable bed slope. A steady flow discharge of  $15 \text{ m}^3/\text{s}$  is maintained at the upstream boundary while a water depth of 0.7484m is maintained at the exit. The Manning's roughness coefficient used for simulation is 0.03 and the Froude number of the flow ranges from 0.40 to 0.77.

An 81-by-4 mesh is used to simulate the case as shown in Figure 20 with the boundary conditions of discharge at the inlet and water depth at the exit.

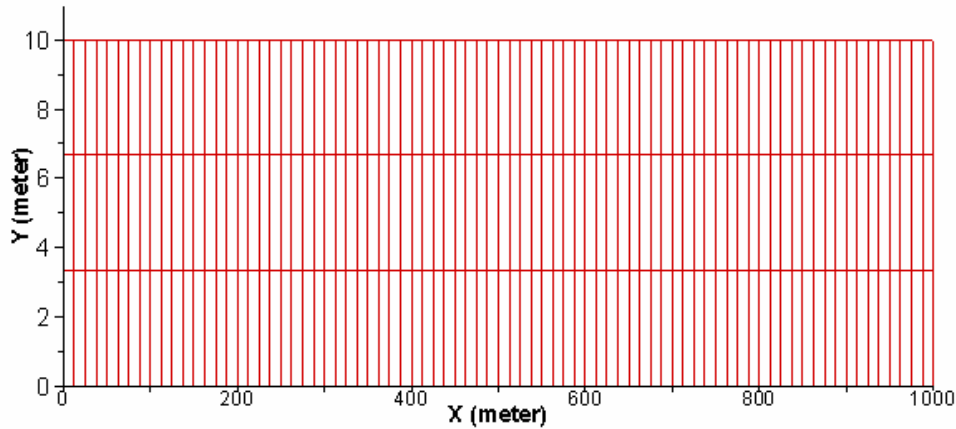


Figure 20. An 81-by-4 mesh used for simulation for test 1 of MacDonald (1996)

Simulated water surface elevation and water depth are compared with the analytical solution of MacDonald (1996) in Figure 21 and Figure 22. Also, the diffusive wave solver is used to simulate the case and results from the diffusive wave solver are also shown. It is seen that the simulated water surface elevation and water depth are almost the same as the analytical solution, while the water depth result of the diffusive wave solver produces slight errors.

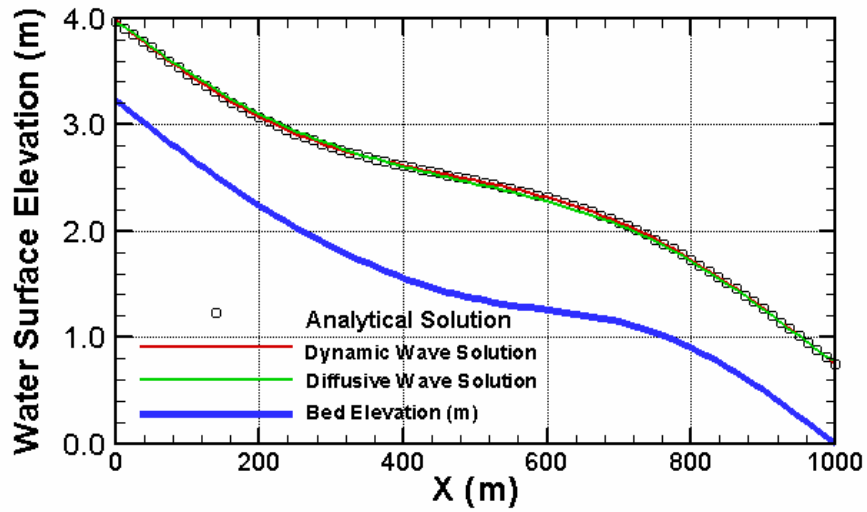


Figure 21. Comparison of simulated water surface elevation with analytical solution for test case 1 of MacDonald (1996)

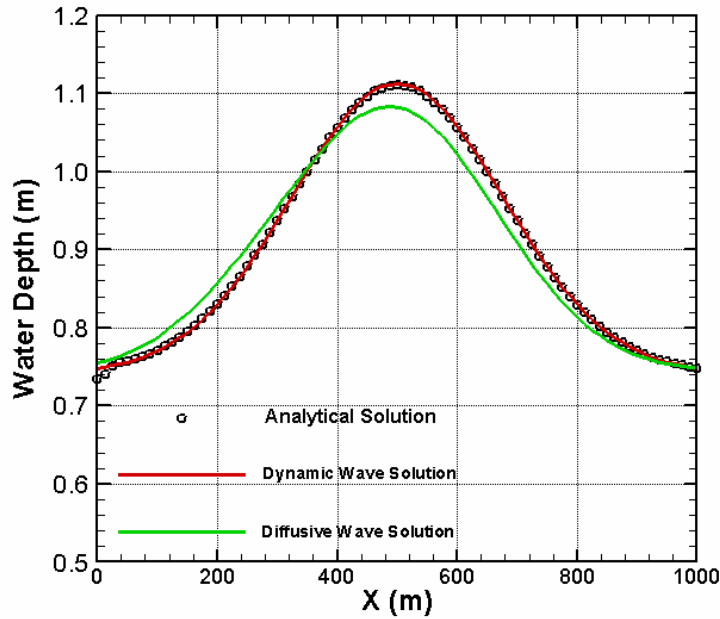


Figure 22. Comparison of simulated water depth with analytical solution for test case 1 of MacDonald (1996)

## 8.4 1D Transcritical Flow in a Channel

Test case 6 of MacDonald (1996) is a transcritical flow that has a smooth transition from subcritical to supercritical flow with a hydraulic jump. It is selected to test the dynamic wave solver of SRH-W. The test case has a horizontal extent of 150m by 10m with a variable bed slope. A steady subcritical flow

discharge of  $20 \text{ m}^3/\text{s}$  is maintained at the upstream boundary while a water depth of  $1.7\text{m}$  is maintained at the exit. The Manning's roughness coefficient is  $0.031752$ .

A  $121\text{-by-}4$  uniform Cartesian mesh is used that is similar to the 1D subcritical flow case in Figure 20. A discharge is specified at the subcritical inlet while water depth is specified at the subcritical exit.

Simulated results are plotted in Figure 23 that show the 3D view of the bed and water surface elevations with color of the water surface representing the Froude number. It is seen that the subcritical flow at the inlet quickly transitions to supercritical, and a hydraulic jump is then formed downstream. Simulated water surface elevation and water depth profiles are compared with the analytical solution of MacDonald (1996) in Figure 24 and Figure 25. Also, the diffusive wave solver is used to simulate the case and results from the diffusive wave solver are also shown. It is seen that the dynamic wave solution compares well with the analytical including capturing of the hydraulic jump. On the other hand, the diffusive wave missed the hydraulic jump completely and a smooth transition of the water surface elevation is simulated. This indicates that the diffusive wave solver is inappropriate for modeling hydraulic jumps. However, the simulated results of the diffusive wave solver is checked against the analytical solution of the diffusive wave equation. It is shown that a comparison between the model and the analytical results are quite good.

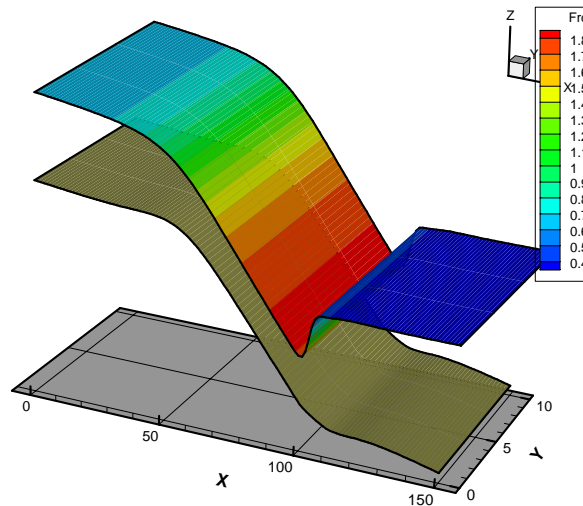


Figure 23. 3D view of bed elevation and simulated water surface elevation for test case 6 of MacDonald (1996)

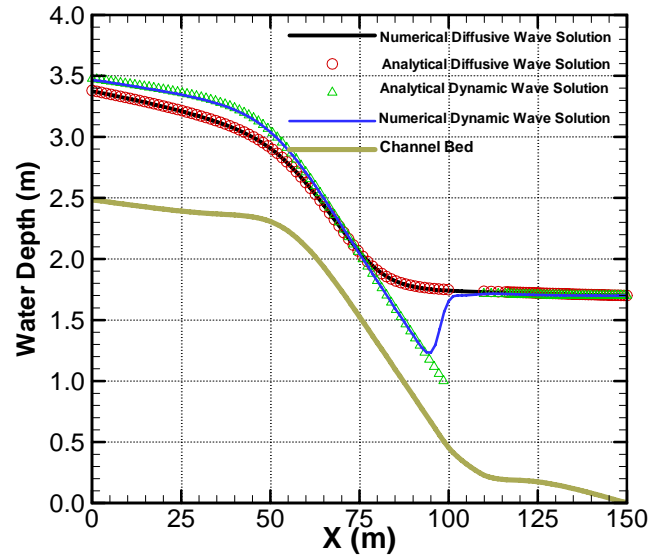


Figure 24. Comparison of simulated water surface elevation with analytical solution for test case 6 of MacDonald (1996)

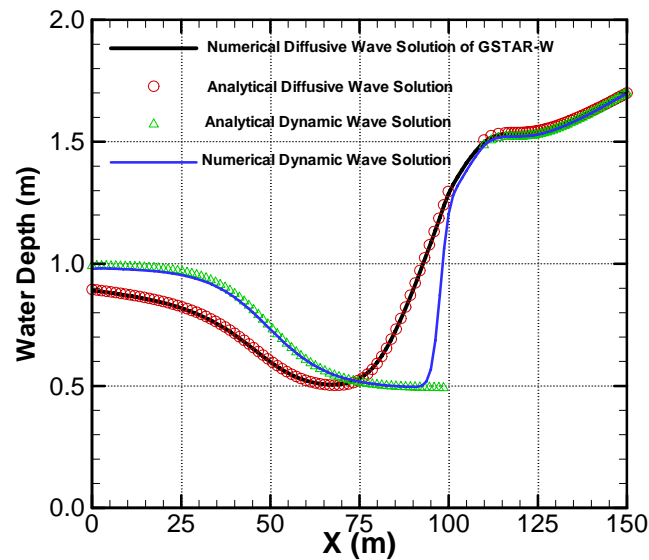


Figure 25. Comparison of simulated water depth with analytical solution for test case 6 of MacDonald (1996)

## 8.5 2D Diversion Flow in a Channel

A channel bifurcation occurs often in open channel flows, and flow features are complex in the diversion area. This test case simulates a channel diversion case measured and studied by Shetta and Murthy (1996). It serves as a 2D test case with flow separations.

The solution domain consists of a main channel, with 6.0m in length ( $X$  direction) and 0.3m in width ( $Y$  direction), and a side channel normal to the main channel at  $X=3.0$ m. The side channel has a length of 3.0m and width of 0.3m. A quadrilateral mesh system was used to cover the solution domain and the portion of the mesh at the diversion is shown in Figure 26, along with the  $X$  and  $Y$  coordinate system. Overall, the main channel has a mesh of 120-by -30 elements and the side channel has 40-by-30 mesh elements.

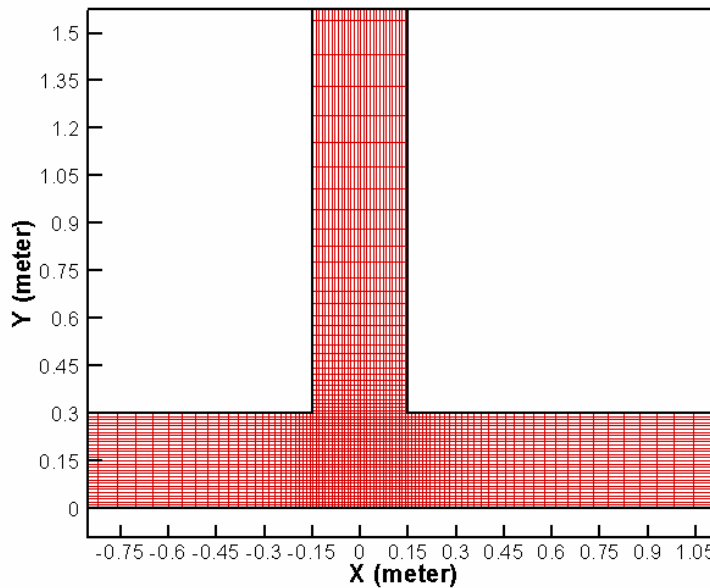


Figure 26. Part of the quadrilateral mesh used for simulation of the diversion flow

The simulated case has a main channel flow discharge of  $0.00567 \text{ m}^3/\text{s}$ , water surface elevation of 0.0555m at the exit of the main channel ( $X=6.0$ m), and water surface elevation of 0.0465m at the exit of the side channel ( $Y=3.3$ m). The Manning's roughness coefficient is 0.012 and the parabolic turbulence model is used for the simulation.

Simulated results are compared with measured data of Shettar and Murthy (1996) for the water surface elevation along both walls of the main and side channels (Figure 27 and Figure 28) and depth averaged velocity profiles in both channels (Figure 29 and Figure 30). The water surface elevation in the main channel is predicted well but discrepancy is noticeable in the side channel. Also, the velocity near the bottom wall ( $Y=0$ ) of the main channel is over-predicted. These discrepancies, mostly associated with areas of flow separation, are due to the inability of the turbulence model to predict the size of flow separation accurately. Results may be improved with the use of the  $k-\varepsilon$  turbulence model instead of the parabolic model used.

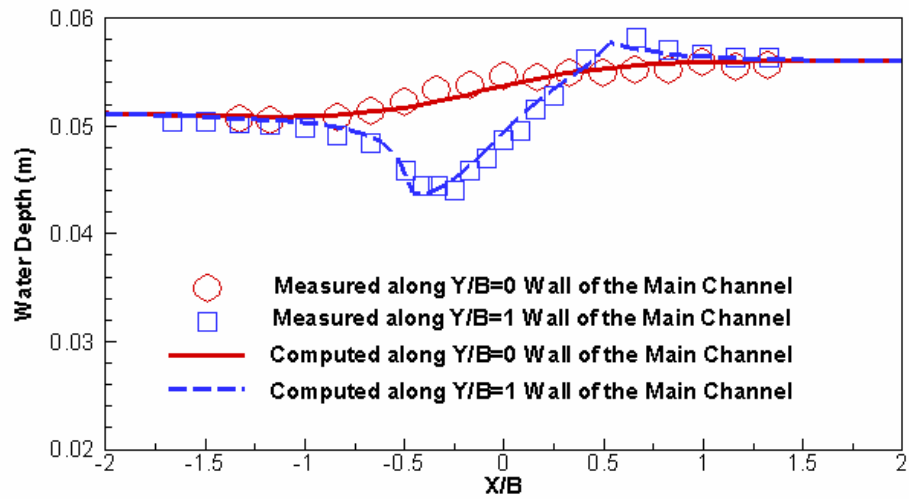


Figure 27. Comparison of water surface elevation along both walls of the main channel for the Shettar and Murthy (1996) case.

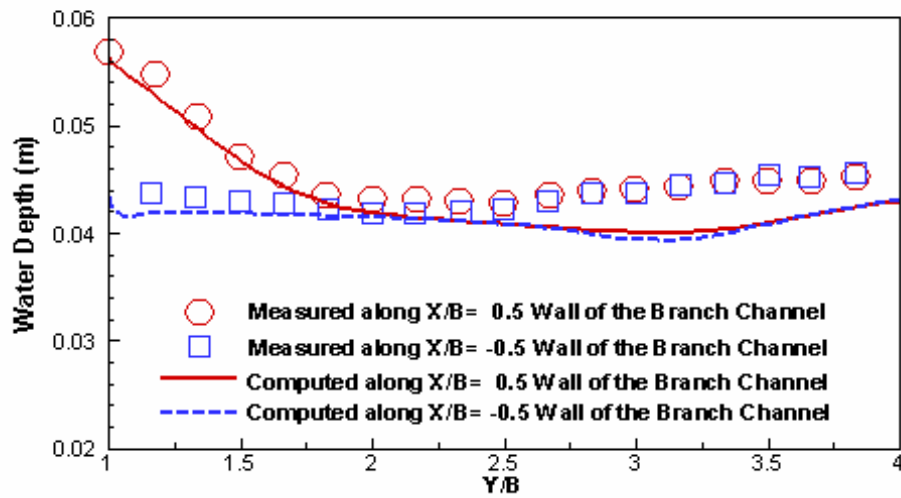


Figure 28. Comparison of water surface elevation along both walls of the side channel for the Shettar and Murthy (1996) case.



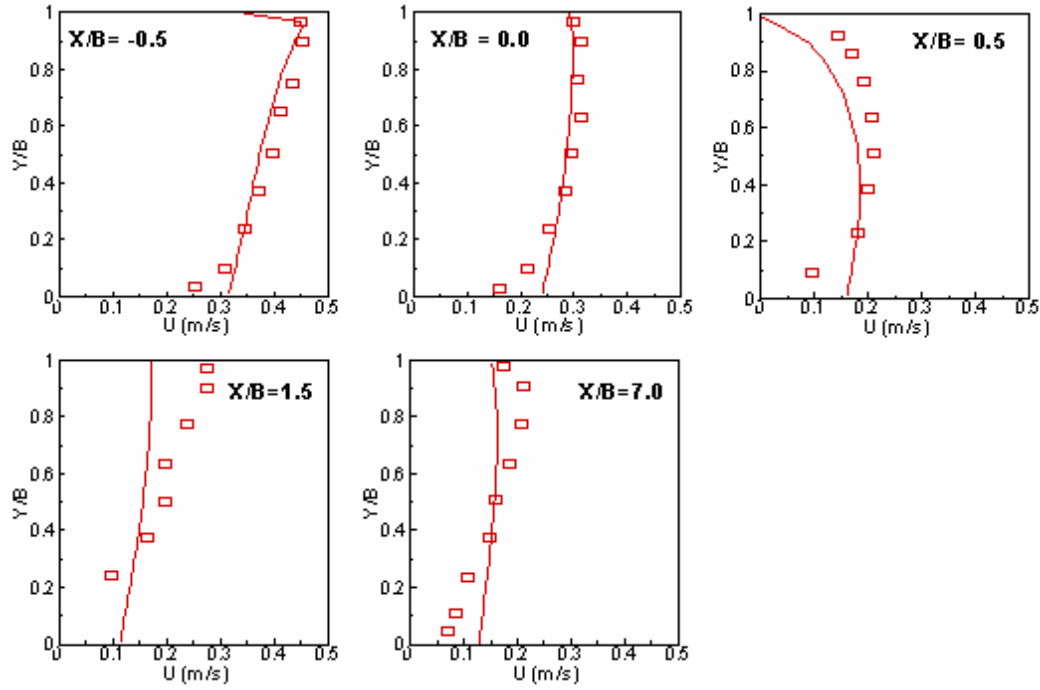


Figure 29. Comparison of x-velocity ( $U$ ) profiles at selected  $x$  locations in the main channel for the Shettar and Murthy (1996) case.

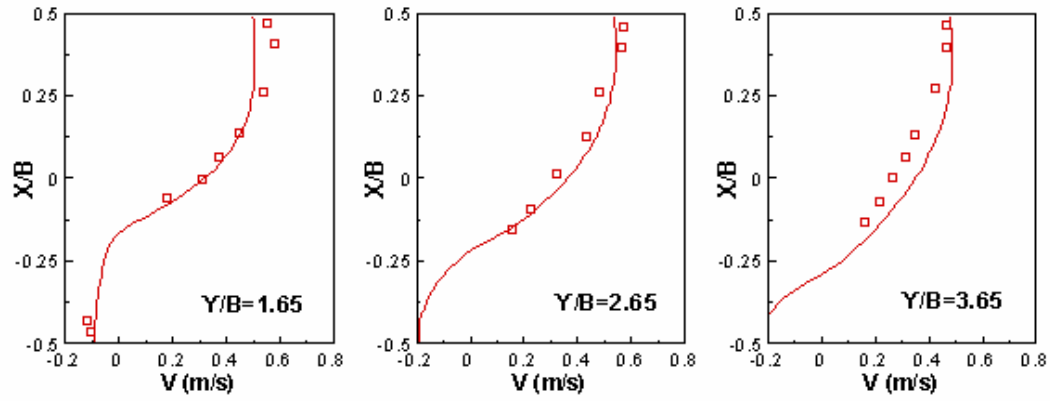


Figure 30. Comparison of y-velocity profiles at selected  $y$  locations in the side channel for the Shettar and Murthy (1996) case.



# CHAPTER 9

## APPLICATION CASES

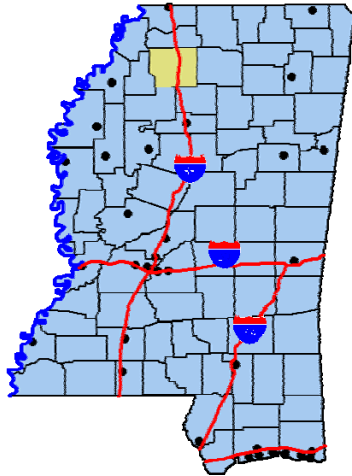
SRH-W has been applied to many projects for practical applications and this chapter focuses on presentation and discussion of selected applications and validation cases. Each case discussed has a separate project report that provides much more detail and the user is referred to the respective reports for further information.

### 9.1 Goodwin Creek Experimental Watershed Runoff

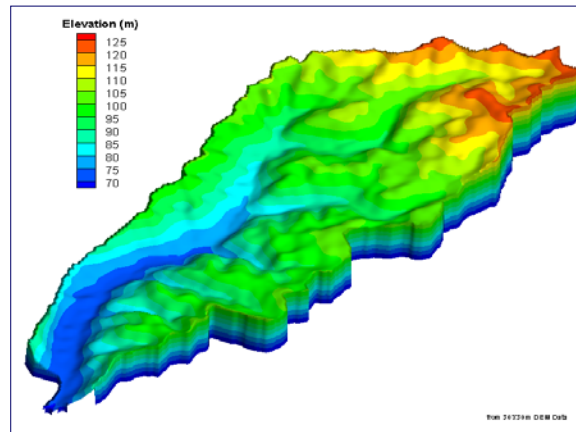
The rainfall-runoff model of SRH-W is applied to a watershed as part of a more practical verification study. One good case is the Goodwin Creek Experimental Watershed that has a large database compiling the precipitation, runoff, sediment, and GIS data over a decade. In addition, this watershed is also the subject of extensive studies by faculty and students at Colorado State University using CASC2D and its variants (e.g., Sanchez, 2002). Therefore, this watershed may serve multiple purposes in testing and validating SRH-W. The Goodwin Creek digital elevation model (DEM), land use and soil maps are available at 30-meter resolution and are used as major model inputs to SRH-W. Most of these data are available from the thesis of Sanchez (2002). A number of different mesh topologies and solvers, available within SRH-W, are tested and compared, as well as comparisons with results of CASC2D and field measured data.

#### 9.1.1 Watershed Description

The Goodwin Creek Experimental Watershed is located in Panola County, Mississippi, near Batesville (see Figure 31). It has a size of 21.3 km<sup>2</sup> situated in the bluff hills of the Yazoo River basin of northern Mississippi, with the outlet at latitude 89°54' 50" and longitude 34° 13' 55". It is a tributary of Long Creek that flows into the Yocona River, one of the main rivers of the Yazoo River Basin. The watershed is under research management by the National Sedimentation Laboratory (NSL), Agricultural Research Service (ARS), and it is organized and instrumented for conducting extensive research on upstream erosion, stream erosion sedimentation, and watershed hydrology (Shields *et al.* 1995; Alonso *et al.* 1995; Alonso *et al.* 1996; Kunhle *et al.* 1996; Kunhle and Willis 1998). The watershed has an extensive database consisting of runoff, sediment, and precipitation from 1981 until 1996 available at the NSL web site.



The County the Watershed  
Belongs to on the State Map



(b) Watershed Topography

Figure 31. Goodwin Creek Watershed Location and Topography

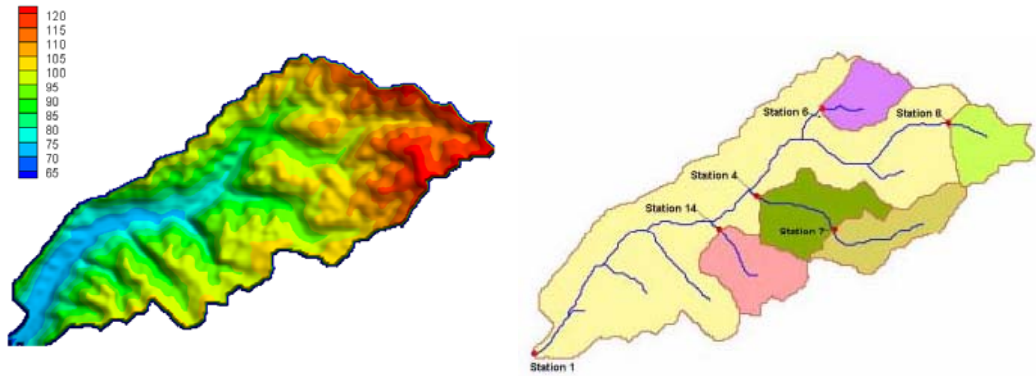
### 9.1.2 Digital Elevation Model

The watershed consists of fourteen nested subcatchments with drainage areas ranging from 1.6 to 21.3 km<sup>2</sup>. At each drainage outlet, a flow-measuring flume was constructed and data at the measuring stations are available. Terrain elevation ranges from 71 to 128 m above mean sea level, with an average channel slope of 0.004 in Goodwin Creek (Figure 31).

A digital elevation model (DEM) of the Goodwin Creek watershed is available at 30-meter resolution and data are preprocessed first using TOPAZ to obtain a depressionless DEM that is displayed in Figure 32a (Sanchez 2002). The channel network and watershed are then delimited from the smoothed 30-meter DEM. For the present simulation, six flume monitoring gage stations are used and the corresponding catchments are displayed in Figure 32b. The areas of six catchments are listed in Table 1.

Table 1. Computed and documented catchment areas (Blackmarr 1995)

Gage Number	14 (has)	4 (has)	7 (has)	8 (has)	6 (has)	1 (has)
Computed (30-m DEM)	165.02	357.82	162.98	137.56	111.49	2065.59
Documented	162.6	356.5	162.5	155.5	120.5	2145.25



(a) Surface Elevation Based on 30-m DEM (b) Monitoring Gages and Subcatchments

Figure 32. Digital elevation model and subcatchments used in the Goodwin Creek watershed.

### 9.1.3 Soil Types

Two major soil associations are mapped in Goodwin Creek. The Collins-Falaya-Grenada-Calloway association is mapped in the terrace and flood plain areas. These are silty soils, poorly to moderately well drained and include much of the cultivated area in the watershed. The Loring-Grenada-Memphis association has developed on the loess ridges and hillsides. These are well to moderately well drained soils on gently sloping to very steep surfaces and include most of the pasture and wooded area in the watershed. The soil characteristics of each area are described below (Blackmarr 1995); the soil type distribution map, based on 30-m resolution and used for the present simulation, is shown in Figure 33.

- Calloway (Ca): Fine-silty, mixed, thermic Glossaquic Fragiudalfs; soils are somewhat poorly drained, strong acid or medium acid silt loam soils formed in deposits of loess in upland positions of low relief (terraces). A fragipan is present generally at a depth of 16 inches.
- Collins (Cm): Coarse-silty, mixed, acid, thermic Aquic Udifluvents; soils are moderately well drained, strongly to medium acid, that have formed in silty alluvium on nearly level bottom lands. These silt loam soils occur primarily along the stream in the bottom area and are the location of much of the cultivation in the watershed. Cotton is the predominant crop but has been supplanted somewhat in recent years by soybeans.
- Falaya (Fa): Coarse-silty, mixed, acid, thermic Aerice Fluvaquents; soil consists of somewhat poorly drained, strong to very strong acid silt loam soils that developed in silty alluvium on nearly level bottom land. Most of the Falaya is cultivated.
- Grenada (Gr): Fine-silty, mixed, thermic Glossic Fragiudalfs; soil consists of moderately well drained, strong to very strong acid silt loam soils that

have developed in thick loess deposits on uplands or terraces. A fragipan is present at a depth of about 24 inches.

- Gullied Land (Gu): It consists of areas that are severely eroded, severely gullied, or both. The surface soil and much of the subsurface soil has been washed away. Most of this is land that was cleared, cultivated and later abandoned. It is now in trees, idle or pastured. It is unsuited for cultivation.
- Loring (Lo): Fine-silty, mixed, thermic Typic Fragiudalfs; soil series is moderately well drained to well drained, strongly to very strongly acid silt loam soils that developed in thick loess on uplands. A fragipan has formed at a depth of about 30 inches.
- Memphis (Ml): Fine-silty, mixed, thermic Typic Hapludalfs; soil series consists of well drained, strongly to very strong acid silt loam soils that developed in thick loess on uplands. In Goodwin Creek, this soil occurs as a mixture with the Natchez and Guin or the Loring. This series has no fragipan within the characterization depth; it is predominantly wooded.
- Mixed Alluvial Land (Mx): Land is poorly drained to excessively drained, strong acid silt loam and coarse sand; no uniformity in the arrangement, depth, color, or thickness of the soil layers. The soil is doughy and very low in organic-matter content and in natural fertility. It is in cultivation (row crops), pasture and trees (hardwoods).

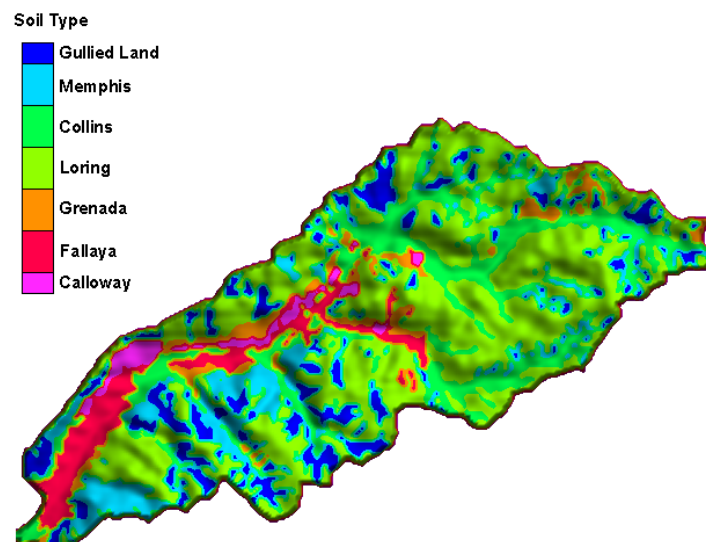


Figure 33. Soil type distribution at the Goodwin Creek

#### 9.1.4 Land Use

Land use and management practices that influence the rate and amount of runoff and sediment delivered to streams from uplands range from timbered areas to row crops. The Goodwin Creek watershed is largely free of land management

activities with 13 percent of its total area being under cultivation and the rest is idle, pasture and forestland. Periodic acquisition of aerial photography and satellite data contributes to a complete aerial coverage of land use and surface conditions. Land use in Goodwin Creek is classified below (Blackmarr, 1995):

- Cultivated Land: consists of three categories: cotton, soybeans and small grain. The field classification is based upon visual confirmation of the crop or by asking the land owner. Types of crops are cotton, soybeans, corn, and small grain.
- Pasture: Classified on the up-keep of the land, the presence of cattle, the presence of fences, and/or asking the land owner.
- Idle Land: Classified on the up-keep of the land, if overgrown with scrub vegetation, the absence of cattle, no fences present, and/or asking the land owner.
- Forest: Classified on the age of the trees, an approximation of age is based on tree height and width which is usually seven years and older.
- Planted Forest: Classified on the age of the trees; as with forest, an approximation of age is based on tree height and width. The range for the classification is from newly planted to seven years old.

In this study, the land use/land cover is reclassified as forest (includes planted forest), pasture (includes idle land), water and cultivated. The land use class distribution is based on 30-m resolution data and is displayed in Figure 34.

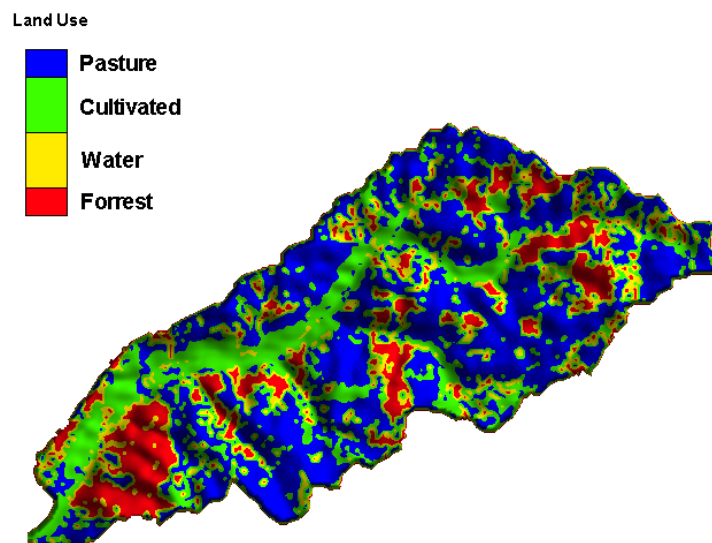


Figure 34. Land Use Class Map at Goodwin Creek

### 9.1.5 Precipitation

The climate at the Goodwin Creek watershed is humid and hot in summer and mild in winter. The average annual rainfall during 1982-1992 was 1440 mm and the mean annual runoff measured at the watershed outlet was  $14 \times 10^6 \text{ m}^3$ . Thirty-two rain gages are uniformly located within and just outside the watershed providing precipitation data. These rain gage data are used as the precipitation input to distributed hydrological models. Figure 35 shows the locations of all rain gages.



Figure 35. Locations of all rain gages at the Goodwin Creek

### 9.1.6 Channel Network and Cross Section Data

A channel network has been delineated from the smoothed 30-m DEM data and a total of eighteen channel reaches have been identified as displayed in Figure 36 (Sanchez, 2002). With the present SRH-W simulation, the diffusive wave channel network solver is applied and constant channel cross-sectional data are used within each reach. The cross-sectional data for each reach have been compiled by the NSL from 1978 until 1988. Average depth and width of the channel cross section for all eighteen reaches are listed in Table 2 (Backmarr, 1995). Rectangular shapes are used in the present simulation.



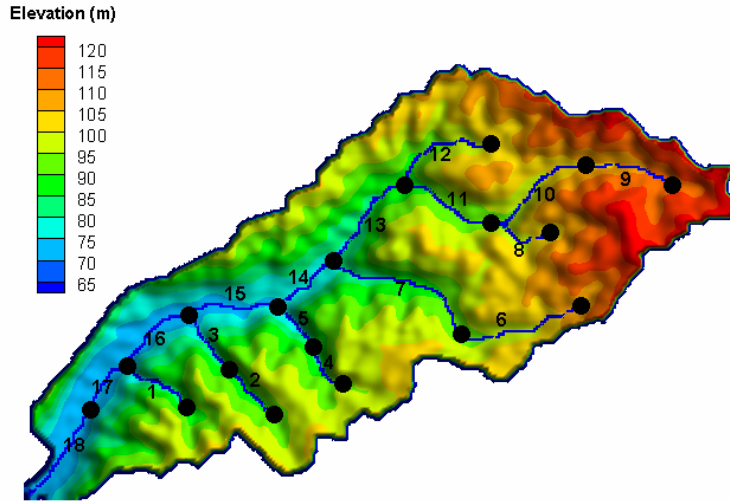


Figure 36. Delineated Channel Network and Reach IDs at Goodwin Creek

Table 2. Average channel width and depth of each reach in Figure 36

Reach ID	Width (m)	Depth (m)
1	25	3.5
2	20	3.0
3	22	3.5
4	27	4.3
5	28	3.1
6	30	3.4
7	30	3.55
8	22	4.1
9	29.4	4.2
10	26	4.35
11	30	4.4
12	22.4	4.0
13	27	4.3
14	30	4.5
15	30	4.7
16	50	5.0
17	48	5.0
18	34	6.05

### 9.1.7 Event Selection and Input Data

In this study, the storm event of October 17, 1981 is chosen for simulation. The same event was also simulated by Sanchez (2002) with CASC2D and data are readily available for comparison. This event began at 9:19 p.m, and had a total

rainfall duration of 4.8 hours with very little rainfall preceding this event. Precipitation data were taken from sixteen of the thirty-two rain gages that are located within and just outside the watershed. The locations of sixteen rain gages, as well as the rainfall intensity time series (30-minute averaged), are displayed in Figure 37. For the event, the total rainfall depth varied from 66 to 78.7 mm with an average value of 73.6 mm. The average rainfall intensity was 14.7 mm/h with a maximum of 51.6 mm/h.

Other input data include the 30-m DEM, and parameters related to different soil types and land use classes discussed above. The same set of parameters used by Sanchez (2002) was used for this SRH-W simulation unless otherwise stated. No attempt has been made to calibrate these parameters to fit the field measured data.

Three infiltration parameters needed for each soil type. The saturated hydraulic conductivity and the suction head were estimated by Sanchez (2002) based on the suggestion of Rawls et al. (1983); the moisture content deficit is assumed uniform in the watershed as no data are available. These values are listed in Table 3. The Manning's roughness coefficient and the interception depth associated with each land use class are estimated by Sanchez (2002) according to the range of possible values found in Wischmeier and Smith (1978), Woolhiser (1975) and Woolhiser et al (1990). The values used in the simulation are listed in Table 4.

For the channel network, the only input is the Manning's roughness coefficient for each channel reach listed in Table 2. The same coefficient is used for all eighteen reaches and its value will be discussed later.

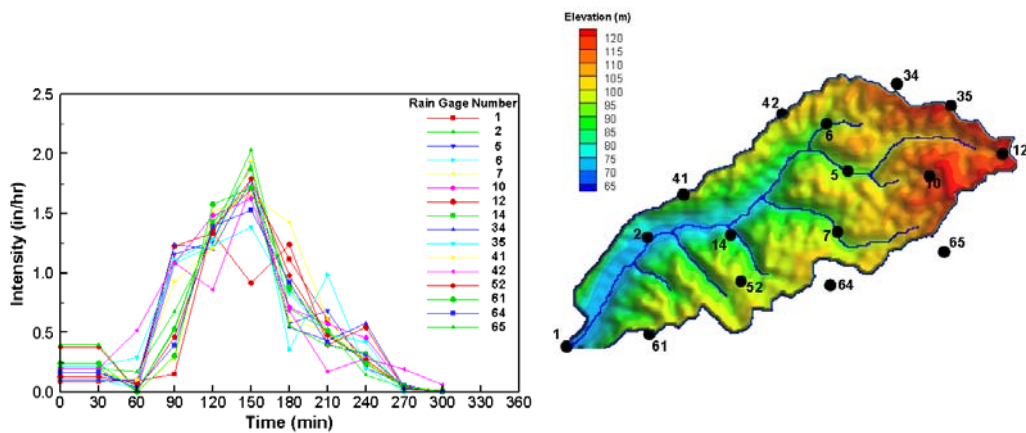


Figure 37. Storm intensity time series and locations of 16 rain gages for the event of Oct. 17, 1981 at Goodwin Creek

Table 3. Soil infiltration parameters for each soil type at the Goodwin Creek

Soil Type	Drainage Condition	$K_s$ (cm/hr)	$\Psi_f$ (cm)	$\theta_s - \theta_i$ ( $cm^3 / cm^3$ )
Calloway	Poor	0.35	22	.33
Fallaya	Poor	0.32	14	.33
Grenada	Moderate	0.37	17	.33
Loring	Mod/Well	0.38	22	.33
Collins	Mod/Well	0.36	18	.33
Menphis	Well	0.45	22	.33
Gullied Land	Poor	0.40	15	.33

Table 4. Land use parameters for each land use class at the Goodwin Creek

Land Use Class	Roughness Coefficient.	Interception (mm)
Forest	0.25	1.5
Water	0.01	0
Cultivated	0.1	0.8
Pasture	0.2	1.0

### 9.1.8 Description of Mesh Topologies

A number of meshes and solver options are used to simulate the selected storm event and they are listed below:

- 30m-by-30m raster mesh with CASC2D solver;
- 30m-by-30m raster mesh with SRH-W; both explicit and implicit solvers;
- A mixed element (both triangles and quadrilaterals) unstructured mesh; both explicit and implicit solvers.

The combination of above scenarios serves several purposes in terms of testing and validating SRH-W.

CASC2D uses only a raster mesh; so the 30m-by-30m raster mesh, as displayed in Figure 38, is used for simulation by CASC2D. This mesh is at the original DEM resolution and is the best possible topography representation. With CASC2D, channel network representation is the same as the diffusive wave channel network solver in SRH-W. That is, overland mesh elements (30m-by-30m squares in this case) are used to represent the channel network. These channel occupied elements are assigned the channel cross-sectional properties in Table 2, plus the Manning's roughness coefficient of 0.035 for all channel reaches. There are several limitations of this channel representation on a raster mesh. When channel width exceeds the element size (30 meter for the present case), the representation is

unrealistic. Also, such a channel representation makes the channel actually zigzag along the raster mesh so the actual reach length may not be accurate, which will be discussed later. With CASC2D simulation, the time step ( $dt$ ) was chosen as 0.5 second as  $dt=1.0s$  leads to divergence. The same time step (0.5s) was also used by Sanchez (2002).

The same 30-m resolution raster mesh is also used with SRH-W simulation for both explicit and implicit solvers. This is to demonstrate that the arbitrarily shaped element method (ASEM) implemented in SRH-W works on any mesh including the raster mesh. The major difference from CASC2D is that only active elements that cover the watershed are used by SRH-W and inactive elements are completely ignored and not part of the input. The raster mesh used by SRH-W has 22,942 square elements and is shown in Figure 39. The rest of the input data, such as the precipitation, soil map and properties, land use map and properties, and channel network representation and parameters are all the same as those used for the CASC2D simulation. With SRH-W, different time steps may be used for the overland runoff simulation and the channel network simulation. For the diffusive wave channel network solver option,  $dt=0.5s$  is used for all simulations. As for the overland runoff simulation, different time steps may be used. Up to  $dt=5s$  may be used with the explicit scheme while up to  $dt=5$  minutes may be used with the implicit scheme.

Finally, a mixed element unstructured mesh is created for the SRH-W simulation. This is the most general and flexible mesh topology and is intended to test and verify the SRH-W implementation of the ASEM. It is also used to demonstrate the general use of SRH-W for practical applications.

The final mesh is displayed in Figure 40 with a zoomed-in view of the mesh near the watershed exit in Figure 41. This mesh was generated within SMS with inputs of the watershed boundary lines and the channel network lines. The 1D quadrilateral mesh is generated on the channel network first with the flexibility of choosing the channel width. The rest of the watershed is then filled with combined elements of triangles and quadrilaterals. The side of each element is maintained approximately to 30 meter resolution though there is quite a spread. Once the 2D mesh is generated, the elevation of each mesh point is resampled from the 30-meter DEM using the bi-linear interpolation algorithm. The final mesh consists of 38,718 elements (14,873 triangles, 23,845 quadrilaterals). Note one important difference of this unstructured mesh from the raster mesh in that the channel may be exactly represented eliminating the two limitations of the raster mesh discussed above.

The soil type and land use class maps on the unstructured mesh are resampled from the corresponding 30-meter raster maps using the nearest-point method. The time step for the diffusive wave channel network solver is fixed at 0.5s while varied time steps are used for the overland runoff simulation. The explicit scheme

may use a time step up to 2.5s while the implicit scheme may use a time step up to 120s.

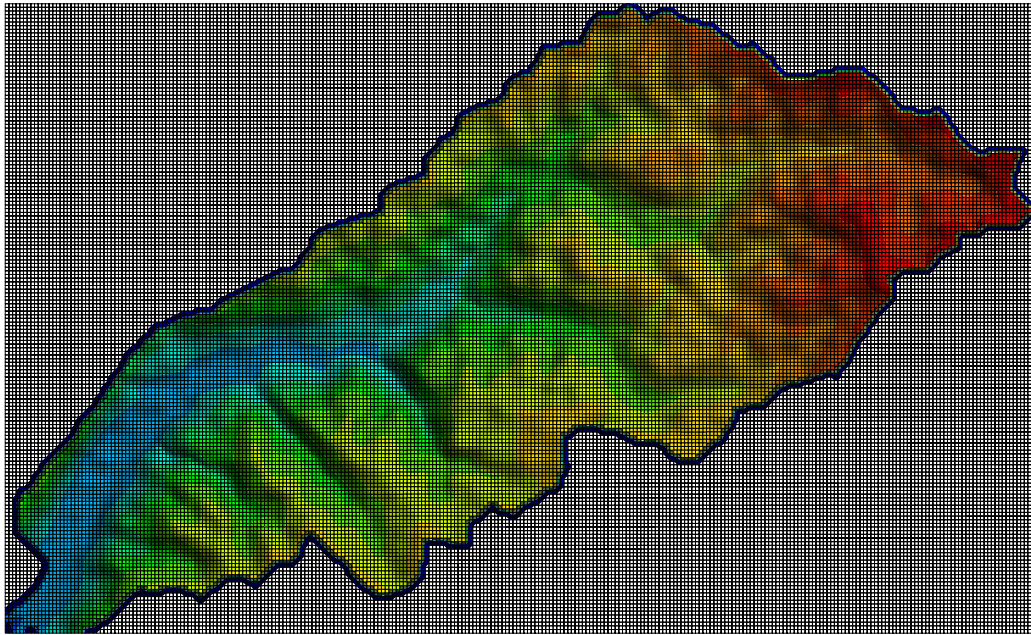


Figure 38. 30-meter Raster Mesh Used for CASC2D

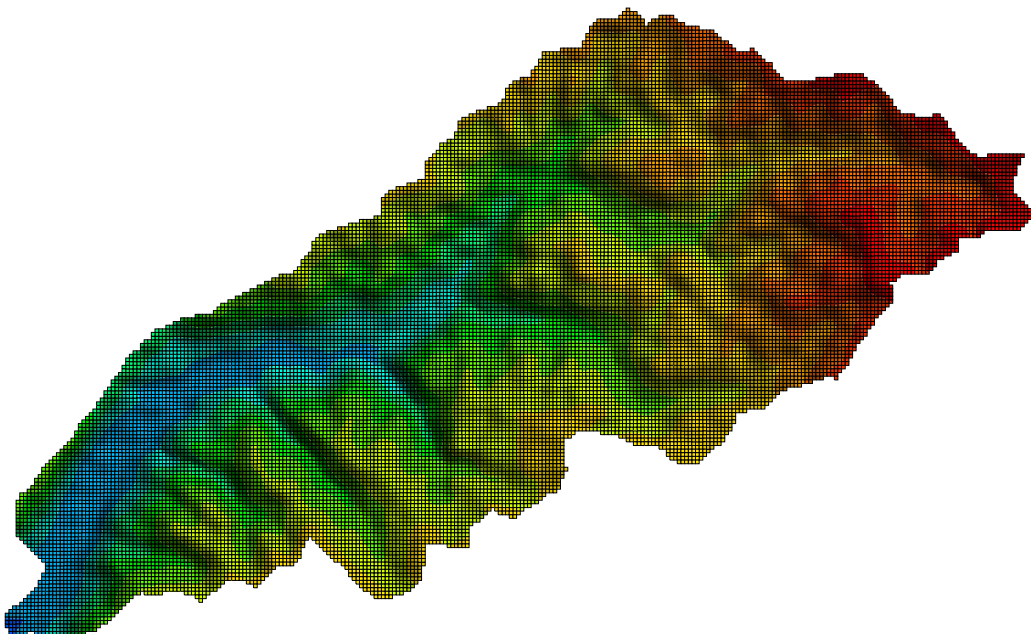


Figure 39. Active 30-Meter Raster Mesh Used for SRH-W

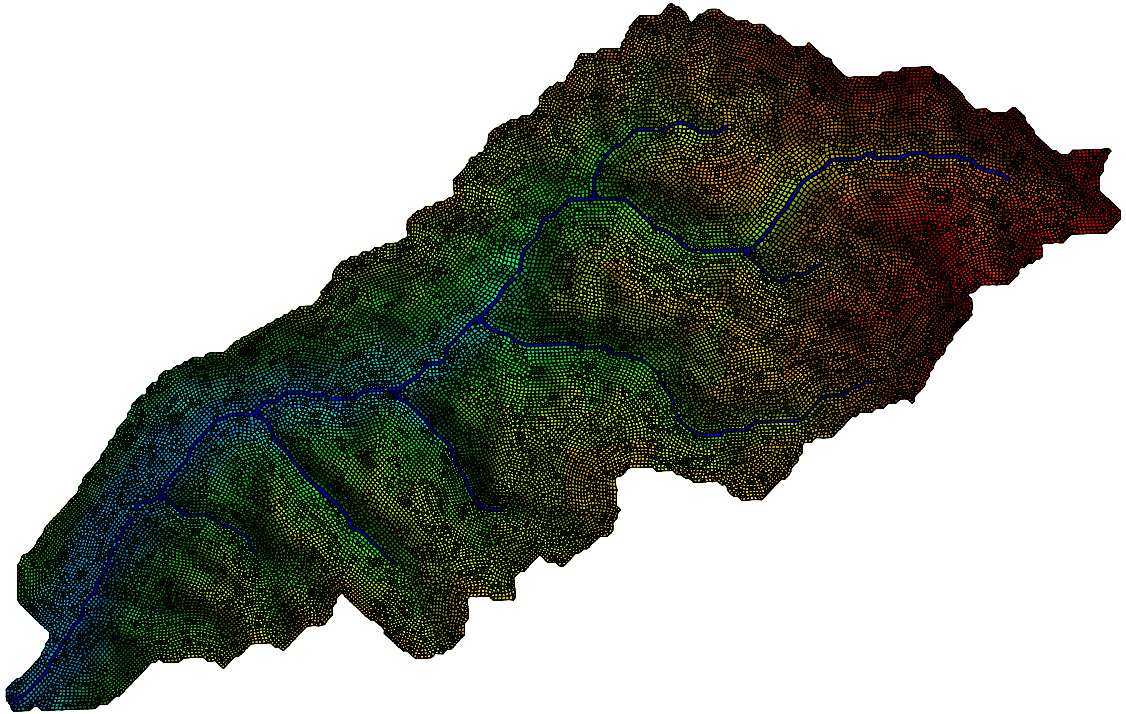


Figure 40. Mixed Element Unstructured Mesh Used for SRH-W

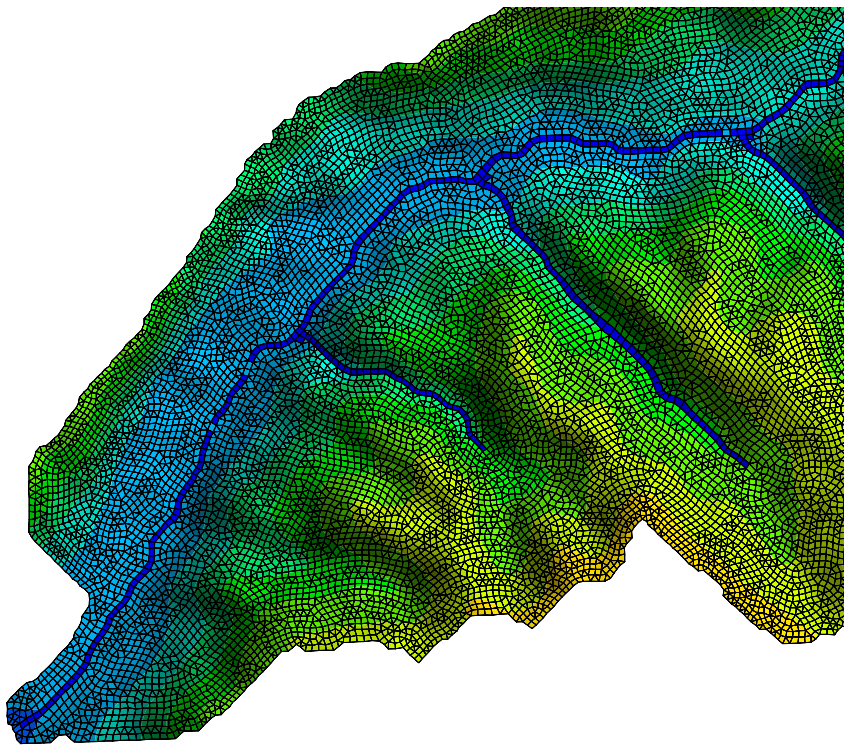


Figure 41. Zoomed-In View of the Unstructured Mesh Near Exit



### 9.1.9 Results and Discussion

Simulated flow hydrographs at six gage stations (see Figure 32b) are obtained and compared in Figure 42 with the raster mesh. The following findings are obtained based on the comparisons:

- Almost the same solutions are predicted by SRH-W with explicit and implicit schemes and with different time steps. Only one curve, therefore, is plotted in the figure with SRH-W results. These simulations indicate that SRH-W implementations for different functionalities are consistent as required.
- With the same raster mesh and same input data, results from the CASC2D and SRH-W are close to each other though SRH-W results are consistently smaller than those of CASC2D. This comparison serves as verification that SRH-W is implemented correctly and it solves the right equation. The slight difference between the two codes may be attributed to the resistance equation used. SRH-W uses equation (4.4) but CASC2D used  $\alpha_x = \sqrt{S_{fx}}$  and  $\alpha_y = \sqrt{S_{fy}}$ . This is equivalent of using a smaller Manning's coefficient with the CASC2D; and it explains why CASC2D consistently predicts a higher hydrograph than SRH-W.
- At the watershed exit (gage 1), peak flow and time to peak are correctly predicted but flows during recession are slightly over-predicted. At internal gages, the rising and falling limbs of the hydrograph and the time to peak were simulated correctly for most cases. However, the peak flows were underestimated for three gage stations. It is noticed that significant under-prediction of the peak occurred for the smallest sub-catchments only (gage 6, 8 and 14). Therefore, the errors may be attributed to sources such as the accuracy of precipitation and the delineated channel.

The second set of comparisons involves results produced from the mixed element unstructured mesh. Note that the input data for the unstructured mesh simulation are the same as those used for the raster mesh except that resampling is needed for spatially distributed data such as the elevation, soil type map, and land use map. The resampling is actually performed within SRH-W.

The major difference between the general unstructured mesh and the raster mesh is the representation of the channel network. With the unstructured mesh, channel reaches are represented naturally by a 1D quadrilateral mesh that follows the channel alignment, as well as the banklines. With the raster mesh, however, channel reaches are described by zigzag patterns and the channel width is limited by the available square mesh size. In order to see the difference between the two representations, initial simulations were carried out with the unstructured mesh using exactly the same channel cross-sectional properties (the channel Manning's coefficient is 0.035). Results are displayed in Figure 43. The predicted hydrograph at the watershed exit is different from the measured data though errors at other internal gage stations are much smaller. A general trend may be observed

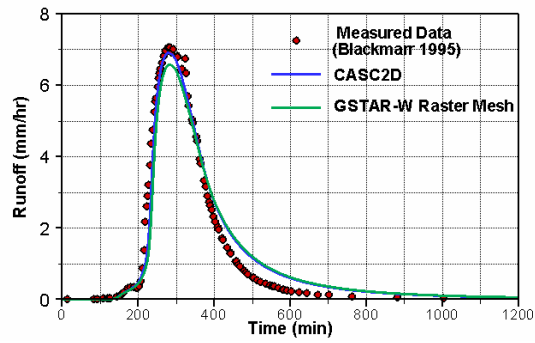
that larger errors are associated with stations with a longer channel reach length and the watershed exit station has the longest length.

It is conjectured that the errors of the unstructured mesh are not due to the failure of the model but to the difference in channel representation. Note that the channel length represented by the raster mesh is longer than that by the unstructured mesh. The above conjecture was verified by increasing the channel length of the unstructured mesh to approximate the one represented by the raster mesh. This exercise was done and results are shown in Figure 44. It is seen that results are much improved and they agree with each other. This exercise demonstrates that the channel parameter, the Manning's roughness coefficient, was calibrated using the wrong channel length represented by the raster mesh. It should be recalibrated using the correct length used by the unstructured mesh. Such an effort was carried out. The final calibrated Manning's coefficient is 0.06 (versus 0.035 used by the raster mesh) and results with this value are shown in Figure 45. It is seen that agreement is very good except at gage 14.

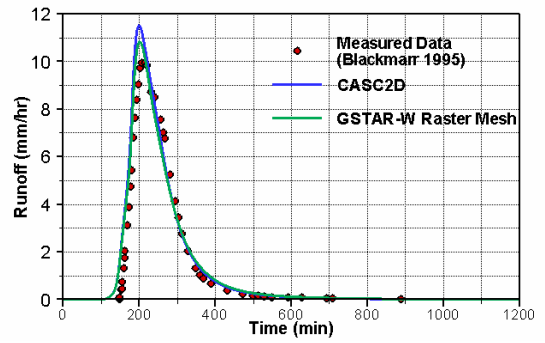
The above results show that some form of corrections should be exercised with respect to channel length when a raster mesh is used to represent the channel. Without the correction, the calibrated roughness coefficient may be in error.

Finally, the spatial distributions of the precipitation and the simulated water depth over the watershed are displayed in Figure 46 and Figure 47 at different times. These plots show the advantages of distributed simulations which provide very detailed information about where the runoff has the highest rate. The information helps to evaluate the impact of different land use and management practices on the runoff, and the associated erosion and sedimentation.

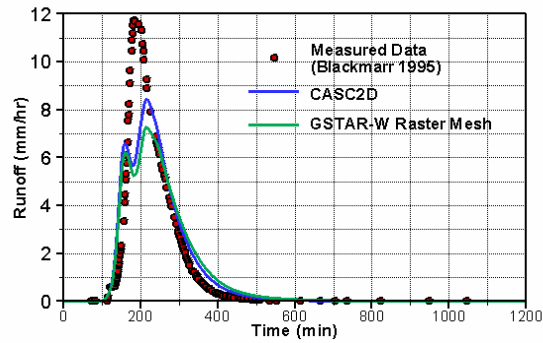




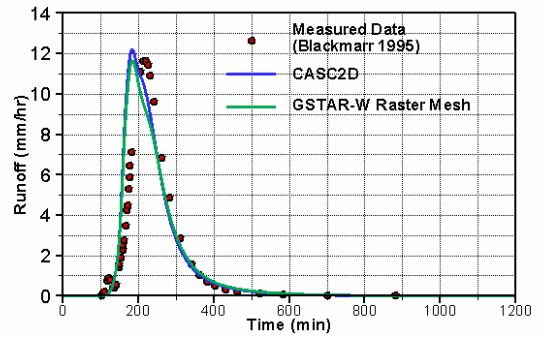
(a) at gage 1



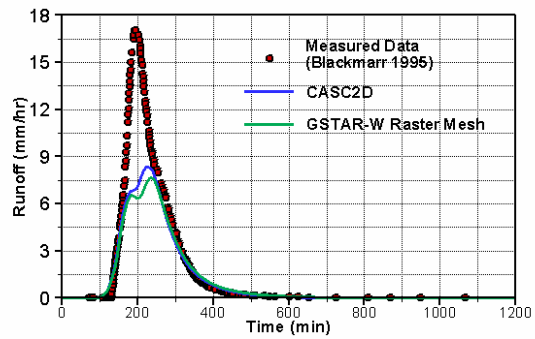
(b) at gage 4



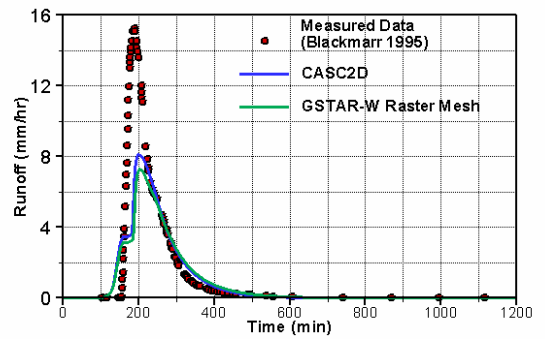
(c) at gage 6



(d) at gage 7

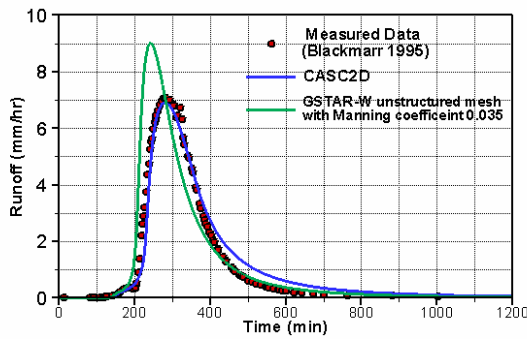


(e) at gage 8

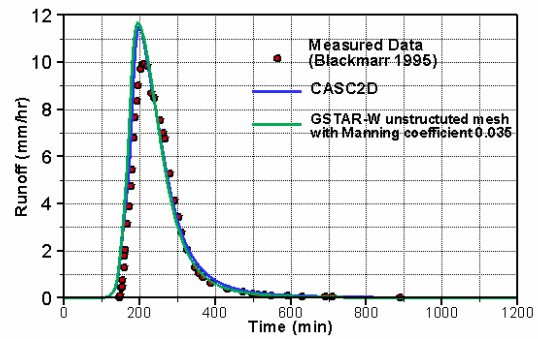


(f) at gage 14

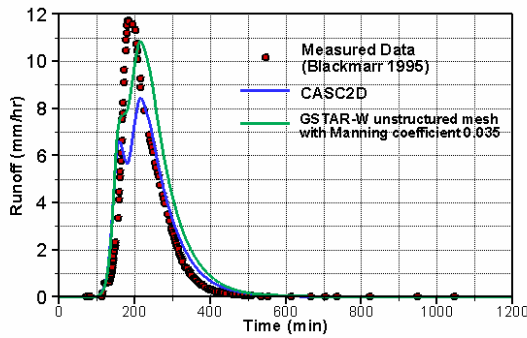
Figure 42. Comparison of Hydrographs: Raster Mesh (GTAR-W is the former name of SRH-W)



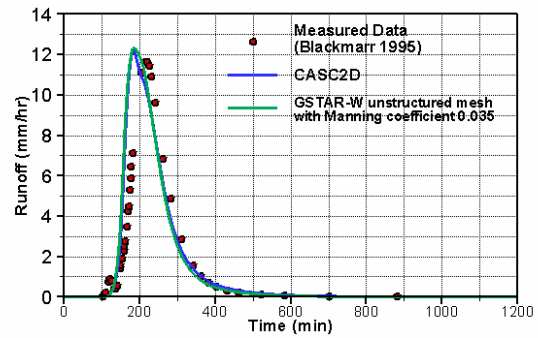
(a) at gage 1



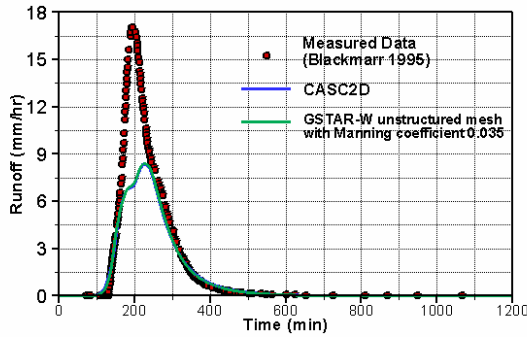
(b) at gage 4



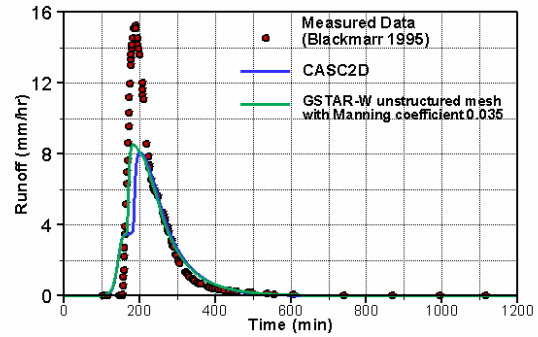
(c) at gage 6



(d) at gage 7

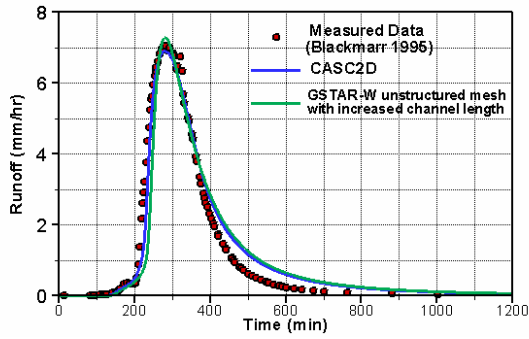


(e) at gage 8

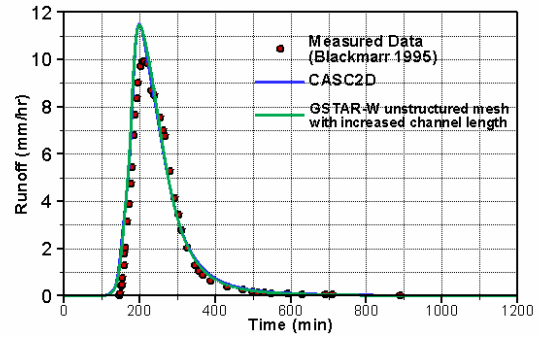


(f) at gage 14

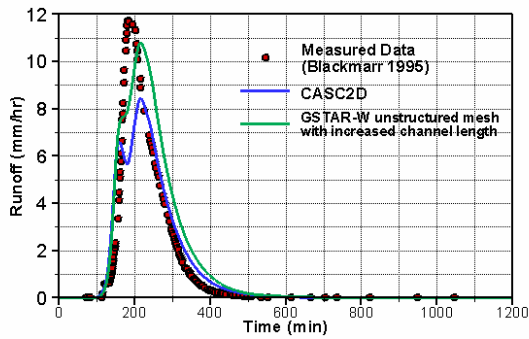
Figure 43. Comparison of Hydrographs: Unstructured Mesh with 0.035 Channel Manning Coefficient (GTAR-W is the former name of SRH-W)



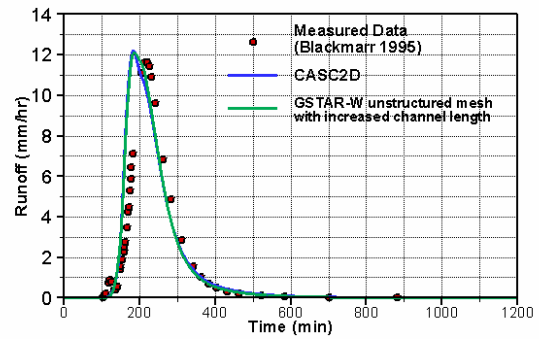
(a) at gage 1



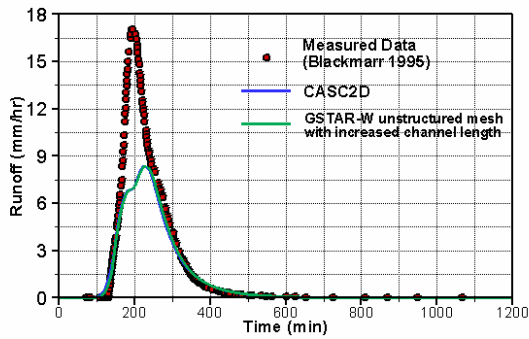
(b) at gage 4



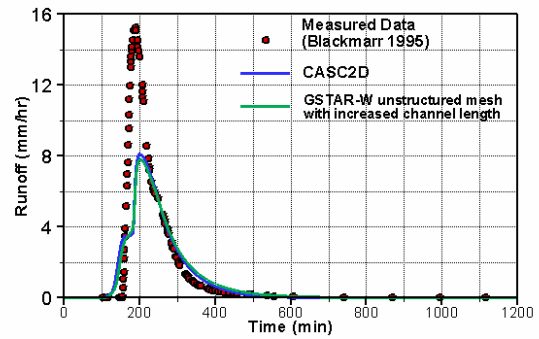
(c) at gage 6



(d) at gage 7

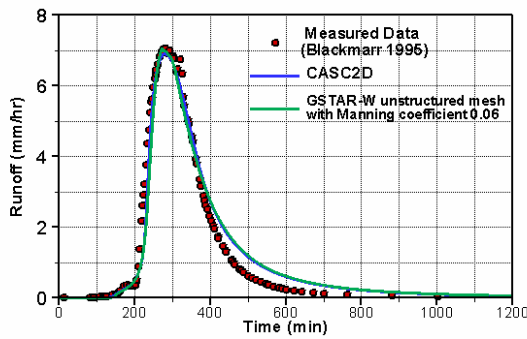


(e) at gage 8

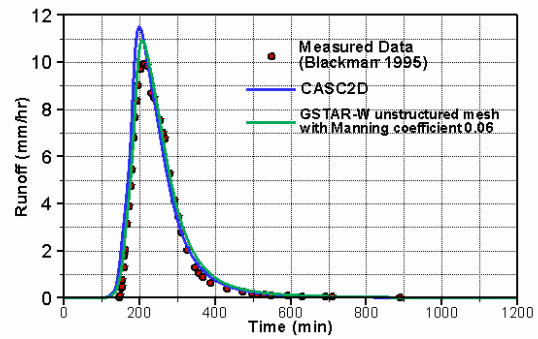


(f) at gage 14

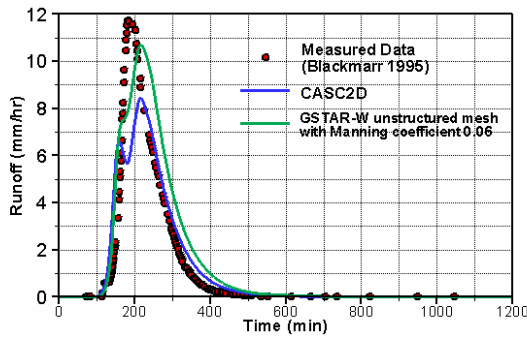
Figure 44. Comparison of Hydrographs: Unstructured Mesh with Increased Channel Length (GTAR-W is the former name of SRH-W)



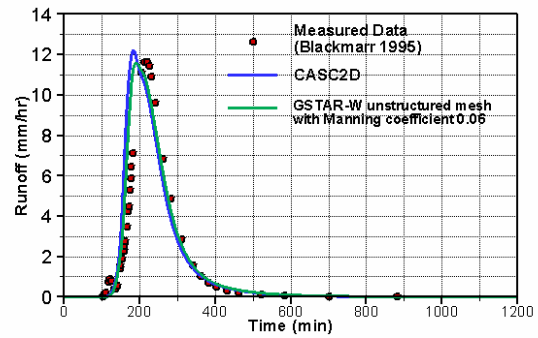
(a) at gage 1



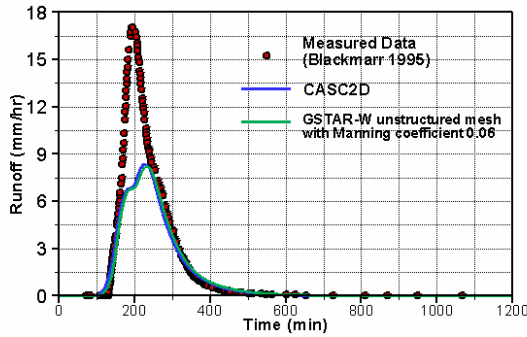
(b) at gage 4



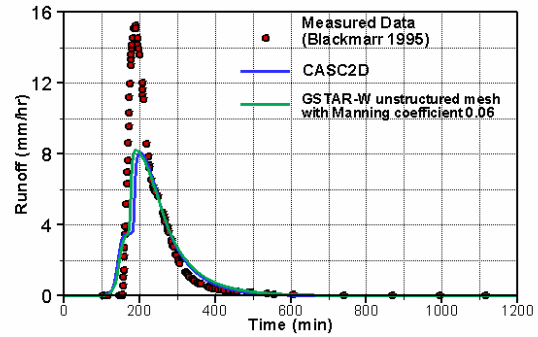
(c) at gage 6



(d) at gage 7



(e) at gage 8



(f) at gage 14

Figure 45. Comparison of Hydrographs: Unstructured Mesh with 0.06 Channel Manning Coefficient (GTAR-W is the former name of SRH-W)

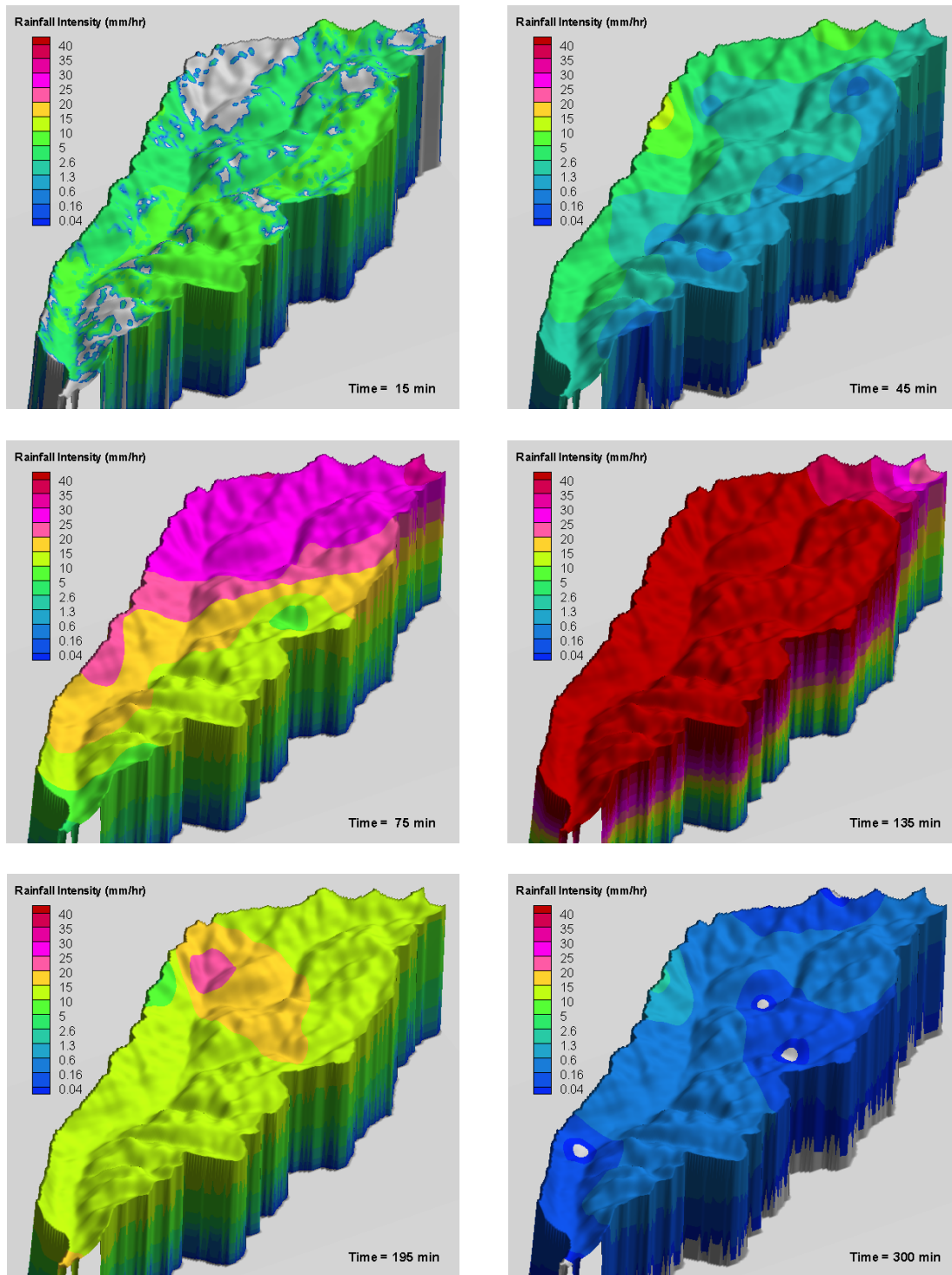


Figure 46. Rainfall Intensity Spatial Distribution at Different Times

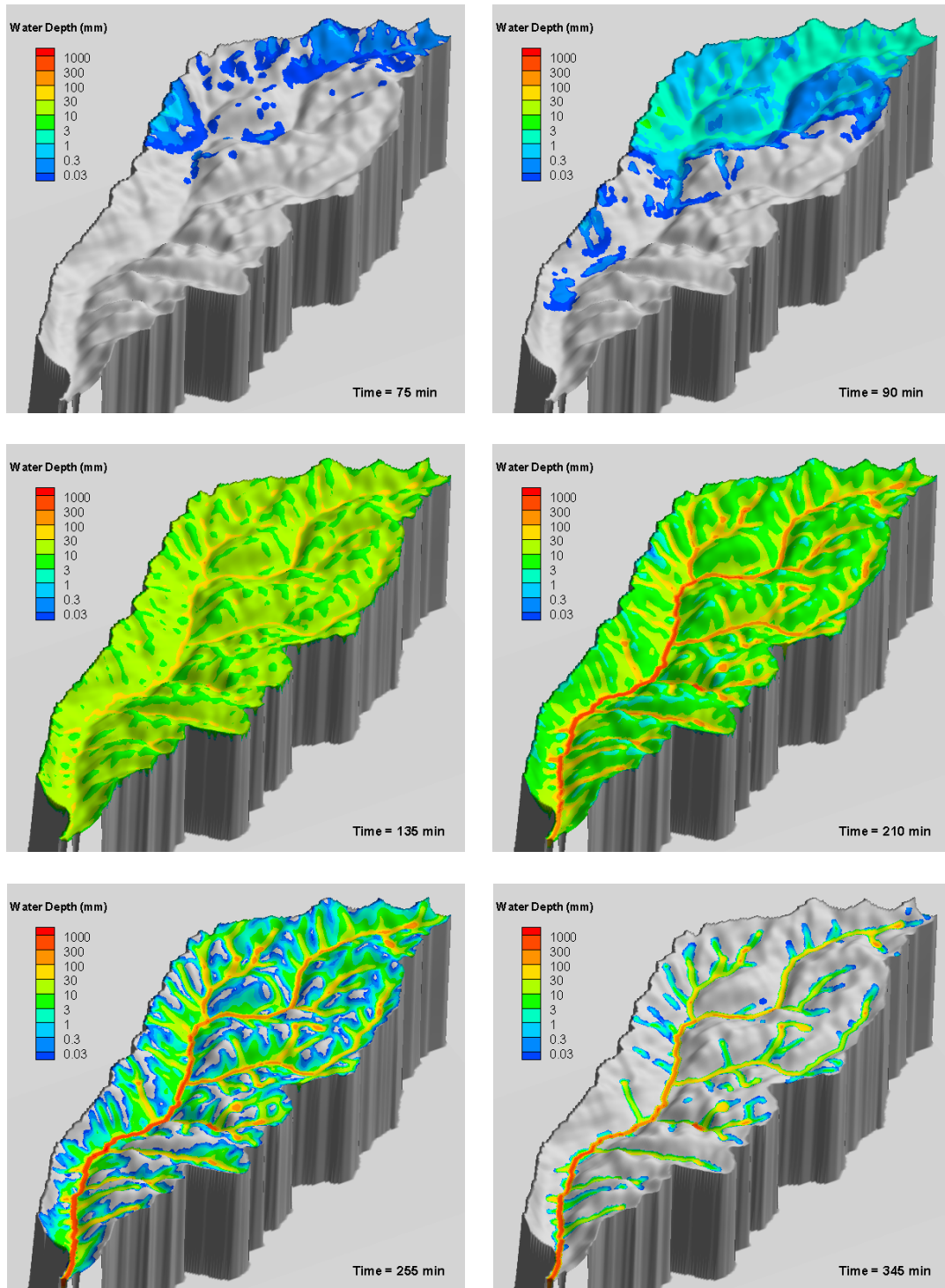


Figure 47. Simulated Water Depth Distribution over Watershed at Different Times



## 9.2 Savage Rapids Dam Removal Study

This section presents application of SRH-W to a dam removal study, the Savage Rapids Dam. The Savage Rapids Dam is located in southwestern Oregon on the Rogue River, five miles upstream from the city of Grants Pass. It is owned and operated by Grants Pass Irrigation District and has been used for diverting irrigation flows since 1921. The full removal of the dam and construction of a new pumping station are under design by the Bureau of Reclamation, due to lack of compliance of the existing fish ladders and screens to the current National Marine Fisheries Service criteria. SRH-W is used to simulate various scenarios to provide design data and assistance. Only the calibration and verification study is reported below. Detailed application results of SRH-W may be found in the project report by Bountry and Lai (2006). Additional discussion of results may be found in Bountry et al. (2006).

### 9.2.1 Topography and Mesh

The simulation reach extends from the Savage Rapids Park, 0.5 mile upstream of the dam, to about 0.45 mile downstream of the dam. The topography for the reach is reconstructed from a number of surveys conducted between 1999 and 2005 (Bountry and Randle 2003) (see Figure 48). A quadrilateral mesh is developed that consists of 20,145 elements and 20,468 nodes with a typical element size of 5 by 12 feet. A 3D view of the topography and part of the mesh is displayed in Figure 49.

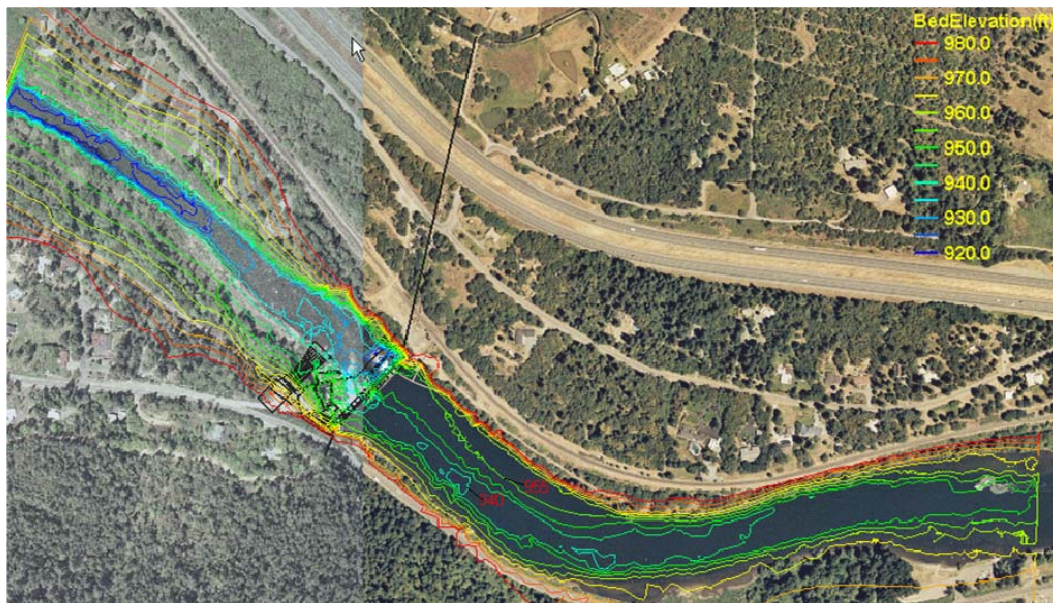


Figure 48. Plainview and bed elevation contours of the simulated area for the Savage Rapids Dam removal project

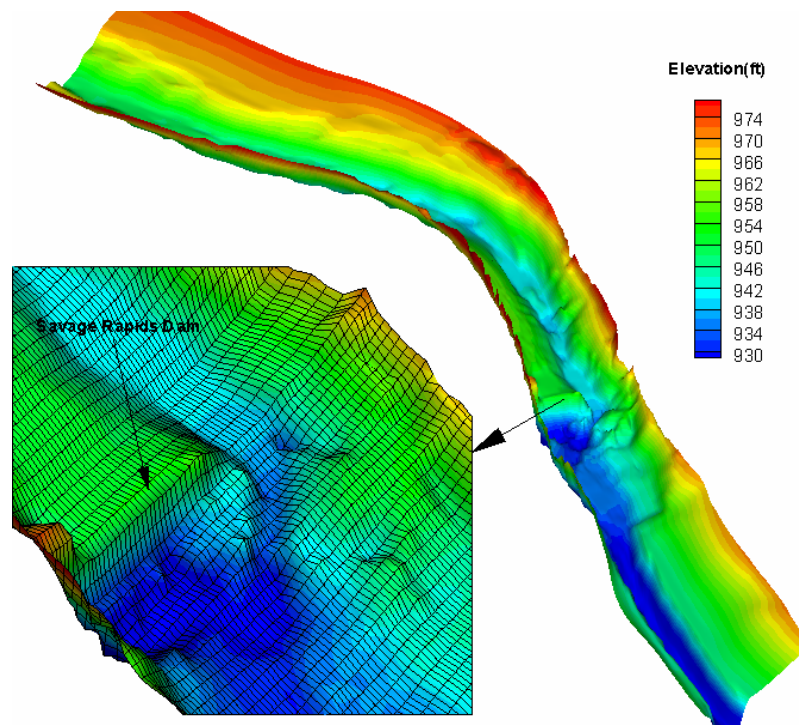


Figure 49. A Perspective View of the Topography of the Modeled River Reach.

### 9.2.2 Case Modeled, Boundary Conditions, and Other Parameters

The measured data, water surface elevation and velocity vectors, during the April 2002 survey (Bountry and Randle 2003) was chosen to calibrate and verify the SRH-W model. This case represents a drawn-down flow with a discharge of 2,800  $\text{ft}^3/\text{s}$ . All flow was through the two radial gates near the left side of the dam. The measured water surface elevation is used to calibrate the Manning roughness coefficient that is assumed to be uniform throughout the reach. Once calibrated, the model results are then compared with the measured velocities and flow patterns. Both diffusive wave and dynamic wave solutions are obtained so that a comparison may be made between the two solvers.

A water surface elevation of 935.53ft was specified at the downstream boundary. This elevation was obtained from the calibrated one dimensional HEC-RAS model as described by Bountry and Randle (2003). At the upstream boundary, a flow discharge of 2,800 $\text{ft}^3/\text{s}$  was applied where a uniform distribution of velocity is assumed with the flow normal to the boundary. The calibrated flow loss coefficient is 0.05 for the diffusive wave model and 0.04 for the dynamic wave model. Finally, the depth-averaged parabolic model is used for the turbulence viscosity used by the dynamic wave model (Rodi 1993).



### 9.2.3 Comparison of Water Surface Elevation

The calibrated model results are compared with the measured water surface elevation along the thalweg in Figure 50. Both the diffusive wave and the dynamic wave model agree with the measured elevation well. Major discrepancy between the two models is mostly limited to an area near the radial gates where a hydraulic jump exists due to the dam. As anticipated, the dynamic wave model predicts the existence of the jump, while the diffusive wave model is incapable of simulating the hydraulic jump. The diffusive wave model tends to predict a smooth variation of elevation over the jump. Based on experiences with other applications of SRH-W, it is recommended that the jump area should be modeled with a higher loss coefficient in order to predict the water elevation change, although the uniform coefficient works fine for the Savage Rapids Dam application.

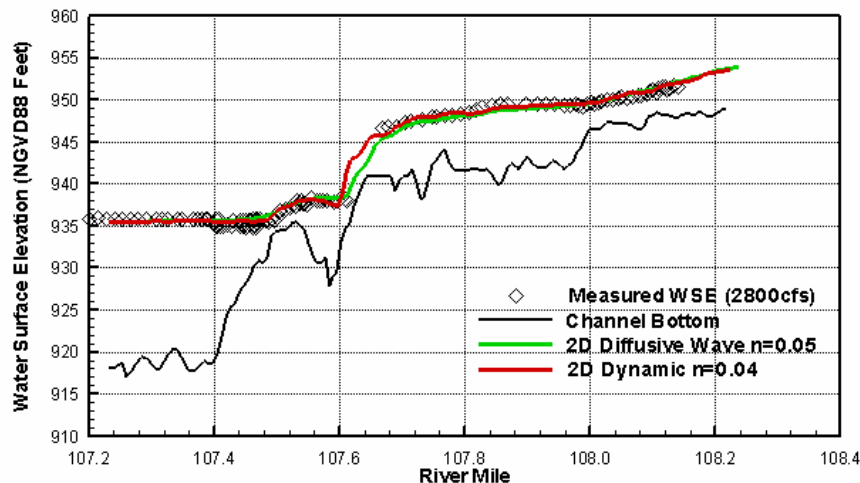


Figure 50. Comparison of Predicted and Measured Water Surface Elevations

### 9.2.4 Comparison of Velocities and Flow Patterns

Next, the computed velocity vectors and flow patterns are compared with the measured data so that the flow hydraulics may be compared in greater detail. It is noted that a good prediction of the water surface elevation does not guarantee a good prediction of velocities and flow patterns.

The ADCP-measured depth-averaged velocity data are available and the measurement points are displayed in Figure 51. Upstream of the dam, eight cross sections were surveyed and they are numbered consecutively in the figure. Downstream of the dam, two areas are compared: One is immediately downstream of the dam but near the right side; another is downstream of the

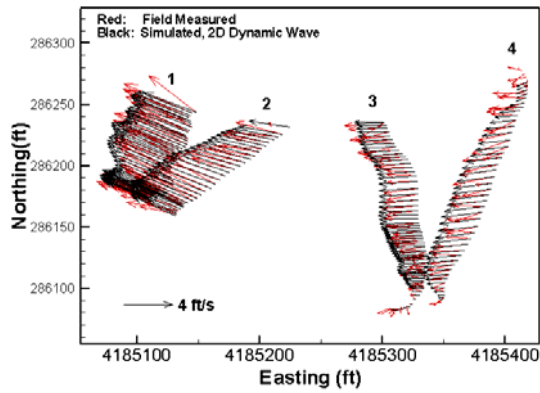
excavated channel from the radial gates. Complex eddies were formed at the time of the survey in both areas.



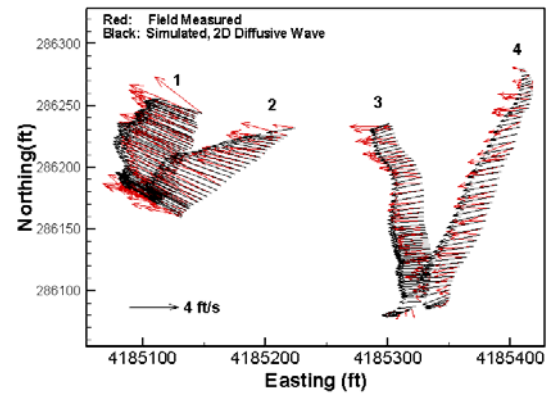
Figure 51. Velocity Measurement Points for the Simulated River Reach (Points are Shown in Red)

A comparison of predicted and measured velocity vectors at eight cross sections upstream of the dam is displayed in Figure 52 and Figure 53. Agreement is favorable for both models except at a few locations. Overall, the difference between the dynamic wave and the diffusive wave solutions is not appreciable. The dynamic wave model is capable of predicting the flow separation on the left bank of cross sections 3 and 4 while the diffusive wave model is not.

A comparison of velocities and flow patterns is shown downstream of the dam in Figure 54. It is clear that the diffusive model is incapable of predicting any eddies and therefore, the velocity results in such areas are in gross error. On the other hand, the dynamic wave model is quite good in predicting the eddy structures. It is noted that the two-eddy structures on the right of the jet stream from the excavated channel is well predicted both in terms of size and location. In addition, the eddy on the left of the jet stream is also predicted. These results indicate that the dynamic wave model has to be used if eddies or flow separation are of interest.

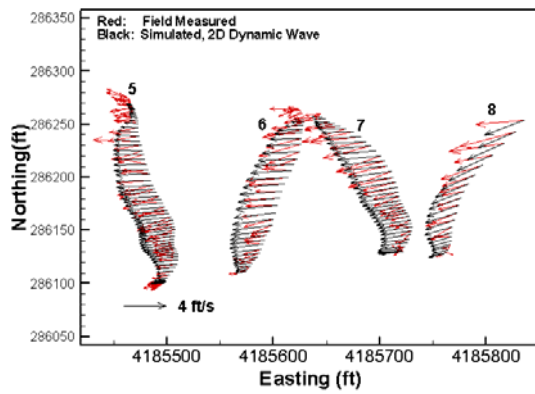


(a) Dynamic Wave Solution

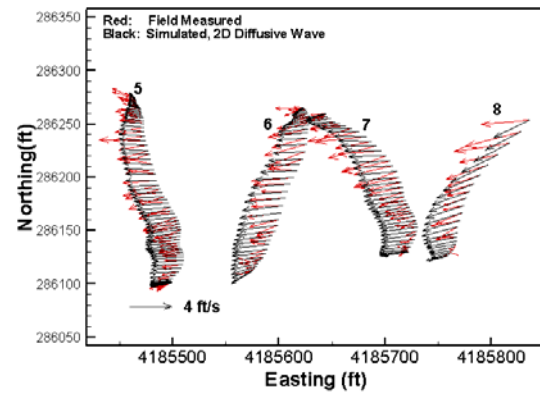


(b) Diffusive Wave Solution

Figure 52. Comparison of Predicted and Measured Velocity Vectors at Cross Sections 1 to 4



(a) Dynamic Wave Solution



(b) Diffusive Wave Solution

Figure 53. Comparison of Predicted and Measured Velocity Vectors at Cross Sections 5 to 8

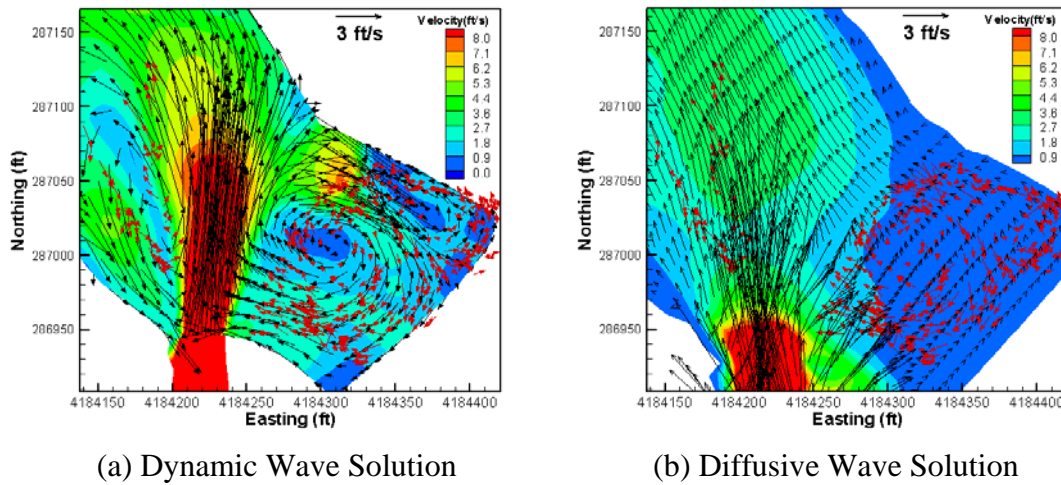


Figure 54. Comparison of Velocity Vectors and Flow Patterns downstream of the Dam

### 9.3 Study of Sandy River and Columbia River Interaction

The Sandy River Delta Dam (SRD Dam) is located near the confluence of the Sandy and Columbia Rivers, east of Portland, Oregon. As a result of its closure in 1938 to improve fish passage through the Sandy River, flow has been redirected from the east (upstream) distributary to the west (downstream) distributary of the delta. The east distributary has since partially filled with sediment and supports dense riparian vegetation, including aged cottonwoods. Although once the main distributary channel, the east distributary is currently only activated under high flow conditions on the Sandy or Columbia Rivers. The study area is shown in Figure 55.

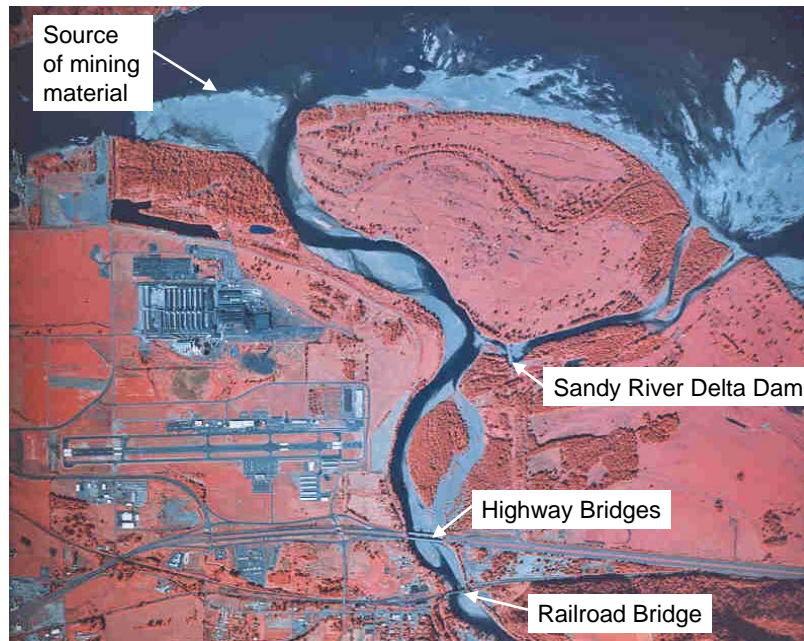


Figure 55. Aerial photo of the study area at the Sandy River Delta

Increased understanding of the ecological functions of the natural channel configuration and requirements of anadromous fish has initiated a reassessment of the role of the SRD Dam in improving fish passage. Recent efforts to improve aquatic habitat conditions have considered the removal of the SRD Dam. SRH-W was used to more effectively evaluate possible effects related to removal of the SRD Dam. Both hydraulic and sediment studies were carried out but only the hydraulic results of the model calibration study are discussed. More details of the study may be found in the project report by Lai et al. (2006).

### 9.3.1 Solution Domain, Mesh, and Flow Roughness

The solution domain was selected based on the stated objectives of the project and was guided later by the topographic and bathymetric data; it is displayed in Figure 56. The solution domain encompassed about 9.5 miles of the Columbia River and 2.6 miles of the Sandy River with an area of about 12.8 square miles.

The final mesh is displayed in a series of figures from Figure 57 to Figure 59. A combination of quadrilateral and triangular elements was used that provided the best compromise between the accuracy and computing time. The main river channels were mostly covered with quadrilateral cells that allow mesh stretching while the remaining areas were mostly covered with combined triangular-quadrilateral cells. The final mesh contained a total of 37,637 cells.





Figure 56. Solution domain for the Sandy River Delta simulation. West (left) side of the Columbia River is the exit boundary, east (right) side is the inlet boundary, and south (bottom) side is the inlet boundary of the Sandy River

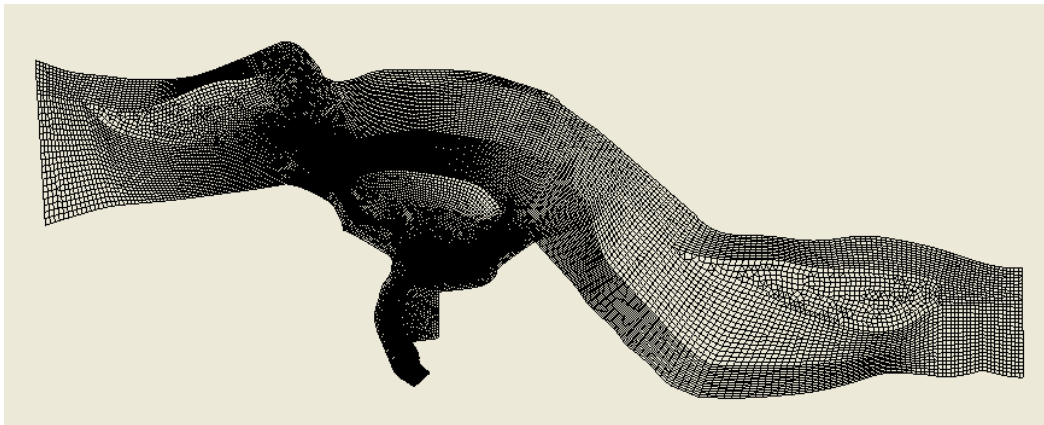


Figure 57. Mesh for the Sandy River Delta project: entire solution domain.

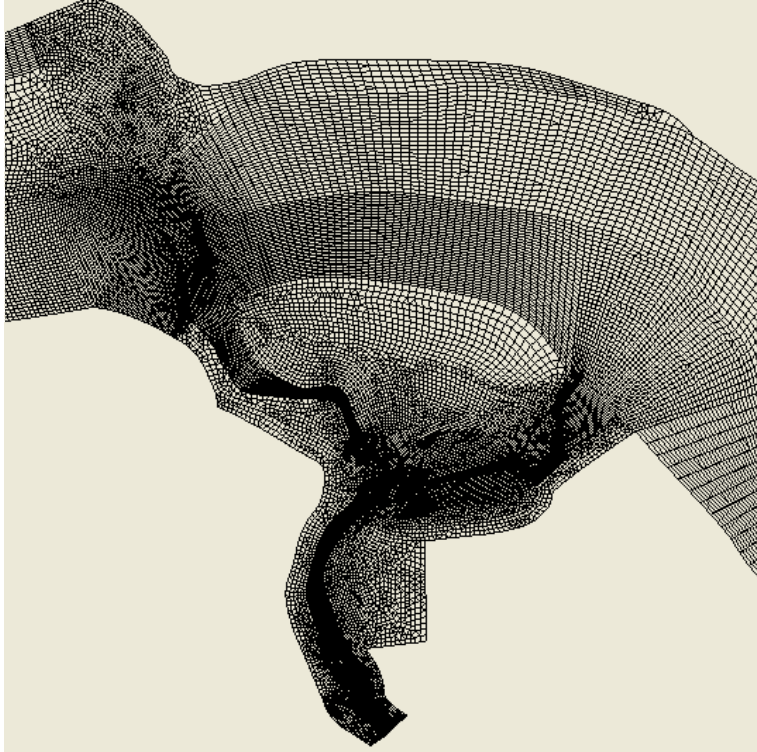


Figure 58. Mesh for the Sandy River Delta project: the Sandy River Delta area

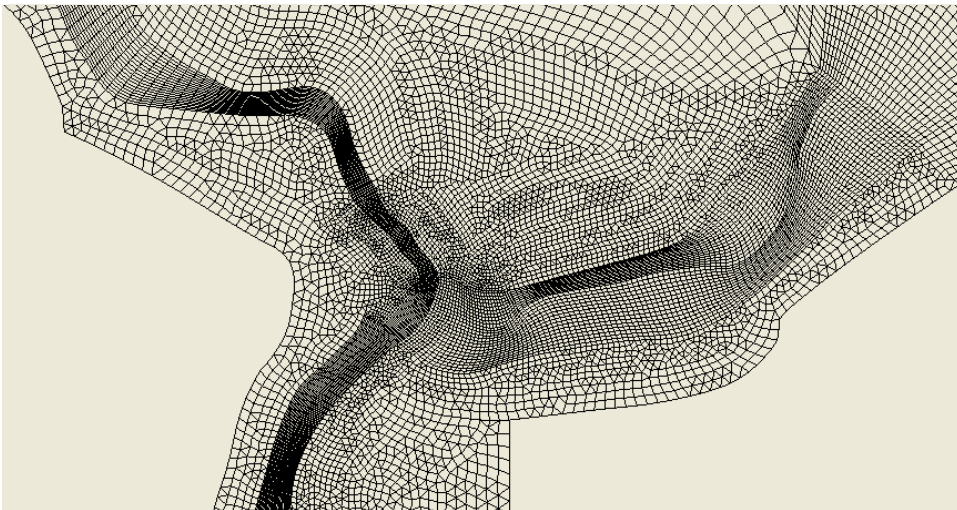


Figure 59. Mesh for the Sandy River Delta project: Dam area.

Topography data were obtained from several sources, including Lidar data and cross section survey data, to represent existing conditions. The bathymetric data were in point form (Easting, Northing, and elevation) and were interpolated onto the mesh points. The bed elevation contour plot and a perspective view of the topography are shown in Figure 60 and Figure 61.

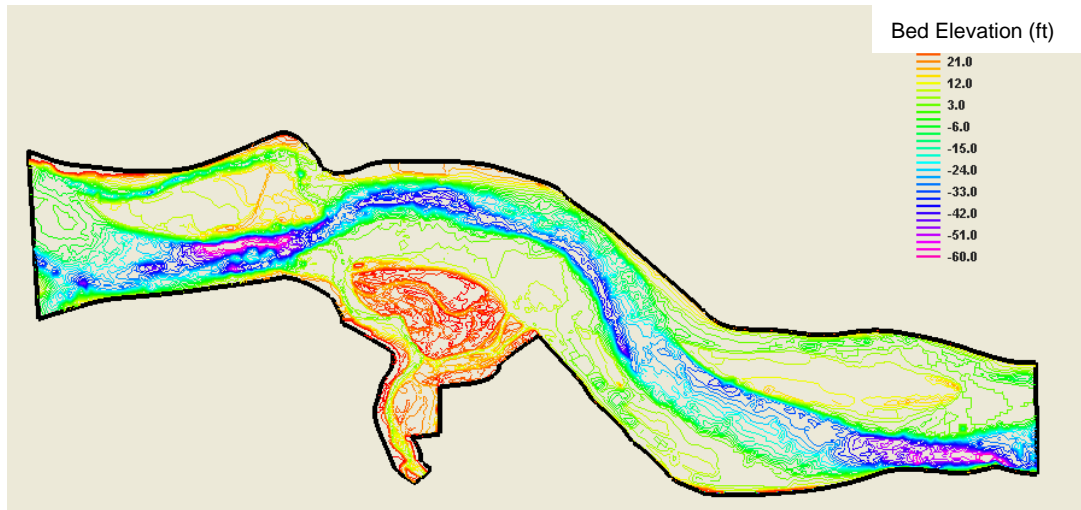


Figure 60. Contour plot of the bed elevation for the Sandy River Delta project

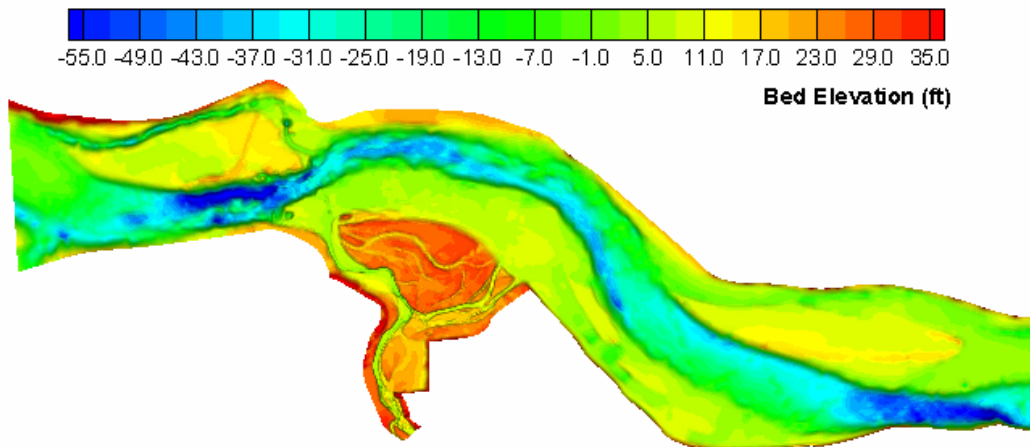


Figure 61. 3D perspective view of the topography for the solution domain.

Flow resistance was calculated with the Manning's roughness equation in which the Manning's coefficient ( $n$ ) was needed as the model input. In this project, the solution domain was divided into a number of roughness zones as shown in Figure 62 according to the underlying bed properties. Note that zones 1, 2 and 3 represent the main channel of the Sandy River, and zones 4 and 5 represent the main channel of the Columbia River. Zone 6 consists mostly of sand bars and less vegetated areas, while zone 7 represents islands and floodplains with more vegetation. Each zone was assigned a Manning's  $n$  value that was determined through a calibration study by comparing with the field data of October 2005. After a number of simulation runs, the final calibrated Manning's coefficients were listed in Table 5.



Table 5. Calibrated Manning's Coefficients in Different Zones Shown in Figure 62

Zone Number	1	2	3	4	5	6	7
Manning's $n$	0.035	0.06	0.15	0.035	0.035	0.035	0.06

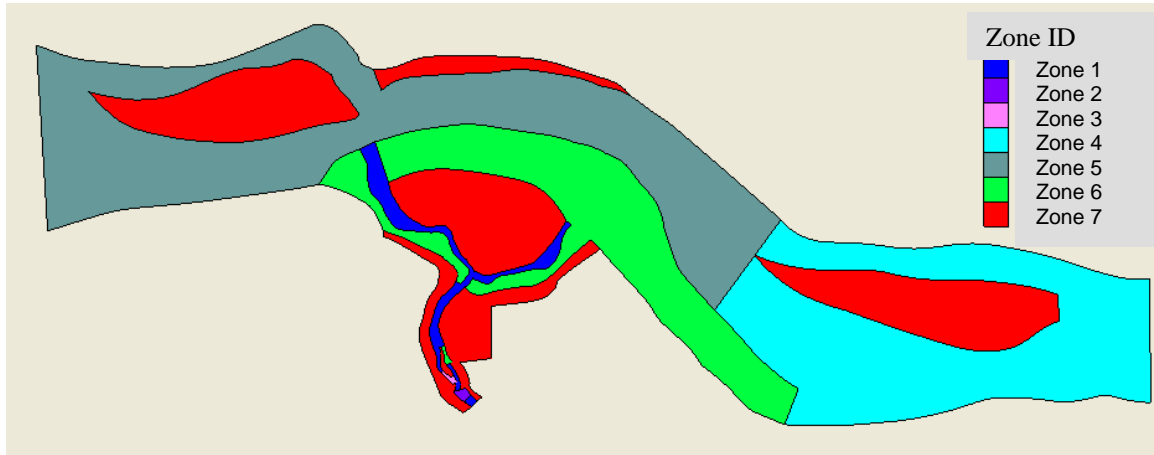


Figure 62. Roughness zones used for the Sandy River Delta Project

### 9.3.2 Input Data

Existing condition simulation was carried out corresponding to the field measured condition on October 12, 2005. The trip of October 2005 indicated that flow conditions were quite unsteady for both the Columbia River and the Sandy River, due mainly to the tidal influence and flow release from the Bonneville Dam. Flow unsteadiness often leads to difficulty in model calibration. Following a careful examination of the field data, conditions corresponding to the trip of October 12, 2005, were used for calibration.

The following input data were used for the model calibration study:

- Flow discharge for the Sandy River was set at 377 cfs, as recorded at the USGS Gage #14142500 (Sandy River below Bull Run River, near Bull Run, OR) on October 12, 2005. At one cross section of the Sandy River, field data from October 2005 estimated that the discharge was about 342 cfs based on the ADCP bottom tracking data.
- Flow discharge through the Columbia River was fixed at 123,000 cfs, which represented the average flow release from the Bonneville Dam on October 12, 2005. Releases from Bonneville Dam that day were very unsteady with a reported range of 118,000 to 132,000 cfs. Discharges calculated at several Columbia River cross sections from measured ADCP bottom tracking velocity data ranged from 98,310 to 125,700 cfs.

- The water surface elevation at the exit of the Columbia River reach was needed as the downstream boundary condition and the field measured elevation was used. The measured elevation, however, was quite unsteady and two distinct elevations were identified: 4.75 feet and 5.50 feet. Both elevations were used for the model calibration, which led to the development of two calibration runs: one low elevation case (4.75 feet) named Run #1, and another high elevation case (5.50 feet) named Run #2. Post-simulation analysis indicated that the difference in elevation at the exit boundary only influenced results near the confluence area of the Sandy River and Columbia River.

### 9.3.3 Comparison of Water Surface Elevation

Three sets of results were obtained with the calibrated hydraulic model, and they are named Run #1, #2 and #3. Run #1 and Run #2 reflect effects due to different water surface elevations specified at the exit boundary of the Columbia River reach. The two runs also indicate the sensitivity of model results to the exit boundary condition. Run #1 used the low elevation condition (4.75 feet), and Run #2 was based on the high elevation condition (5.50 feet). Both Run #1 and Run #2 used a Manning's coefficient of 0.15 for zone 3 in Figure 62. A third run (Run #3) was added to examine the impact of using a different Manning's coefficient in zone 3. Run #3 used the same downstream boundary condition as Run #1, but used a Manning's coefficient of 0.08 in zone 3 (versus 0.15 with Run #1 and #2).

The simulated water surface elevations on the Sandy River project reach are compared with the field data of October 2005 in Figure 63. The following observations may be made:

- The hydraulic model predicted the water surface elevation along the Sandy River quite well despite uncertainty in measured data and the unsteady nature of the flow in the field. The thalweg profile was also plotted in Figure 63 to demonstrate how well the model predicted water surface elevation despite large fluctuations in the bed topography. The difference between the field-measured and model-predicted elevation was typically within 0.3 feet, except near the confluence of the west distributary of the Sandy River and the Columbia River. This difference at the west confluence is likely associated with tidal fluctuations during the survey of October 2005.
- Major elevation changes at riffle and pool areas of the Sandy River reach were also predicted by the model. This indicates that the bed topography represented the riffle and pool areas correctly and that the model also represented the flow loss correctly.
- Uncertainty in the value of the Manning's  $n$  at Zone 3 may be obtained with results of Run #3. Reducing  $n$  from 0.15 to 0.08 alone led to a drop in

water surface elevation upstream of the zone by about 0.65 feet for the calibrated case. It should be noted that model-predicted elevations in other parts of the reach are not affected by this change. This assures that uncertainty in the roughness of zone 3 is limited to zone 3 only. A Manning's roughness coefficient of 0.08 was used when the model was applied to flood flow scenarios.

Comparison of water surface elevations on the Columbia River reach are shown in Figure 64. Again on the Columbia River, the river flow was quite unsteady and two distinct water surface elevations were identified. When different water surface elevations were used as the exit boundary conditions, represented by Run #1 and Run #2, the SRH-W model predicted water surface elevations within the range of the measured values. Comparison of the field-measured and model-predicted water surface elevations demonstrates a satisfactory agreement along the Columbia River reach.

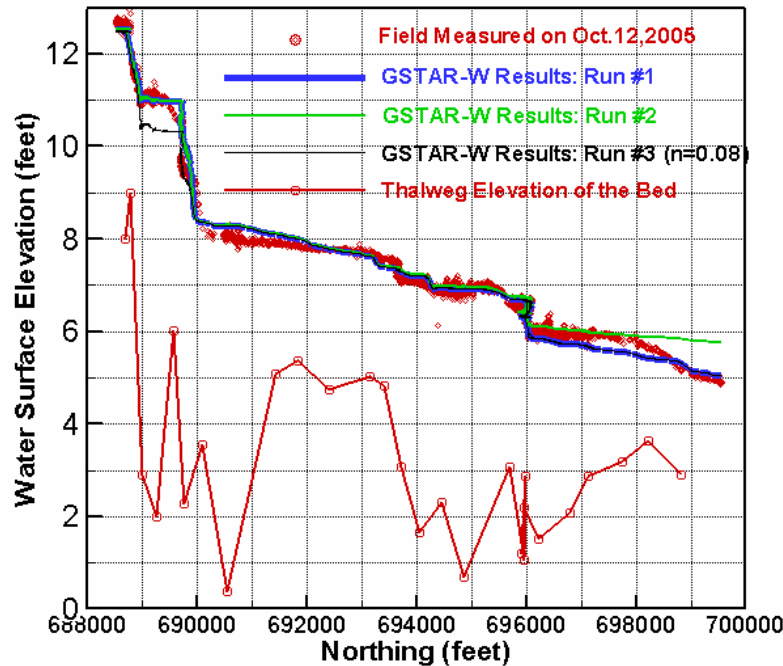


Figure 63. Comparison of simulated and field-measured water surface elevations along the Sandy River reach for October 12, 2005 flow conditions (GTAR-W is the former name of SRH-W)

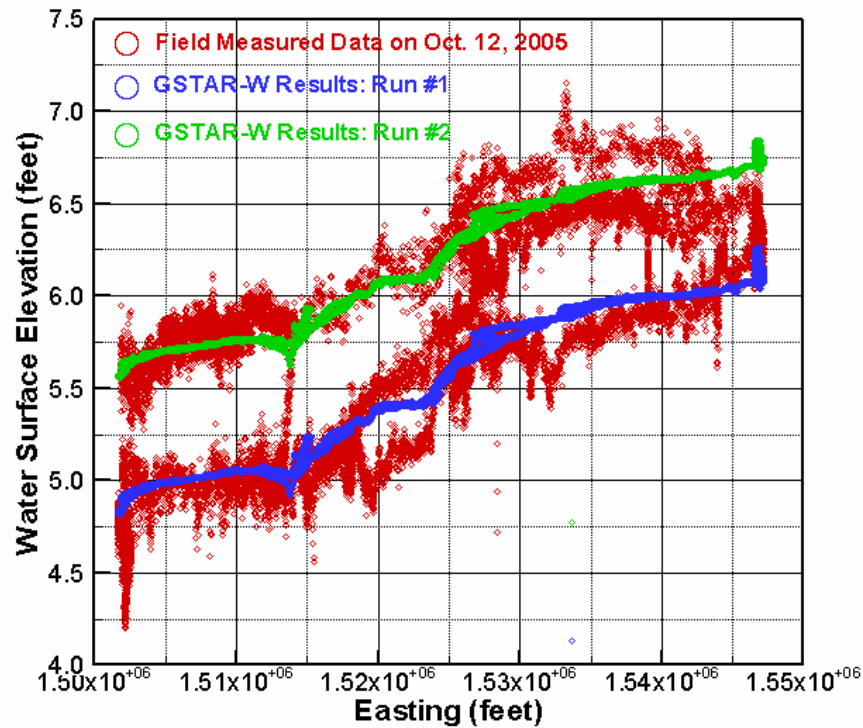


Figure 64. Comparison of simulated and field-measured water surface elevations along the Columbia River reach for October 12, 2005 flow conditions (GSTAR-W is the former name of SRH-W)

### 9.3.4 Comparison of Flow Velocity

Verification of the model was further carried out by comparing predicted and field-measured velocity results. ADCP measured velocity data were collected along both the Sandy and Columbia Rivers. An ensemble of ADCP data is a combination of water velocity (profile) and bottom tracking (boat velocity) data, and can be comprised of an average of several water velocity pings and several bottom pings. A ping is a single pulse of acoustic energy. Sandy River depth-averaged velocity data were processed from the ADCP velocity profiles (Water Mode 12) with 12 sub-pings. The Columbia River depth-averaged velocity data were from a single ADCP ensemble (velocity profile).

In both rivers, a measured data point represents an instantaneous, depth-averaged velocity for a single location. As a result, the data can be noisy, and averaging several adjacent velocity profiles is recommended in some situations. Research indicates that spatial averaging, sampling time, and sampling frequency affects the accuracy of mean velocity estimates (González-Castro *et al.*, 2000). However, no averaging of the field data was performed in this study for comparison with the model results, as we were only interested in evaluating if the simulated data fell within the range of measured data. An effort was made to remove all extreme outlier velocity data from the field-measured dataset.

Nevertheless, the dataset may still contain some erroneous data points (as can be seen from several velocity vectors presented). This does not affect the model calibration, but may contribute to a portion of the observed noise in the field-measured data.

Field-measured and model-predicted velocity magnitude comparisons at all measurement points were made for both the Sandy River (Figure 65) and the Columbia River (Figure 66). Although field data were noisy, results of the comparison are quite satisfactory. The large fluctuations in measured velocity values may be attributed to flow unsteadiness created by local geometry features, such as boulders and large turbulent eddies, and partly due to a few erroneous field data points.

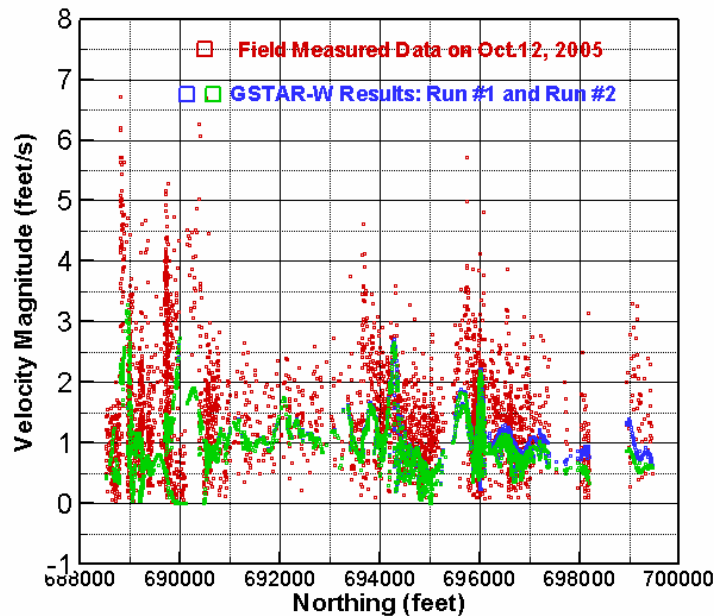


Figure 65. Comparison of simulated and field-measured velocity magnitudes along the Sandy River reach for October 12, 2005 flow conditions (GTAR-W is the former name of SRH-W)

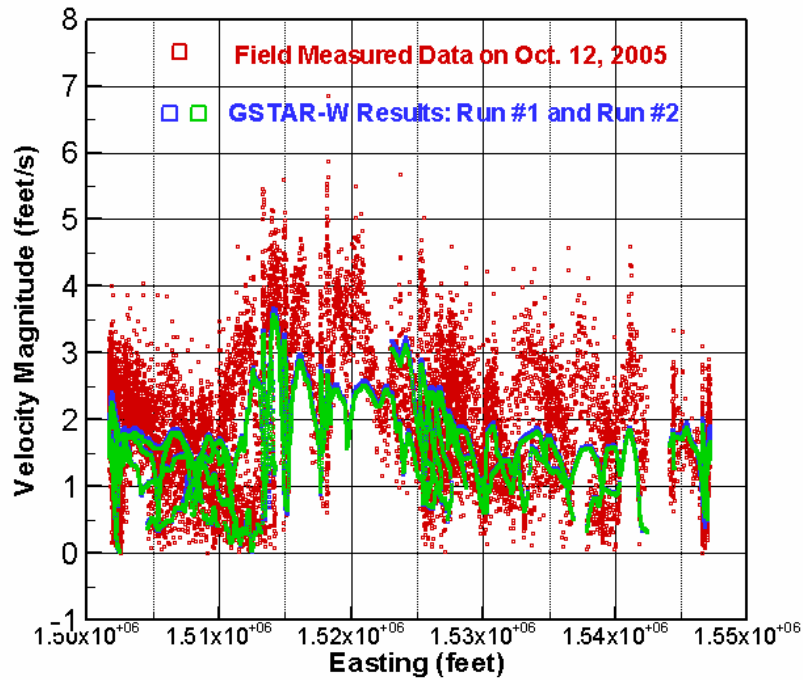


Figure 66. Comparison of simulated and field-measured velocity magnitudes along the Columbia River reach for October 12, 2005 flow conditions (GTAR-W is the former name of SRH-W)

Comparison of velocity was achieved through assessment of velocity vectors in different regions of the river reaches. Seven regions were used for comparison (Figure 67) and results are shown in Figure 68 to Figure 74. In view of uncertainty associated with some of the field data, the comparison between the field-measured and model-predicted data is deemed satisfactory.

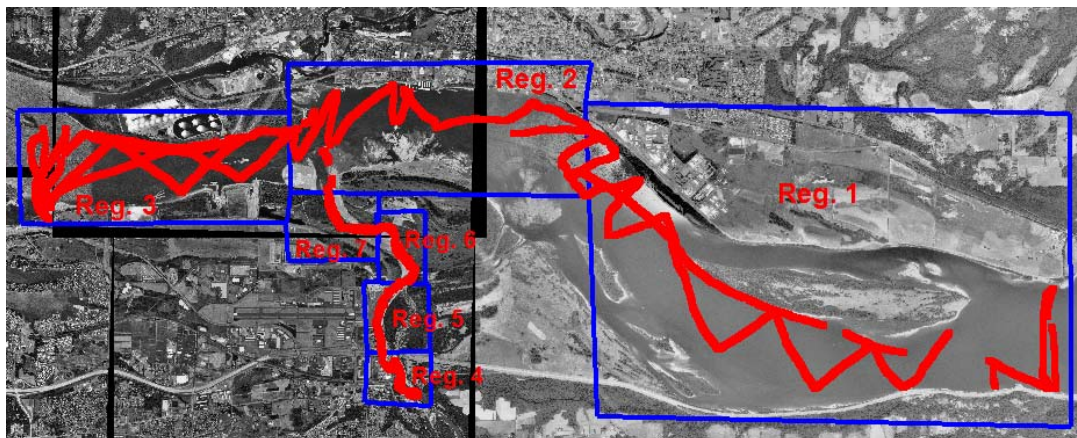


Figure 67. Seven regions (blue boxes) used for velocity vector comparison; Red points are the locations where velocity measurements were made

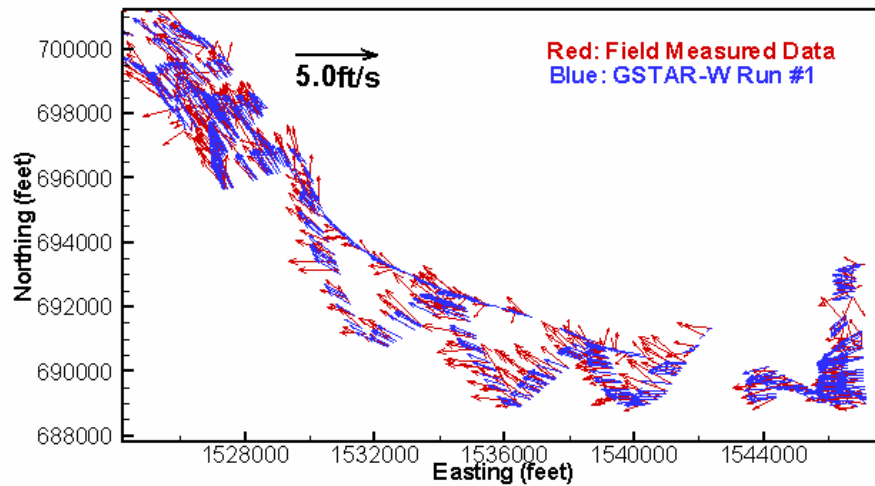


Figure 68. Comparison of velocity vectors in Region 1 (GTAR-W is the former name of SRH-W)

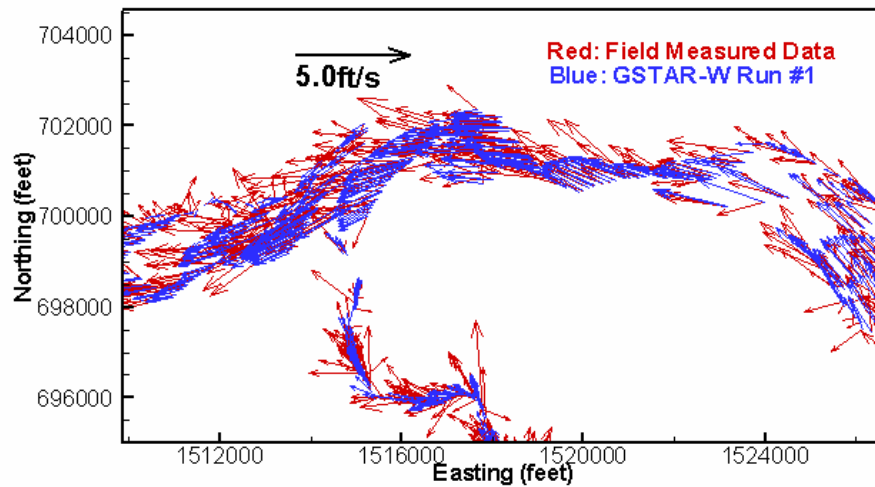


Figure 69. Comparison of velocity vectors in Region 2 (GTAR-W is the former name of SRH-W)



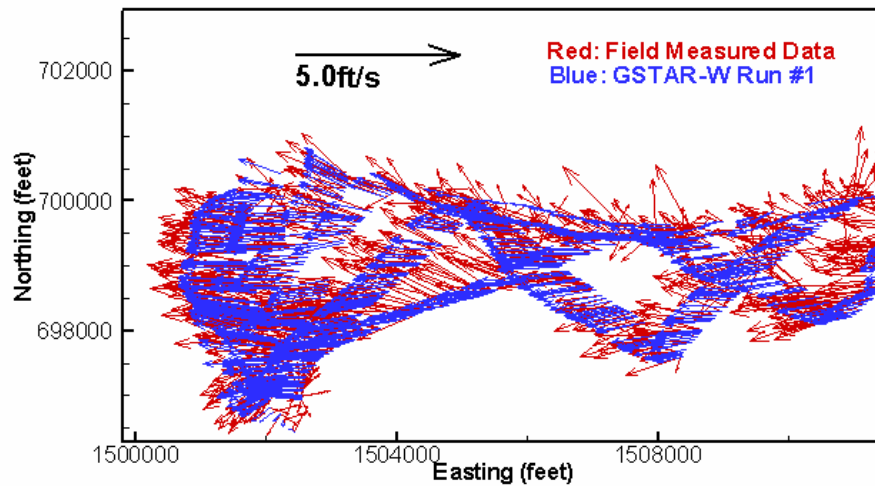


Figure 70. Comparison of velocity vectors in Region 3 (GTAR-W is the former name of SRH-W)

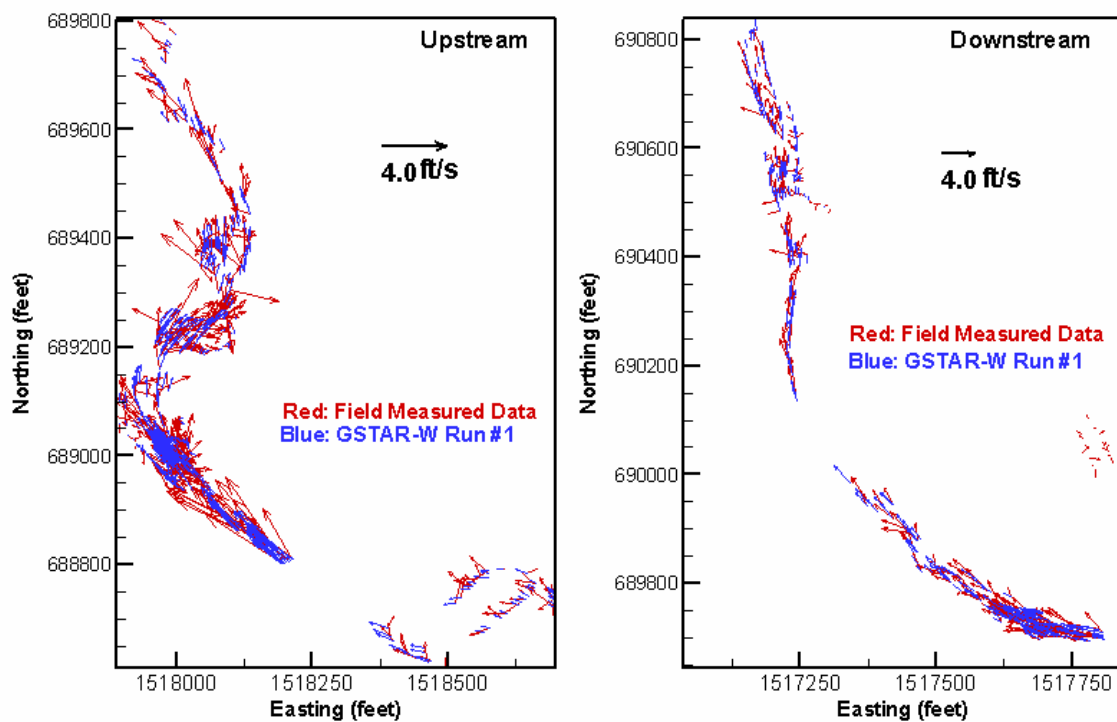


Figure 71. Comparison of velocity vectors in Region 4: Left is upstream and right is downstream portion of the region (GTAR-W is the former name of SRH-W)



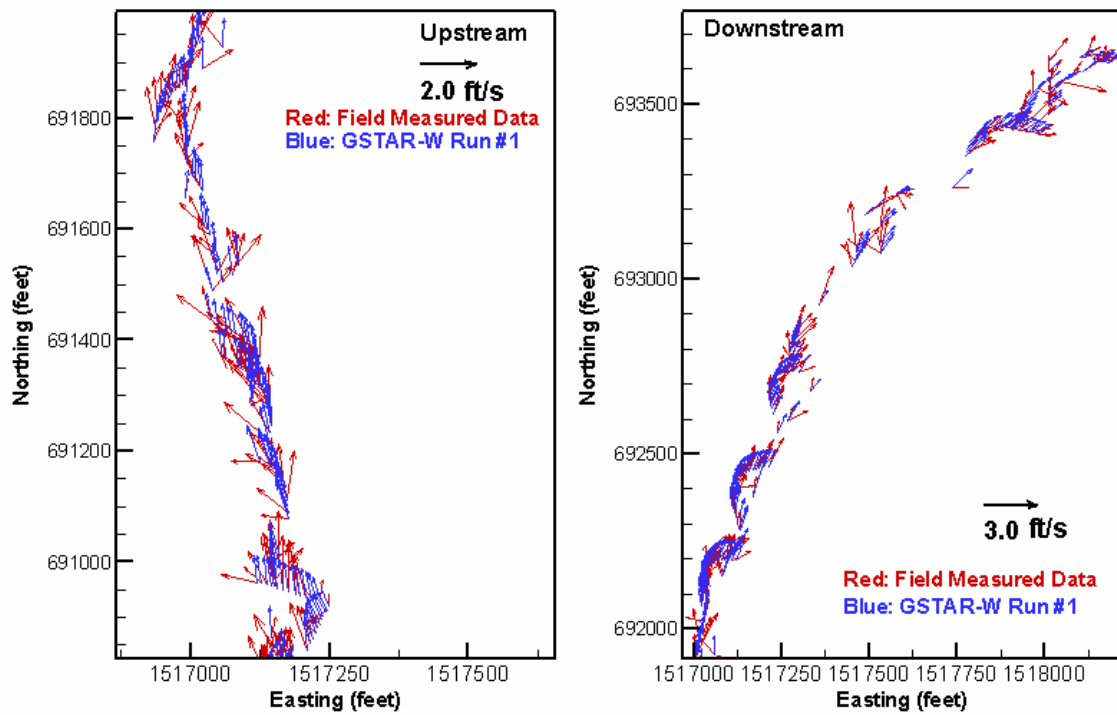


Figure 72. Comparison of velocity vectors in Region 5: Left is upstream and right is downstream portion of the region (GTAR-W is the former name of SRH-W)

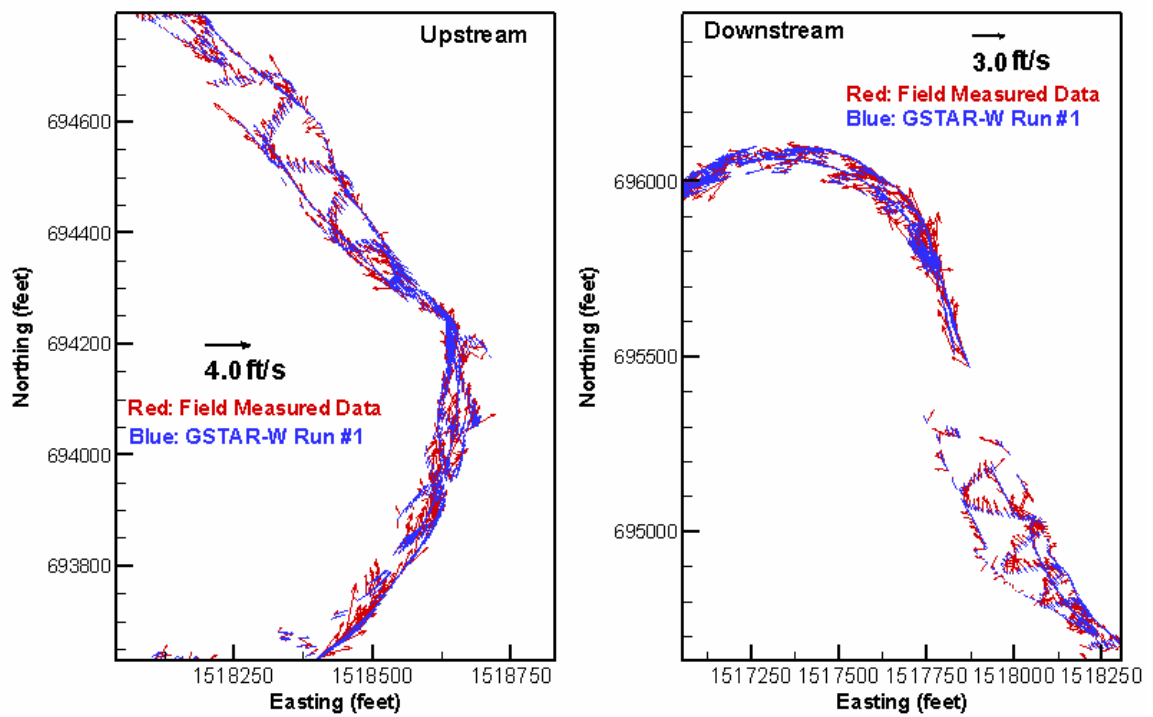


Figure 73. Comparison of velocity vectors in Region 6: Left is upstream and right is downstream portion of the region. (GTAR-W is the former name of SRH-W)

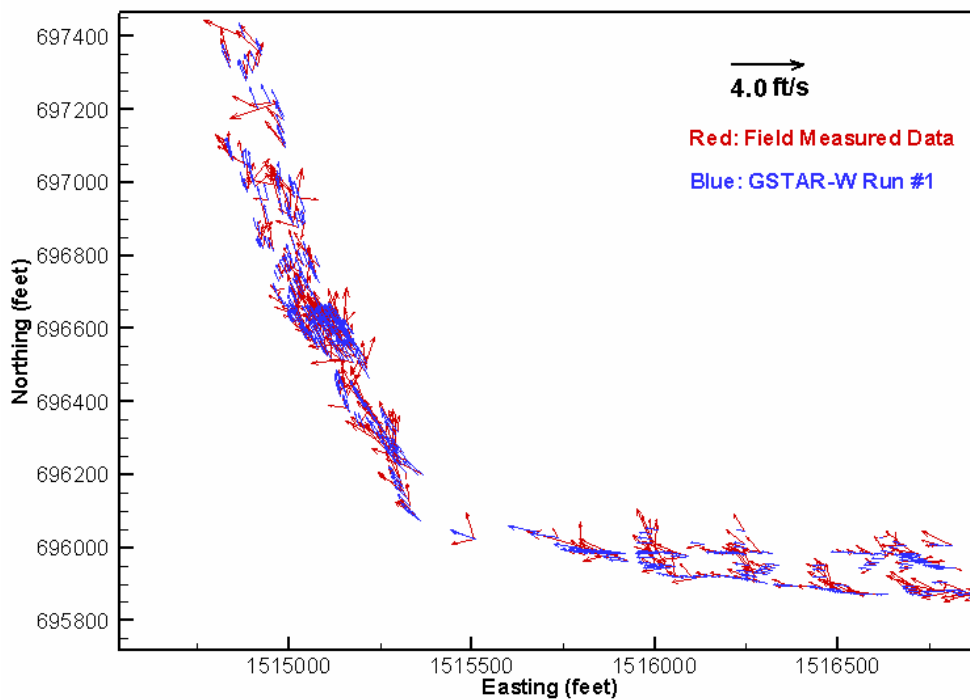


Figure 74. Comparison of velocity vectors in Region 7 (GTAR-W is the former name of SRH-W)

## 9.4 Other Application Cases

In addition to the projects discussed in this manual, SRH-W has also been applied to other projects with various purposes, such as temporary channel diversion, levee setback, stream habitat, cofferdams, etc. The following is a list of available project reports carried out at Reclamation for additional applications using the SRH-W:

- “Numerical Hydraulic Modeling and Assessment in Support of Elwha Surface Diversion Project,” by Bountry and Lai (2006).
- “Numerical Modeling Study of Levee Setback Alternatives for Lower Dungeness River, Washington”, Lai and Bountry (2006).
- “Identifying Stream Habitat with a Two-Dimensional Model – Report to the Yakima River Basin Water Storage Feasibility Study, Washington”, Hilldale and Mooney (2006).
- “Addendum to Analysis of Sediment Transport Following Removal of the Sandy River Delta Dam,” by Lai et al. (2006).



## REFERENCES

- Alonso, C. V., Bingner, R. L., and Kuhnle, R. A. (1995). "Sediment yield from watersheds with eroding channels," *Water Resources Engineering: Proceedings of the First International Conference*, ASCE, 1183-1187.
- Alonso, C. V. (1996). "Hydrologic research on the USDA Goodwin Creek experimental watershed, northern Mississippi," *Procs. 16th AGU Hydrology Days*, Colorado State University, 25-36.
- Barling, R.D., Moore, I.D., and Grayson, R.B. (1994). "A quasi-dynamic wetness index for characterizing the spatial distribution of zones of surface saturation and soil water content," *J. Water Resources Research*, 30(4), 1029-1044.
- Bathurst, J. C., Wicks, J. M., and O'Connell, P. E. (1995). "Chapter 16: the SHE/SHESED basin scale water flow and sediment transport modeling system." *Computer Models of Watershed Hydrology*, V.P. Singh, ed., Water Resources Publications, Littleton, Colo. 563-594.
- Beven, K.J., and Kirkby, M.J. (1979). "A physical-based variable contributing area model of basin hydrology," *Hydrol. Sci. Bull.*, 24, 43-69.
- Beven, K.J., (1981). "Kinematic subsurface storm flow," *Water Resour. Res.*, 17(5), 1419-1424.
- Beven, K.J. (1985). *Distributed Models in Hydrological Forecasting*, edited by M.G. Anderson, and T.P. Burt, John Wiley, NY, 425-435.
- Blackmarr, W. A. (1995). "Documentation of hydrologic, geomorphic, and sediment transport measurements on the Goodwin Creek experimental watershed, northern Mississippi, for the Period 1982-1993 - Preliminary Release." *Research Report No.3 (CD-ROM)*, U.S. Dept. of Agriculture. Agricultural Research Service.
- Bountry, J.A. and Randle, T.J. (2003). "2D numerical model results at proposed intake sites for full dam removal," Project Final Report, Technical Service Center, Bureau of Reclamation, Denver, CO.
- Bountry, J.A. and Lai, Y.G. (2006). "Numerical modeling of flow hydraulics in support of the Savage Rapids Dam removal." Project Final Report, Technical Service Center, Bureau of Reclamation, Denver, CO.
- Bountry, J.A., Lai, Y.G., and Randle, T.J. (2006). "Comparison of numerical hydraulic models applied to the removal of Savage Rapids Dam near Grants Pass, Oregon", 8<sup>th</sup> Federal Interagency Conference, Reno, NV, April 2-6, 2006.

- Brakensiek, D.L. (1967). "Kinematic flood routing," *Transactions of the ASAE* 10(3): 340-343.
- Bras, R. L. (1990). *Hydrology, an introduction to hydrologic science*, Addison - Wesley.
- Chow, V. T., Maidment, D. R. and Mays L. W. (1988). *Applied Hydrology*. New York: McGraw-Hill.
- DHI Software (1996). "MIKE 21 Hydrodynamic Module Users Guide and Reference Manual," Danish Hydraulic Institute - USA, Eight Neshaminy Interplex, Suite 219, Trevose, PA. (Check the following website: <http://www.dhisoftware.com/MIKE21/> )
- Dietrich, W.E., Wilson, C.J., Montgomery, D.R., and Bauer, J.M.R. (1992) "Erosion thresholds and land surface morphology," *J. Geology*, 20: 675-679.
- diGiammarco, P., Todini, E. and Lamberti, P. (1996), "A conservative finite element approach to overland flow: the control volume finite element formulation," *J. Hydrology*, 175, 267-291.
- Downer, C. W. (2002). "Identification and modeling of important streamflow producing processes," Ph.D. Dissertation, Department of Civil and Environmental Engineering, The University of Connecticut, Storrs, CT 06269, USA.
- Dunne, T. and Black, R.D. (1970). "An experimental investigation of runoff production in permeable soil," *Water Resources Research* 6(2), 478-490.
- Eagleson, P. S. (1970). *Dynamic hydrology*, McGraw-Hill.
- González-Castro, J.A., Oberg, K., and J.J. Duncker (2000). "Effect of temporal resolution on the accuracy of ADCP measurements," *Proceedings of the ASCE 2000 Joint Conference on Water Resource Engineering and Water Resources Planning and Management, July 30- August 2, 2000*, Minneapolis, Minnesota, edited by R.H. Hotchkiss and M. Glade, 9 pp.
- Govindaraju, R.S., Jones, S.E., and Kavvas, M.L. (1988). "On the diffusion wave model for overland flow 1. solution for steep slopes," *Water Resour. Res.*, 24(5), 734-744.
- Green, W.H. and Ampt, G. (1911). "Studies of soil physics, part I – the flow of air and water through soils," *J. Ag. Sci.* 4:1-24
- Henderson, F. M., and Wooding, R. A. (1964). "Overland flow and groundwater flow from a steady rainfall of finite duration," *J. Geophysical Research*, 69(8), 1531-1540.
- Horton, R.E. (1933). "The role of infiltration in the hydrologic cycle," *American Geophysical Union Transactions* 14, 446-460.
- Iwagaki, Y. (1955). "Fundamental studies on the runoff analysis by characteristics disaster prevention," *Res. Inst. Bull.* 10, Kyoto University.

- Jaber, F.H. and Mohtar, R.H. (2003). "Stability and accuracy of two-dimensional kinematic wave overland flow modeling," *Advances in Water Resources*, 26, 1189-1198.
- Johanson, R. C., Imhoff, J.C., Kittle Jr., J.L., and Donigian, A.S. (1984). "Hydrological Simulation Program - FORTRAN (HSPF): User Manual for Release 8.0," EPA 600/3-84-066, Environmental Research Laboratory, U.S. EPA, Athens, Georgia.
- Johnson, B. E., Julien, P. Y., Molnar, D.K. and Watson, C.C. (2000). "The two-dimensional upland erosion model CASC2D-SED," *Journal of the American Water Resources Association*, 36(1), 31-42.
- Julien, P. Y. and Saghafian, B. (1991). "CASC2D users manual - A two dimensional watershed rainfall-runoff model." *Civil Eng. Report, CER90-91PYJ-BS-12*, Colorado State University, Fort Collins, Fort Collins, CO.
- Julien, P. Y., Saghafian, B. and Ogden, F. L. (1995). "Raster-based hydrologic modeling of spatially-varied surface runoff," *Water Resource Bullitin, AWR*., 31(3), 523-536.
- Kuhnle, R. A., Bingner, R. L., Foster, G. R., and Grissinger, E. H. (1996). "Effect of land use changes on sediment transport in Goodwin Creek." *Water Resources Research*, 32(10), 3189-3196.
- Kuhnle, R. A. and Willis, J. C. (1998). "Statistics of sediment transport in Goodwin Creek." *ASCE J. Hydraulic Engineering*, 124(11), 1109-1114.
- Lai, Y.G., So, R.M.C., and Przekwas, A.J. (1995). "Turbulent transonic flow simulation using a pressure-based method," *Int. J. Engineering Sciences*, 33(4), 469-483.
- Lai, Y.G. (1997). "An unstructured grid method for a pressure-based flow and heat transfer solver," *Numerical Heat Transfer, Part.B*, 32, 267-281.
- Lai, Y.G. (2000). "Unstructured grid arbitrarily shaped element method for fluid flow simulation," *AIAA Journal*, 38(12), 2246-2252.
- Lai, Y.G., Weber, L.J., and Patel, V.C. (2003a). "Non-hydrostatic three-dimensional method for hydraulic flow simulation - Part I: formulation and verification," *ASCE J. Hydraulic Engineering*, 129(3), 196-205.
- Lai, Y.G., Weber, L.J. and Patel, V.C. (2003b). "Non-hydrostatic three-dimensional method for hydraulic flow simulation – Part II: validation and application," *ASCE J. Hydraulic Engineering*., 129(3), 206-214.
- Lai, Y.G. and Yang, C.T. (2004). "Development of a numerical model to predict erosion and sediment delivery to river systems, progress report No.2: sub-model development and an expanded review," Department of the Interior, Bureau of Reclamation, Technical Service Center, Denver, Colorado.
- Lai, Y.G., (2005). "River and watershed modeling: current effort and future direction", *US-China Workshop on Advanced Computational Modeling in*

*Hydroscience & Engineering*, September 19-21, 2005, Oxford, Mississippi, USA.

- Lai, Y.G., (2006), "Watershed erosion and sediment transport simulation with an enhanced distributed model," *3<sup>rd</sup> Federal Interagency Hydrological Modeling Conference*, Reno, NV, April 2-6, 2006.
- Lai, Y.G., Holburn, E.R., and Bauer, T.R. (2006). "Analysis of sediment transport following removal of the Sandy River Delta Dam," Project Final Report, Technical Service Center, Bureau of Reclamation, Denver, CO.
- Leavesley, G.H., Lichty, R.W., Troutman, B.M., and Saindon, L.G. (1983). "Precipitation-runoff modeling system: User's Manual," USGS Water Resources Investigations Report 83-4238.
- Lighthill, M.L. and Whitham, G.B. (1955) "On kinematic waves, I. flood movement in long rivers," *Proc. Roy. Soc.*, A229, 281-316.
- MacDonald, I., (1996). "Analysis and computation of steady open channel flow," Ph.D. Thesis, Dept. of Mathematics, Univ. of Reading, U.K.
- Mein R.G. and Larson, C.L. (1973). "Modeling infiltration during a steady rain," *Water Resour. Res.* 9(2): 384-394.
- Ogden, F.L. and Saghafian, B. (1997). "Green and Ampt infiltration with redistribution," *ASCE J. Irrigation & Drainage Engineering*, 123(5), 386-393.
- Overton, D.E. and Brakensiek, D.L., (1973), "A kinematic model of surface runoff response," *IAHS Pub.*, 9, 110-112.
- Patankar, S.V. (1980). *Numerical Heat Transfer and Fluid Flow*, McGraw-Hill, New York.
- Peric, M., Kessler, R., and Scheuerer, G. (1988). "Comparison of finite volume numerical methods with staggered and collocated Grids," *Computers in Fluids*, 16(4), 389-403.
- Rastogi, A., and Rodi, W. (1978). "Prediction of heat and mass transfer in open channels," *J. Hydraulic Division, ASCE*, 104(3), 397-420.
- Rawls, W. J., Brakensiek, D. L., and Miller, N. (1983). "Green-Ampt infiltration parameters from soils data." *Journal of Hydraulic Engineering*, 109(1), 62-69.
- Rhie, C.M. and Chow, W.L. (1983). "Numerical study of the turbulent flow past an airfoil with trailing edge separation," *AIAA Journal*, 21(11), 1526-1532.
- Rodi, W. (1980). "Turbulence models and their applications in hydraulics," Monograph, IAHR, Delft, The Netherlands.
- Rodi, W. (1993). "Turbulence models and their application in hydraulics," 3<sup>rd</sup> Ed., IAHR Monograph, Balkema, Rotterdam, The Netherlands.



- Sanchez, R. R. (2002). "GIS-based upland erosion modeling, geovisualization and grid size effects on erosion simulations with CASC2D-SED," Ph.D. Thesis, Civil Engineering, Colorado State University, Fort Collins, CO.
- Sharika, U., Senarath, S. Ogdon, F.L., Downer, C.W., and Sharif, H.O. (2000). "On the calibration and verification of two-dimensional, distributed, Hortonian, continuous watershed models," *Water Resour. Res.*, 36(6), 1495-1510.
- Shettar, A.S., and Murthy, K.K. (1996). "A numerical study of division of flow in open channels," *J. Hydraulic Research*, 34(5), 651-675.
- Shields, F. D., Knight, S. S., and Cooper, C. M. (1995). "Rehabilitation of watersheds with incising channels." *Water Resources Bulletin*, 31(6), 971-981.
- Singh, V. P. (1995). *Computer Models of Watershed Hydrology*, Water Resources Publication, Highlands Ranch, Colorado.
- Singh, V.P., and D.K. Frevert (eds.) (2002a). "Mathematical models of small watershed hydrology," Water Resources Publications, LLC, Highlands Ranch, Colorado.
- Singh, V.P., and D.K. Frevert (eds.) (2002b). "Mathematical models of large watershed hydrology," Water Resources Publications, LLC, Highlands Ranch, Colorado.
- Stephenson, D. and Meadows, M.E. (1986). *Kinematics Hydrology and Modeling*, Elsevier, Amsterdam, 250 pp.
- Therrien, R., Panday, S.M., McLaren R.G., Sudicky, E.A, Demarco, D.T., Matanga, G.B., and Huyakorn, P.S. (2003). "HydroSphere: a three-dimensional numerical model describing fully-integrated subsurface and surface flow and solute transport," User's Manual of HydroSphere, a Draft.
- US Army Corps of Engineers, (1996), "Users Guide to RMA2 - Version 4.3," US Army Corps of Engineers, Waterway Experiment Station - Hydraulic laboratory, Vicksburg, MS.
- Van Rijn, L.C. (1987). "Mathematical modeling of morphological processes in the case of suspended sediment transport," Delft Hydraulics Communication No.382.
- Vanderkwaak, J. (1999). "Numerical simulation of flow and chemical transport in integrated surface-subsurface hydrological systems," Ph.D. Thesis, Earth Sciences, University of Waterloo, Waterloo, Ontario Canada.
- Vieira, J.H.D. (1983). "Conditions governing the use of approximations for the Saint Venant equations for shallow surface water flow." *J. Hydrology*, 60, 43-58.
- Williams, J. R., Jones, C.A., and Dyke, P.T. (1984). "A modeling approach to determining the relationship between erosion and soil productivity," *Transaction of the ASAE*, 27, 129-144.

- Williams, J. R., Nicks, A.D., and Arnold, J.G. (1985). "Simulator for water resources in rural basins," *ASCE J. Hydraulic Engineering*, 111(6), 970-986.
- Wischmeier, W. H., and Smith, D. D. (1978). *Predicting Rainfall Erosion Losses: A Guide to Conservation Planning*, Agricultural Handbook np.537, USDA, Science and Education Administration.
- Woolhiser, D.A. and Liggett, J.A. (1967). "Unsteady, one-dimensional flow over a plane – the rising hydrograph," *Water Resour. Res.*, 3(3), 753-771.
- Woolhiser, D. A. (1975). "Simulation of unsteady overland flow." *Unsteady Flow in Open Channels*, K. Mahmood and V. Yevjevich, eds., Fort Collins, CO.
- Woolhiser, D. A., Smith, R. E., Sharif, H. O., and Goodrich, D. C. (1990). "KINEROS, a kinematic runoff and erosion model: documentation and user manual." *ARS-77*, USDA, Agricultural Research Service, 130p.
- Woolhiser, D. A. (1996), "Search for physically based runoff model - A hydrologic El Dorado?" *J. Hydraul. Eng.*, 122(3), 122-129.
- Wu, W. and Siddle, R.C. (1995). "A distributed slope stability model for steep forested basins," *Water Resources Research*, 31(8): 2097-2110.
- Yang, C.T., Lai, Y.G., Randle, T.J., and Dario, J.A. (2003), "Development of a numerical model to predict erosion and sediment delivery to river systems: Progress Report No.1: review and evaluation of erosion models and description of SRH-W approach," Department of the Interior, Bureau of Reclamation Technical Service Center, Denver, Colorado.

# APPENDIX A

## ON MESH GENERATION USING SMS

This appendix describes how to prepare a SRH-W mesh using SMS. It is not the intent of this Appendix to train a user to use SMS; for such a purpose a user should consult the SMS user's manual or resort to the SMS training classes. Instead, this Appendix focuses only on how to interface between SMS and SRH-W. Note that only a portion of the SMS capabilities are used by SRH-W. The modules used include the Map, Mesh, and Scatter Points. Below is a typical sequence of mesh generation procedures using SMS:

(1) Upon entering SMS, a user needs to make sure that the **COVERAGE** of the application is set to **GENERIC 2D MESH** under the MAP module and Feature Objects/Coverage option. This way, upon completion of mesh generation within SMS, the mesh will be stored in the 2D Generic Mesh format. Project\_Name.2DM file stores the mesh information and is used by the SRH-W as the mesh input.

(2) The first SMS module used is usually the SCATTER Module in which the topography of the to-be-simulated area is defined. The topography of the simulation area may be defined by a file containing ASCII data of all survey points or contour lines stored in formats such as DXF. A DXF file may be converted into scatter points to define the topography with the SMS MAP Module, DXF → Scatter Points option. The topography information contained in the SCATTER module and is used later to obtain to bed elevation at mesh points through interpolation.

(3) The first step in mesh generation is to use the MAP Module to create the boundaries of the solution domain. Boundaries are represented with Feature Objects (nodes and arcs) with the SMS MAP Module. The topography data contained in the SCATTER Module or aerial photos may be used to sketch out the solution domain. The size and location of the boundaries may be determined by factors such as the interested simulation area, the largest discharge to be simulated, etc. If possible, one solution domain is used for all possible discharges under the same topography. SRH-W determines the wet and dry areas automatically and a larger domain may be used if an inundation extent is unknown.

(4) Once the solution domain is determined and created, the next step is to divide the solution domain into combinations of polygons using the feature objects (nodes and arcs). Polygons are automatically generated within SMS MAP Module with the Feature Objects/Build Polygons option, once all feature arcs are generated and completed. Note that the polygon creation step is very important in several ways. Firstly, each polygon may be meshed independently within the

MESH Module, thus it may be used as a way to distribute the mesh density. For example, the main channel may be represented by a polygon so that a quadrilateral mesh is generated (with PATCH in SMS) and more mesh points may be used in the polygon. In the floodplain areas, however, polygons may be meshed with triangles (with PAVING in SMS) and many fewer points may be used. A sample mesh is shown in Figure A1 to illustrate the mesh distribution. Secondly, a polygon may be assigned a material type and the material type is used by SRH-W to assign landuse properties such as the Manning's roughness coefficient. This way, different polygons may be used to represent different landuse characteristics.

(5) Once all polygons are generated, the next step is to generate a mesh for each polygon and assign a material type to it. A pop-up window will appear to carry out the task by clicking the polygon within the MAP Module. Several mesh types are available with SMS, and the most useful ones are the PATCH and PAVING. PATCH creates a quadrilateral structured mesh and works on four sided polygons only while PAVING creates a triangular unstructured mesh and works on any polygons. It is recommended that the main channel be meshed with PATCH and the remaining areas be meshed with PAVING. The mesh density and distribution may be changed and the polygon/material type may be assigned within the pop-up window. A user should consult the SMS manual for more detail on mesh generation. Do not be afraid to make mistakes as SMS allows you to revisit the mesh generation and change/modify the mesh any way necessary.

(6) Once all polygonal meshes are generated, the mesh may be assembled together by using the Feature Objects/Map→ 2D Mesh option within the MAP Module. "Merging Triangles" option may be used to reduce the number of cells while keeping the mesh points the same. This completes the 2D mesh generation and the mesh may be displayed for examination. Steps (4) to (6) may be repeated to optimize the mesh until a final mesh is obtained.

(7) Once the mesh is finalized, the bed elevation of each point is interpolated from the scatter data sets created in Step (2). This is accomplished by going to the SCATTER Module and using the Scatter/Interpolate-to-Mesh option. The bed topography represented by the mesh may be examined by plotting the contour lines in the Display Option. Also, check that linear elements are used for the mesh (versus the Quadratic) by displaying the mesh points. If midpoints of element edges are displayed, elements are quadratic. Conversion from quadratic to linear may be carried out within the MESH Module with the Elements/Linear – Quadratic option.

(8) Finally, NODESTRINGS are created within the MESH Module. Each nodestring represents a boundary segment of the solution domain and is used by SRH-W to specify the boundary types and boundary conditions (see the BOUNDARY SEGMENT DEFINITION command). All boundaries of the solution domain and all mesh points on boundaries should be included in the

nodestrings. Or, SRH-W preprocessor, *srhpre11*, will issue an error message. A user should take a note of the nodestring order when it is created as the order is designated as the nodestring ID. For example, the first created node string has an ID of 1, and the fifth nodestring has an ID of 5, etc. The nodestring ID will be used to specify boundary conditions with SRH-W. If a user forgot the nodestring IDs for a mesh, the mesh file, *project\_name.2DM*, may be viewed to decide the order (and ID) that is listed near the end of the file. It is recommended that “special” boundary segments be created first as the nodestrings. “Special” refers to those boundary segments that are to be manually defined as non-default boundaries using the BOUNDARY SEGMENT DEFINITION command. Typical special boundaries include the upstream inlets and downstream exits. The default setting of SRH-W v1 is as follows: for non-watershed application all boundaries are setup as solid walls (WALL); and for watershed application all boundaries are setup as fixed elevation (FIX-H) with zero water depth.

(9) The above procedures complete the mesh generation process and if the project file is saved with the name of project-name, an ASCII mesh file will be created by SMS with the name of project-name.2DM. This 2DM file will be used by SRH-W.

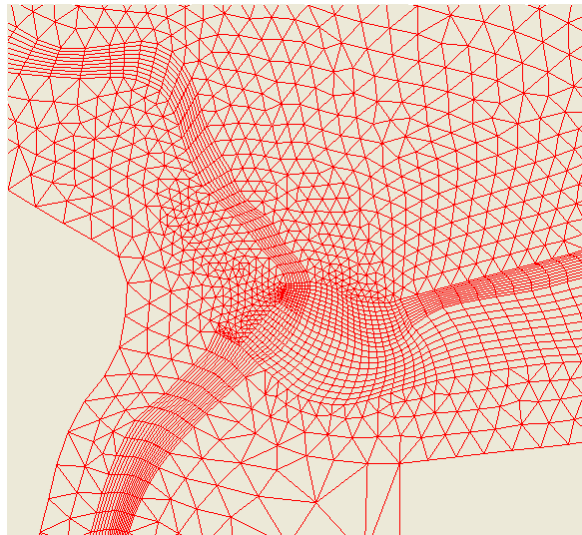


Figure A1. A Sample Mesh to Represent Main Channel and Floodplain



# APPENDIX B

## INPUT AND OUTPUT FORMATS

This appendix provides a description on how some of the input and output formats are used with SRH-W.

### B.1 SMS Format

SMS format is used for output, and is to store the simulation results, final or intermediate, so that SMS or ArcGIS may be used to view and process the results.

### B.2 TECPLOT Format

TECPLOT format is used for output, and is to store the simulation results, final or intermediate, that may be used by TECPLOT, another post-processing graphical software. Users are referred to the TECPLOT user's manual for details about the TECPLOT program.

### B.3 PLOT3D Format

PLOT3D format is exclusively used for single or multi-block structured mesh. The mesh file is in the form of ASCII with double precision data. The PLOT3D format of the mesh may be created with the following FORTRAN statement:

```
write(*,'(16i5)') nblock
write(*,'(16i5)') (nx(i),ny(i),ione,i=1,nblock)
DO iblock=1,nblock
    nxyz=nx(iblock)*ny(iblock)
    write(*,'(1p5e16.8)') (x(ip,iblock),ip=1,nxyz)
    write(*,'(1p5e16.8)') (y(ip,iblock),ip=1,nxyz)
    write(*,'(1p5e16.8)') (z(ip,iblock),ip=1,nxyz)
ENDDO
```

where nblock is the number of mesh blocks, nx(i), ny(i) are the number of mesh points in the I and J directions, respectively, for mesh block i. Note that ione is integer 1 that indicates that the mesh is 2D. Also, (x(i,j) y(i,j) z(i,j)) are the horizontal and bed elevation coordinates for mesh point i and mesh block j.

## B.4 GENERIC Format

GENERIC format is an output format offered by SRH-W v1 as a way of obtaining the simulation results when a user does not have access to graphical packages that use the TECPLOT or SMS formats. With the GENERIC format, a user may convert the result file into other formats so that other readily available post-processing packages may be used. With the GENERIC format, an output file, casename\_GNR.dat, is created.

The GENERIC format file is created with the following FORTRAN statement:

```
write(*,*) FILE-DESCRIPTION      !one record of text
write(*,*) Nvar                  !number of dependent variables
write(*,*) Variable-List        !list of variable names in the file

write(*,*) Nnode,Nelem          !number of nodes & elements

DO Ivar=1,Nvar                  !loop over all variables
  Write(*,*) (Var(i,Ivar),i=1,Nnode)
ENDDO

DO I=1,Nelem                    !loop over all elements
  Write(*,*) Nnd                !number of nodes for the element
  Write(*,*) (NodeID(j),J=1,Nnd) !list of nodes of the element
ENDDO
```



# APPENDIX C

## DYNAMIC INPUT FILE (DIP)

Some of the frequently used parameters, which are set up through *srhpre11*, may also be set up or modified during SRH-W execution. This dynamic setup and change of solution parameters are achieved using the SRH-W Dynamic Input (DIP) file. The DIP file is a text file named casename\_DIP.dat and it has the following format:

```
$DATAC
    parameter assignment statement
$ENDC
```

A sample copy of the \_DIP file may be obtained from the tutorial cases that are available through the SRH-W distribution package.

A number of parameter assignment statements may be listed and each statement has the following syntax:

*parameter-name = parameter-value*

Available parameters which may be changed using the DIP file are listed below:

<b><i>NTSTEP = n</i></b>	<i>n</i> is the total number of time steps to be simulated.
<b><i>NITER = n</i></b>	the number of iterations within each time step. Typically, <i>n</i> =1 or 2 may be used for steady state simulation; 10 to 20 may be used for unsteady simulation.
<b><i>IREST = l</i></b>	<i>l</i> equals 0 or 1 to specify how the casename_RST.dat is used for initial condition setup. IREST=0 means no RST file is used and initial condition is setup using one of the methods available; IREST=1 means it is a continuation run and the execution is restarted from casename_RST.dat.
<b><i>INTERVAL = n</i></b>	used for steady or unsteady simulation; it allows SRH-W to write out intermediate results every <i>n</i> time steps. Output file will have the name of, e.g., casename_TECi.dat.
<b><i>DTNEW = r_time</i></b>	this is to change the flow simulation time step to <i>r_time</i> .
<b><i>ISCHEME = l</i></b>	this allows a user to choose different discretization schemes for the convection term. <i>l</i> =1 is for 1 <sup>st</sup> -order upwind scheme that is the default and recommended for most applications. <i>l</i> =2 is the 2 <sup>nd</sup> -order scheme with damping that provides higher theoretical accuracy but its effectiveness depends on its application.

***RELAX\_H = r*** specify relaxation of the continuity equation to ***r***, where ***r*** typically ranges from 0.001 to 0.5 with a smaller value for heavier relaxation. Typically, 0.1 should work for most problems.

***RELAX\_UV=r*** specify relaxation of the momentum equations to ***r***, where ***r*** typically ranges from 1.0 to 100.0 with a higher value for heavier relaxation. Typically, 1.0 works for most applications.

***A\_TUR = r*** This is to set the depth-averaged parabolic turbulent model coefficient. ***r*** ranges from 0.3 to 1.0; default is 0.7.

## **APPENDIX D**

# **SPECIAL TREATMENT IN MESH ZONES**

This section is intentionally left blank.